PROCEEDINGS

OF THE

AMERICAN PHILOSOPHICAL SOCIETY

HELD AT PHILADELPHIA

FOR PROMOTING USEFUL KNOWLEDGE

VOL. LIV MAY–JULY, 1915 NO. 217

ADDITIONS TO THE FAUNA OF THE LOWER PLIOCENE SNAKE CREEK BEDS (RESULTS OF THE PRINCETON UNIVERSITY 1914 EXPEDITION TO NEBRASKA).

BY WILLIAM J. SINCLAIR.

(*Read April 24, 1915.*)

One of the objects of the Princeton University 1914 Geological Expedition to Nebraska was to acquire, if possible, fossil bones from the Lower Pliocene Snake Creek beds of Sioux County, partly to fill out the exhibition and study collections of the Department of Geology, which were lacking in Pliocene vertebrates, and, partly, to obtain some additional light on the fauna of the Great Plains region in Lower Pliocene time, with the purpose of establishing a broader basis for the correlation of Continental Interior and Pacific Coast Tertiary deposits. In both respects the expedition was thoroughly successful, which I attribute, in large part, to the enthusiastic support of my assistants, Messrs. A. C. Whitford, of Lincoln, Nebraska, and Mr. Charles Barner, of Agate, and to the kindness of our temporary neighbors, the various ranchmen on whose ranges the bonebearing deposits lie.

The Snake Creek beds were named and described by Matthew and Cook,[1] and reference should be made to their paper for details not brought out in the pages which follow. The four exposures worked by the Princeton party lie within the limits of the Whistle

[1] "A Pliocene Fauna from Western Nebraska," *Bull. Am. Mus. Nat., Hist.*, N. Y., Vol. XXVI., Art. XXVII., pp. 361–414, 1909.

PROC. AMER. PHIL. SOC., LIV., 217, F, PRINTED JULY 7, 1915.

Creek quadrangle, south of the sandhills on the divide between the Niobrara and the North Platte rivers, in draws at or near the heads of Dry Spotted Tail Creek, Spotted Tail Creek and Snake Creek, as follows: Loc. 1000A, T. 26 N., R. 55 W., Sec. 31 (N. E. ¼); Loc. 1000B, same township and range, but in the southeast quarter of Sec. 33; Loc. 1000C, T. 25 N., R. 55 W., Sec. 3 (S. E. ¼ to middle of section); Loc. 1000D, T. 25 N., R. 54 W., Sec. 2 (N. E. ¼). Of the four, Loc. 1000C, to which the attention of Messrs. Whitford and Barner was called by Mr. John Weir, before my arrival in the field, was particularly productive, yielding some of our best material.

The Snake Creek beds comprise unconsolidated, water-worn gravels, clean, cross-bedded, round-grained sands sometimes streaked with magnetic, and a mortar-like, gray-white material, sometimes in angular fragments and sometimes in cobbles or boulder-like masses, resting with marked erosional unconformity on the Middle Miocene Sheep Creek beds. Rolled pebbles of granite, quartzite, etc., indicate water transportation from the crystalline rocks of the mountains farther west, probably some of the sand is windborne, but a large part of the Snake Creek matrix has not been transported far and consists, sometimes, of subangular fragments resembling in appearance dried mortar, and, sometimes, of gravels, cobbles, and large masses of more or less indurated clay or silt, evidently represented the harder portions of the Sheep beds through which the Snake Creek channels were cut. Many large, slightly rounded masses of Sheep Creek sediment incorporated in the Snake Creek sands and gravels are quite incoherent and could not have stood thorough saturation with water, not to mention transportation to any considerable distance. I think they were derived from the caving of undercut banks along channels incised in the Sheep Creek. Water-worn fragments of silicified wood are common, but are not necessarily remains of a forest contemporary with the Lower Pliocene fauna. Most of it, if not all, is *remanie* material.

The stratification is lenticular, water-worn gravels giving place laterally to cross-bedded sands and jumbled masses of clay boulders. Either gravels, sands or mortar-like fragments may rest with clean sharp contact on the eroded surface of the Sheep Creek, the irregu-

larity of which is increased by land sliding occuring along the sides of the draws where the exposures are found, but much of it is due to changes in the slope of the channel-beds in which the Snake Creek deposits accumulated. Upward, the formation merges into wind-blown sands and silts which cover the prairie top, and it is not always possible to distinguish between them, as bones sometimes occur in the lower layers of the sand above the level of the typical Snake Creek gravels.

Exposures, when found, are along the sides of the draws which have cut down through the Snake Creek beds into the underlying Sheep Creek, and are usually more or less obscured by wind-blown sand overgrown with grass and weeds, so that little in the way of fossils can be seen at the surface except an occasional weathered bone fragment on the bare spots between grass clumps. Occasionally, a larger ungrassed area of sand and pebbles may show a few horse teeth, a jaw fragment or two or the ends of some broken limb bones. All collecting was done by stripping off the surface sod and exposing the Snake Creek-Sheep Creek contact wherever the greater abundance of gravel and bone fragments suggested the presence of a productive "pocket" or lens of bone-bearing gravel. If the preliminary prospecting seemed to warrant further excavation, a large area was cleared and the bank cut back to a vertical face which was worked by undercutting at the level of the contact just mentioned. This was kept up until the productive gravel was exhausted or the repeating caving of the heavy top burden of sand made further work both laborious and dangerous.

The bones are remarkably well preserved, mostly black or of a dark color, and occur in both the gravels, sands and mortar-like conglomerate, becoming scarce as the sand gets clean or the number of clay boulders and cobbles increases. They are all more or less abraded, sometimes by water wear, at other times manifestly by wind-blown sand,[2] and vary in character from rolled bone pebbles to complete skulls. Hardly ever is there association of adjacent parts. Occasionally a *remanie* fossil, washed out of the Sheep

[2] The type skull of *Protolabis princetonianus* sp. nov. was found in soft sand, lying on the left side with the front of the skull tilted downward. The arch and back of the skull on the upper (right) side are pared down to a common level in a manner suggesting sand-blasting.

Creek, is found, but with this exception the bones seem to have been introduced directly into the streams which transported the Snake Creek gravel and, apparently, represent the fauna of the immediate vicinity, as frail teeth and delicate skull and jaw processes remain unbroken, suggesting that the bones have not been moved far. As will be seen by an examination of the Whistle Creek Quadrangle, our collecting localities are somewhat widely scattered and may not all represent the deposits of a single stream, possibly are not all strictly contemporaneous, but as our large collection from locality 1000C contains practically the same forms as are found in the remaining less fossiliferous localities, there is every reason to regard the fauna as a unit. So far as determined, the Snake Creek beds have yielded the following association of forms, those marked (*A*) being preserved in the American Museum, New York, (*P*) in the Geological Museum of Princeton University and (*C*) in the private collection of Mr. H. J. Cook, of Agate, Nebraska.

DOGS.

Amphicyon amnicola (*A*).
Amphicyon sp. indet. (*A*).
?Amphicyon sp. indesc. (*P*).
Aelurodon haydeni validus (*A*).
Aelurodon saevus secundus (*A*).
Aelurodon cf. *wheelerianus* (*P*).
Aelurodon sp. div. indet. (*A, P*).
Tephrocyon hippophagus (*A, P*).
Tephrocyon cf. *temerarius* (*A*).
Tephrocyon cf. *vafer* (*A, P*).
Tephrocyon mortifer (*C*).
Tephrocyon sp. maj. (*A, P*).
?Cyon sp. (*A*).

CIVET-CAT.

Bassariscus antiquus (*A*).

MUSTELINES.

Brachypsalis pachycephalus (*P*).
Brachypsalis obliquidens sp. nov. (*P*).
Martes glareæ sp. nov. (*P*).

CATS.

Pseudælurus near *intrepidus* (*P*).
Cat, non-machærodont (*P*).
Machærodont cat, gen. indet. (*A*).
?Felis cf. *maxima* (*A*).

RODENTS.

Mylagaulus cf. *monodon* (*A*).
Dipoides curtus (*A, P*).
Dipoides tortus (*A*).
Hystricops cf. *venustus* (*A, P?*).
Geomys cf. *bisulcatus* (*A*).

EDENTATES.

Megalonychid, gen. et. sp. indet. (*A, P*).

RHINOCEROSES.

Teleoceras sp. (*A, P*).
Aphelops sp. (*A, P*).
?Cænopus sp. (*A*).

HORSES.

Archæohippus sp. (*P*).
Parahippus cf. *cognatus* (*A, P*).
Hypohippus cf. *affinis* (*A*).
Hypohippus sp. (*P*).
Merychippus cf. *insignis* (*A, P*).
Merychippus close to *calimarius* (*P*).
Hipparion cf. *occidentale* (*A, P*).

Hipparion gratum (*A, P*).
Hipparion cf. *affine* (*A, P*).
Protohippus cf. *placidus* (*P*, probably *A*).
Protohippus near *perditus* (*P*, probably *A*).
Pliohippus cf. *mirabilis* (*P*).
Pliohippus sp. div. (*A*).

PECCARIES.

Prosthennops cf. *crassigenis* (*A*).
Prosthennops sp. (*A, P*).

OREODONTS.

Merychyus (*Metoreodon*) *relictus* (*A*).
Merychyus (*Metoreodon*) *profectus* (*A, P*).
Merychyus (*Metoreodon*) sp. (*A, P*).
Pronomotherium siouense sp. nov. (*P*).

CAMELS.

Protolabis princetonianus sp. nov. (*P*).
Pliauchenia (*Megatylopus*) *gigas* (*A, P*).
Alticamelus procerus (*A, P*).
Alticamelus sp. div. (*A, P*).
?Procamelus sp. div. (*A*).

ANTELOPES AND DEER.

Dromomeryx whitfordi sp. nov. (*P, A*).[3]
Drepanomeryx falciformis gen. et sp. nov. (*P*).
Cervus sp. (*A, P*).
Blastomeryx elegans (*A*).
Blastomeryx cf. *wellsi* (*A*).
Merycodus necatus sabulonis (*A, P*).
Merycodus cf. *necatus* (*A, P*).
Merycodus sp. div. (*A, P*).

BOVIDS.

Neotragocerus improvisus (*A, P*).
Bovid gen. indet. (*A*).
Bison sp. (*A*).

MASTODONS.

Gomphotherium sp. (*P*).
?Mastodon sp. (*P*).

BIRDS.

Aquila danana? (*P*).[4]
Buteo near *borealis* (*P*).[4]

REPTILES.

Crocodile vertebra (*P*).
Lizard jaws (*P*).
Huge land tortoise (*A, P*).

OF UNCERTAIN POSITION.

Part of large mammal jaw (*P*).

The collections obtained by the Princeton expedition have greatly increased the number of Miocene genera represented in the Snake Creek fauna. *Archæohippus* excepted, *Brachypsalis, Pseudælurus, Pronomotherium, Protolabis* and *Dromomeryx* have species in the Upper Miocene, distinct, but not strikingly different from, their Snake Creek successors, rather increasing the close relationship of the fauna with that of the Upper Miocene previously commented on by Matthew and Cook. Additional Pliocene elements are far

[3] *Palæomeryx* sp. of Matthew and Cook.

[4] Represented in the Princeton collection by a fragment of the tarso-metatarsus. Determinations by Dr. Loye Holmes Miller.

less abundant. Perhaps the new horned artiodactyl, *Drepanomeryx*, presenting a type of horn-core not hitherto known in North America, and a mastodon apparently allied to *Mastodon americanus*, may be regarded as belonging to this category. The conception of old and new faunal elements should not be unduly emphasized, because, as our exploration of the Snake Creek beds plainly shows, we do not yet know the extreme upward range in time of a number of Upper Miocene genera and can merely say of the new, supposedly Pliocene, forms that this is their first appearance. A suggestion regarding climatic conditions may be found in the presence of crocodiles and huge land tortoises, the latter rivalling in size those of the Galapagos Islands, indicating, perhaps, that the approaching chill of glacial times had not yet exterminated these cold-blooded types.

DESCRIPTIONS OF NEW GENERA AND SPECIES.

AELURODON sp. compare WHEELERIANUS?

The left ramus of a lower jar with p_4 and m_1 and alveoli for the remaining teeth (No. 12068 Princeton University Geological Museum, collecting locality 1000C) is referable to an *Aelurodon* of about the size of *A. wheelerianus*, from the type of which it differs in the greater length of p_4-m_1, the shorter jaw and the closer crowding of the premolars. It is either too small or too large to be referred definitely to any of the described species of *Aelurodon*, but is hardly complete enough to be made a new specific type.

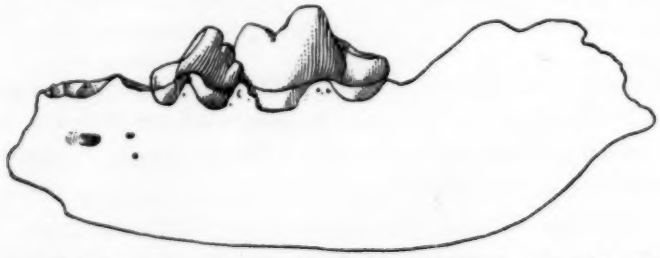

FIG. 1. *Aelurodon* sp., compare *wheelerianus?*, left ramus, side view, No. 12068, two thirds natural size.

?AMPHICYON sp. indesc.

A huge canid, possibly an undescribed species of *Amphicyon*, is represented in the Princeton Snake Creek collection by the right

ramus of the lower jaw, an ulna and some other bones, of which the lower jaw (No. 12078 Princeton University Geological Museum, collecting locality 1000C) is here figured to give some idea of its size and proportions. The fragment retains alveoli for the canine, four double-rooted premolars and the sectorial molar. The first and second premolars are separated from each other by a short space, and from the canine and first molar by long diastemata, whlie the rest of the dentition is in close series.

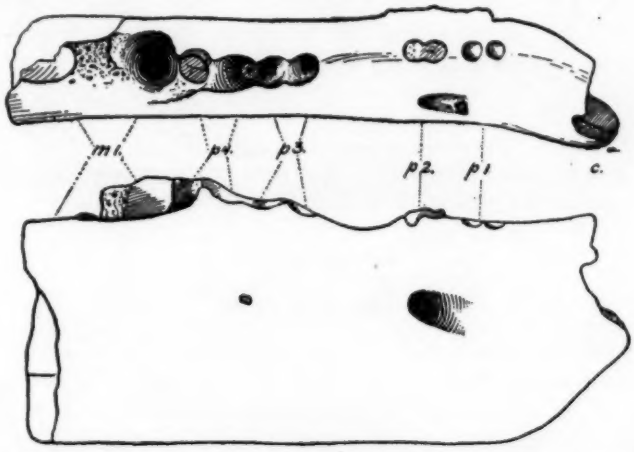

FIG. 2. *?Amphicyon* sp. indesc., No. 12078, right ramus of the lower jaw, side and top views, one half natural size.

BRACHYPSALIS OBLIQUIDENS sp. nov.

Type No. 12070 Princeton University Geological Museum, collecting locality 1000C, the left ramus of the lower jaw with p_2-m_2 and alveoli of the canine and first premolar (Fig. 3). This is a decidedly larger, deeper-jawed, heavier-toothed species than *Brachypsalis pachycephalus,* with the anterior premolars placed very obliquely to the tooth-row and all the teeth closely crowded. It is of about the same size as *Paroligobunis* (*Brachypsalis*) *simplicidens* from the Lower Harrison, but has a larger second molar, a slightly larger sectorial and more closely crowded, obliquely placed anterior premolars.

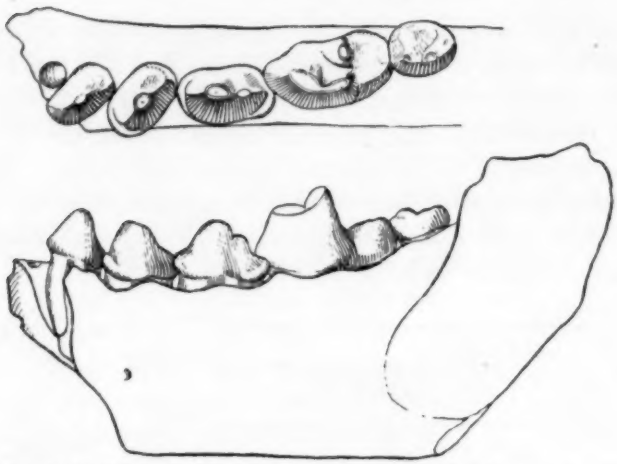

FIG. 3. *Brachypsalis obliquidens,* lower jaw, type specimen, external view, and crown view of the teeth, both natural size, No. 12070.

MEASUREMENTS.

Length, p_1-m_3	56
Length, p_1-p_4	32
Length, m_1-m_3	26
p_3	9¾ × 6
p_2	11 × 7
p_4	13 × 7¾
m_1	17½ × 9
m_2	9 × 7½

MARTES GLAREÆ sp. nov.

Type No. 12071 Princeton University Geological Museum, collecting locality 1000C, the left ramus of the lower jaw with p_3, $_4$ and m_1 and alveoli of the canine, p_1, $_2$ and m_2 (Fig. 4). In size, close to the type of *M. ogygia* Matthew from Horizon E of the Upper Miocene of Colorado, but differing in the presence of p_1 (represented by a small alveolus), the slightly larger, more laterally compressed p_3 which lacks a posterior accessory cusp as in *ogygia* and some existing species, the presence of this cusp on p_4 (only slightly less developed than in specimens referred to *M. americana* with which comparison was made), and the larger heel on m_1. In both *M. ogygia* and *M. glareæ* the metaconid or m_1 is more sharply separated than in specimens referred to *M. americana* which I have

examined. *M. minor* Douglass from near the bottom of the Lower Madison Valley Loup Fork beds and *M. furlongi* Merriam from the Thousand Creek beds, Thousand Creek, Nevada, are smaller forms, while *M. parviloba* Cope from the Middle Miocene of Colorado is a larger animal than either *ogygia* or *glareæ*, and *M.* (*Putorius*) *nambianus* from the New Mexican Loup Fork has a shorter jaw than either of the species just mentioned. It is approached in size by specimens in the Princeton University osteological collection referred to *M. americana*, but differs, in addition to the characters cited above, in the larger heels and heavier anterior basal ledges on the premolars and the greater degree of lateral compression of these teeth.

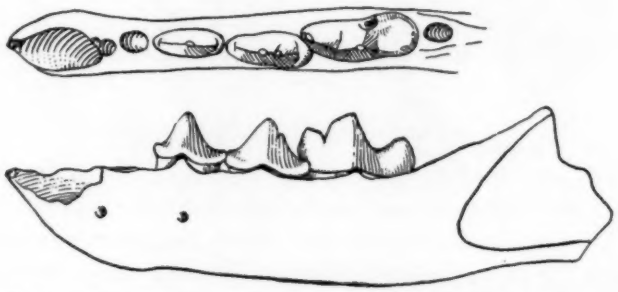

FIG. 4. *Martes glareæ*, lower jaw, type specimen, external view and crown view of the teeth, twice natural size, No. 12071.

MEASUREMENTS.

Length, $p_{\bar{3}}$-$m_{\bar{1}}$	17
$p_{\bar{3}}$	5 × 2
$p_{\bar{4}}$	5.8 × 2.1
$m_{\bar{1}}$	8 × 3

PSEUDAELURUS near INTREPIDUS Leidy.

The presence in the Snake Creek fauna of a cat not far removed from *Pseudaelurus intrepidus* Leidy is indicated by a jaw fragment No. 12081 Princeton University Geological Museum, collecting locality 1000C, which agrees with Leidy's type fairly closely in the dimensions of the jaw, but differs in having the teeth a little smaller and the posterior accessory cusps and heels on the premolars less strongly developed. A further difference, which may be of little importance, is found in the position of the mental foramina which,

in *P. intrepidus*, occur below the alveolus for p_2 and the anterior root of p_3 respectively, while in the Snake Creek form they lie below the posterior root of p_3 and a little in front of its anterior root. The alveolus for p_2 is quite small and must have supported a minute vestigial single-rooted tooth.

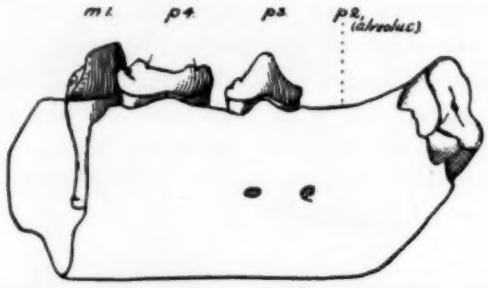

FIG. 5. *Pseudælurus* near *intrepidus*, lower jaw, right side, No. 12081, natural size.

FELID gen. et sp. indet.

A large non-machærodont cat is represented by a fragment of the left mandibular ramus No. 12073 Princeton University Geological Museum, collecting locality 1000A, in which are preserved the alveoli for three incisors, the base of a very large laterally flattened canine and alveoli for two premolars, a very small single-rooted p_2 and a large double-rooted p_3. The chin is not flanged but the symphysial region projects a short distance below the level of the lower border of the jaw.

FIG. 6. Indeterminate felid, fragment of the lower jaw, left side, lateral view, No. 12073, natural size.

Edentate (?Megalonychid).

A single imperfect claw, "definitely recognizable as of Gravigrade relationship" and comparable "with some of the smaller Megalonychidæ" is reported by Matthew and Cook from the Snake Creek beds. Further confirmation of the presence of edentates is found in a navicular bone (Fig. 7) unquestionably of a Gravigrade, about two thirds the size of the navicular of *Megalonyx jeffersoni* and of much the same general type, obtained by the Princeton expedition at collecting locality 1000C.

Fig. 7. Navicular bone of gravigrade edentate, upper and lower views, two thirds natural size, No. 12079.

Mastodons.

Mastodons of two types are indicated in the Princeton Snake Creek collection by several complete molars, most of which seem

Fig. 8. *Gomphotherium* sp., right last lower molar, one half natural size. No. 12064 Princeton University Geological Museum, collecting locality 1000 A.

referable to *Gomphotherium,* with a last lower molar carrying four cross-crests and a heel and having the intervening valleys blocked by large accessory tubercles (Fig. 8). A smaller form (Fig. 9), also with four cross-crests and a heel in $m_{\overline{3}}$, has the summits of the crests much more acute than in the *Gomphotherium* type and the valleys as free from accessory tubercles as in the corresponding tooth of *Mastodon americanus* to which the Snake Creek form is, possibly, related. Accessory ridges occur on the front and rear of the external half of each crest, but are no more strongly developed than in *M. americanus.* The last lower molar of the latter does not decrease in width posteriorly as rapidly as does the tooth here considered, but in other respects they closely resemble each other. The crown is unworn and there is no trace of cement.

FIG. 9. *?Mastodon* sp., left last lower molar, two thirds natural size. No. 12116 Princeton University Geological Museum, collecting locality 1000 A.

INCERTÆ SEDIS.

A fragment of the left ramus of a lower jaw, No. 12091 Princeton University Geological Museum, collecting locality 1000A, has not been determined generically (Fig. 10). The specimen shows alveoli for two incisors and part of the root of a third. The first alveolus is very large and shallow and the second narrow and deep. The fragment of the root of the third incisor is strongly compressed

laterally and almost quadrangular in cross-section. These are followed after an intervening space, throughout which the dental margin of the ramus is broken, by a small, single-rooted, conical

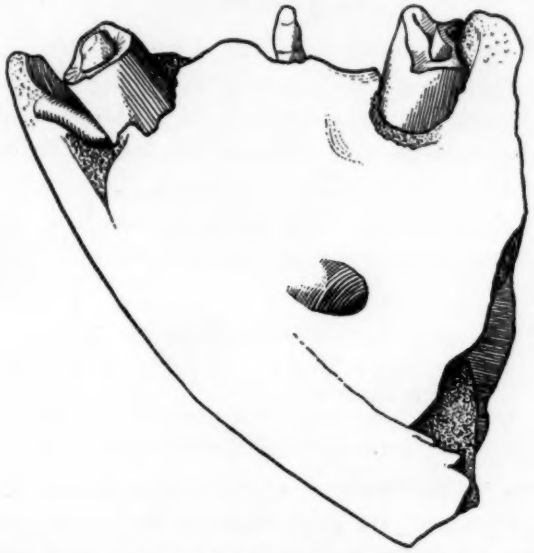

FIG. 10. *Genus incert. sed.* No. 12091, a fragment of the left ramus of the lower jaw, outer side, two thirds natural size.

tooth with enamel-covered crown. A second diastema, with undamaged margin, separates this tooth from the anterior root of a large, evidently deciduous tooth, beneath which, in the jaw, is the cavity for a still larger permanent tooth. The root of $i_{\overline{3}}$ seems to have projected into this cavity where it has been truncated by absorption. The symphysis is firmly fused, a small portion of the right ramus adhering to the left one and showing part of the alveolus for the first incisor of the right side.

MEASUREMENTS.

$i_{\overline{1}}$, anteroposterior diameter of alveolus (approximate)	23
$i_{\overline{1}}$, transverse diameter of alveolus (approximate)	18½
$i_{\overline{2}}$, anteroposterior diameter of alveolus (approximate)	6½
$i_{\overline{2}}$, transverse diameter of alveolus (approximate)	9
$i_{\overline{3}}$, anteroposterior diameter of root	16
$i_{\overline{3}}$, transverse diameter of root	9
?c, anteroposterior and transverse diameters	6

Length of diastema ?c-dp	15
Depth of jaw below middle of dp	107
Thickness of jaw at level of mental foramen	45

ARCHÆOHIPPUS sp.

A small short-crowned $p_{\overline{2}}$ of the right side (No. 12128 Princeton University Geological Museum, colecting locality 1000B) agrees in structure with the upper teeth of *Archæohippus* in the complete union of the metaloph and ectoloph, the distinct protoconule, and open prefossette, there being no anterior median enamel fold on the wall of the metaloph. This horse has not been reported hitherto from any horizon above the Middle Miocene Mascall beds of Oregon.

MEASUREMENTS.

Greatest anteroposterior diameter	13
Greatest transverse diameter	13

PRONOMOTHERIUM SIOUENSE sp. nov.

Type No. 12057 Princeton University Geological Museum, colecting locality 1000C, the right ramus of the lower jaw with $p_{\overline{1}}$-$m_{\overline{3}}$ and alveoli of $i_{\overline{1}}$-c. Tooth crowns worn. A smaller form than

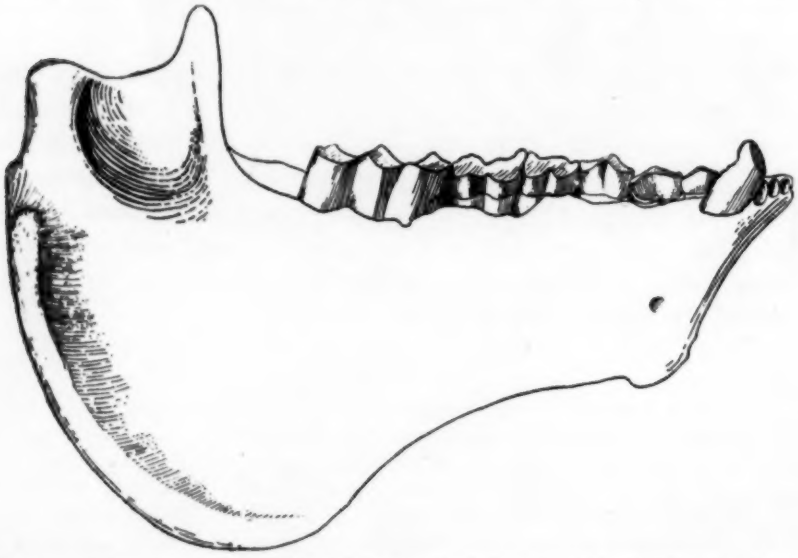

FIG. 11. *Pronomotherium siouense*, lower jaw, type specimen, external view, × ½.

either of the better known Miocene species (*P. laticeps* and *P. altiramis*) from which it can be separated by differences both in size and proportions.

MEASUREMENTS.

Length of jaw	208
Depth beneath p_3	57
Depth beneath m_1	53
Depth beneath back part of m_2	55
Depth beneath last lobe of m_3	94
Depth coronoid to angle	147
Length lower dental series	132+
Length lower premolar-molar series	125
Length lower premolar series	50
Length lower molar series	75

PROTOLABIS PRINCETONIANUS sp. nov.

Type No. 12053 Princeton University Geological Museum, collecting locality 1000C, an uncrushed skull, sand-worn on the right side which lay uppermost, associated with most of the left ramus of the lower jaw, a fragment of the right ramus and an ulna-radius. The limb bone belongs to a camel but may not pertain to the same individual as the skull. In size, there is close agreement with *Protolabis longiceps* Matthew from the Colorado Loup Fork (Pawnee Creek beds), but a comparison of the two skulls brings out certain minor differences which appear to be of specific value. In *P. princetonianus,* the anterior facial vacuity is far larger than in the Colorado form, with the premaxillæ extending above it and reaching farther back than in that species. Another marked difference appears in the absence of an abrupt constriction of the face in front of p^2 which produces the sudden incurving of the tooth row seen in *longiceps* in contrast with the gradual taper of this region in the Princeton specimen. Various differences in dental structures are also noticeable, as follows: p^2 thicker and heavier and p^3 less reduced and with posteroexternal groove deeper than in *P. longiceps;* p^4, if anything, larger in *longiceps* than in *princetonianus.* Lower premolars somewhat less reduced and molar crowns somewhat higher, and posteroexternal groove in p_4 placed nearer hinder end of tooth than in *longiceps;* p_3 with distinct anterior cusp which is absent in the last named form.

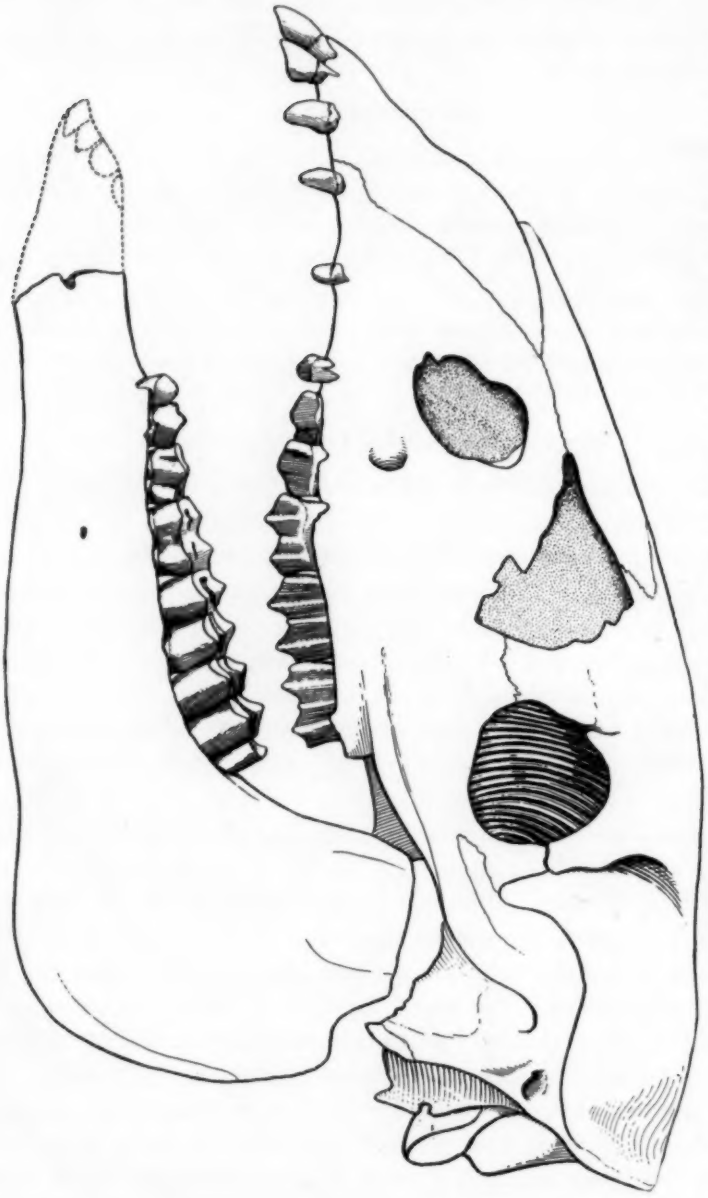

FIG. 12. *Protolabis princetonianus*, type specimen, left side of skull and lower jaw, one half natural size, No 12053. Symphysis of lower jaw restored in outline from another specimen of the same species.

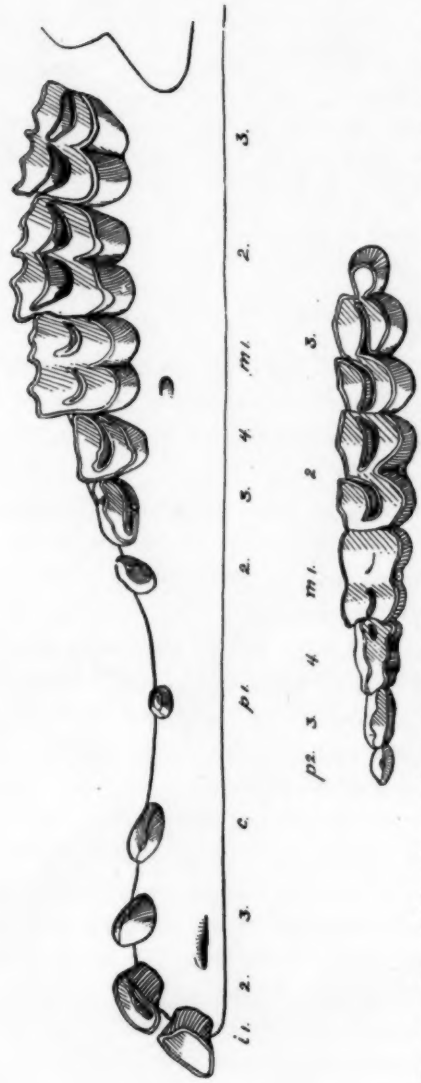

FIG. 13. *Protolabis princetonianus*, type specimen, crown view of the upper and lower teeth, two thirds natural size, No. 12053.

PROC. AMER. PHIL. SOC., LIV. 217, G, PRINTED JULY 6, 1915.

MEASUREMENTS.

Total length of skull (incisors to condyles)				310
Length, i_1-m^3	right	195,	left	199
Length, p^1-m^3	right	121,	left	127
Length, premolar series	right	59½,	left	64
Length, diastema behind i_3	right	11,	left	9
Length, diastema behind c		18		
Length, diastema behind p^1	right	18,	left	20
Length, lower premolar-molar series				106
Length, lower premolars				33
Depth of jaw in front of p_2				32
Depth of jaw below middle of m_2				40
Length of radius				195
Width of radial shaft at middle				24

DREPANOMERYX FALCIFORMIS gen. et sp. nov.

Type No. 12072 Princeton University Geological Museum, collecting locality 1000C, a horn of the left side (lacking tip) and the basal portion of the right horn (Figs. 14, 15).

Frontal not cavernous at base of horns. Horns non-deciduous, rising immediately above upper posterior margin of orbit, sloping backward and upward and at the same time curving inward, at base almost circular, but flattening upward in the transverse plane extending backward and inward from the orbits, producing a scimitar-like structure which curves inward toward its fellow on the opposite side. Horns without any suggestion of twist, proximal half comparatively smooth and free from pits and irregularities, such faint groovings as are present being longitudinal. Distally, and especially toward the outer margin, the surface is rough and pitted, but this seems to be due to sand-blasting or water-wear which has destroyed the outer table of bone. A broad groove is visible throughout the central portion of the shaft on the posterior aspect of the horn. Horns solid throughout, the surface, texture resembling that of the Pronghorn Antelope.

No teeth have been found in the Snake Creek beds which can be referred, even provisionally, to the new form, unless those which have been correlated by Matthew and Cook with their *Neotragocerus improvisus,* and the lower jaw described under that genus in the present paper, should be associated with the curved type of horn found in *Drepanomeryx* rather than with the straight horns of *Neotragocerus.*

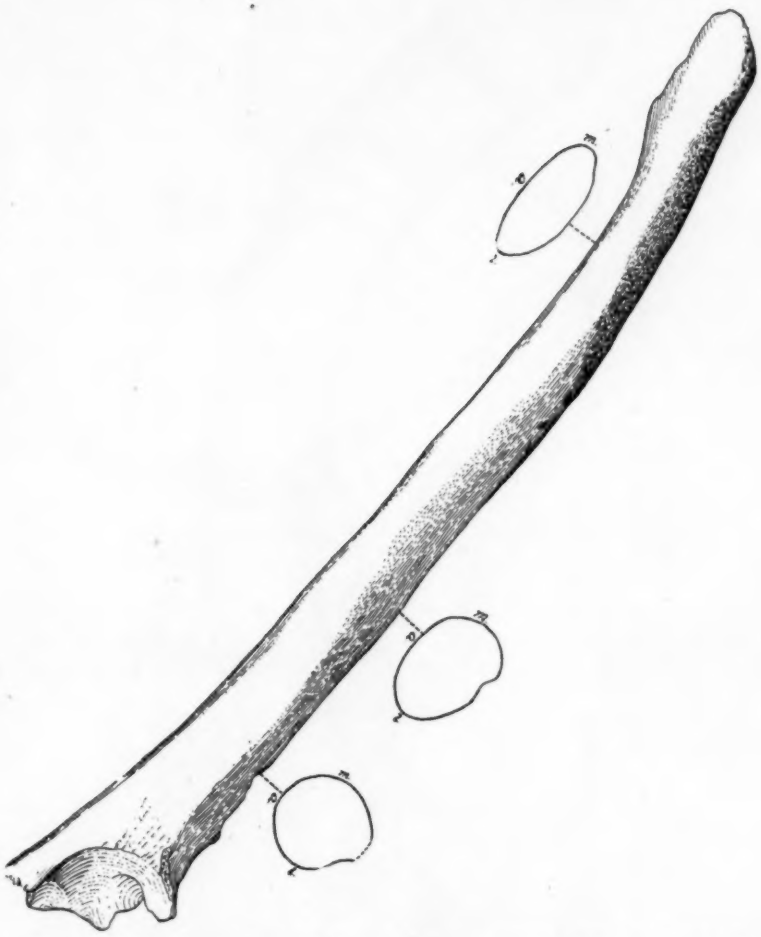

FIG. 14. *Drepanomeryx falciformis,* type specimen, lateral aspect of the left horn, one half natural size, No. 12072. *l, m, a* in cross-sections = lateral, median and anterior margins.

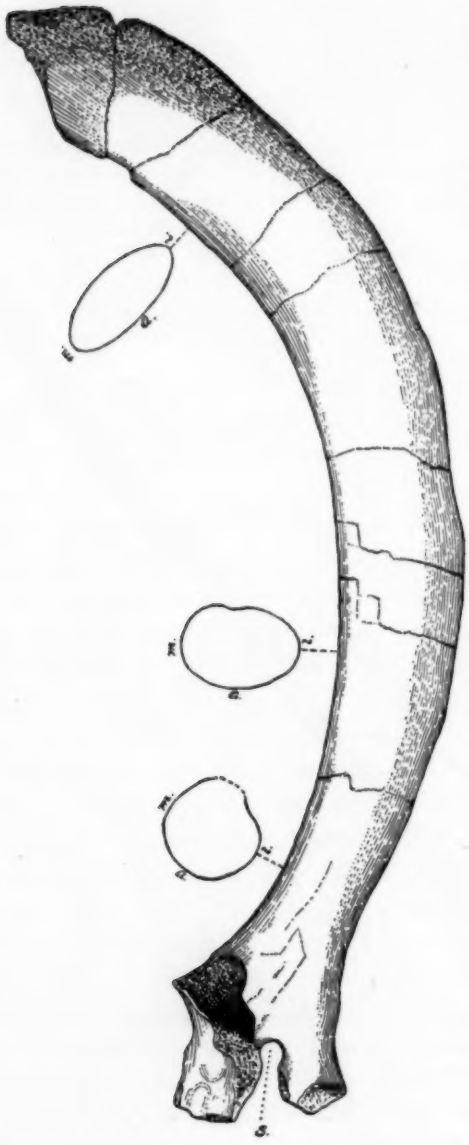

FIG. 15. *Drepanomeryx falciformis*, type specimen, anterior aspect of the left horn, one half natural size, No. 12072. *l*, *m*, *a* in cross-sections = lateral, median and anterior margins; *s*, supraorbital foramen.

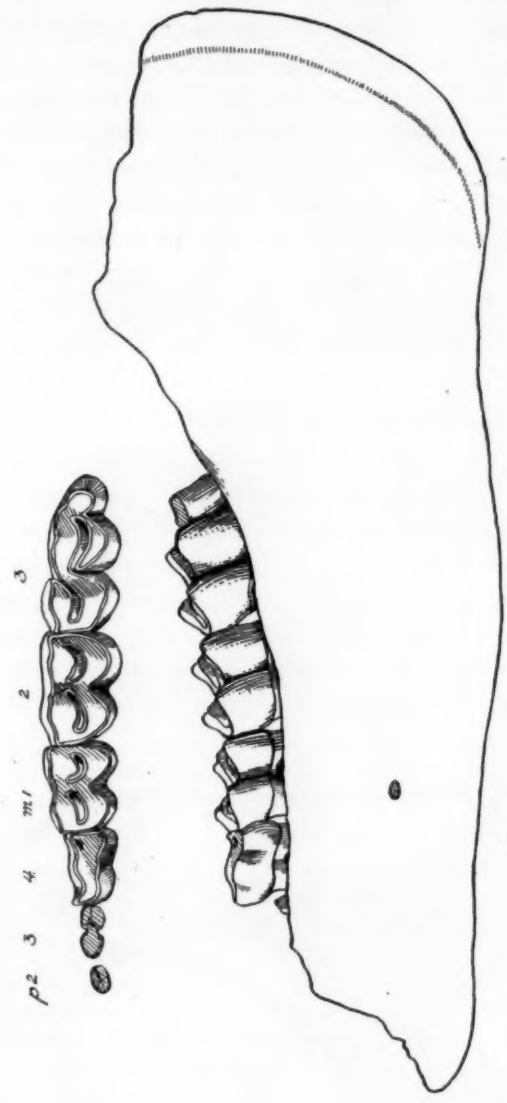

FIG. 16. *?Neotragocerus improvisus*, left ramus of the lower jaw, side view, and crown view of the teeth, two thirds natural size, No. 12106.

NEOTRAGOCERUS IMPROVISUS Matthew and Cook.

The left ramus of a lower jaw (No. 12106 Princeton University Geological Museum, collecting locality 1000C), which is doubtfully referred to this form, supports brachyodont molars which register almost exactly with the upper teeth selected by Matthew and Cook as paratypes of *Neotragocerus improvisus*. With the discovery in the Snake Creek beds of scimitar-shaped horns (*Drepanomeryx* gen. nov.), presumably of antelope-like animals, correlation of the straight *Neotragocerus* type of horn with jaw fragments, both upper and lower, supporting short-crowned teeth becomes even more provisional than it has hitherto been, since either type of horn is large enough to fit an animal of the size of those to which the jaws belonged.

DROMOMERYX WHITFORDI sp. nov.

Type No. 12054 Princeton University Geological Museum, collecting locality 1000C, an associated pair of horn bases (Fig. 17). Paratype No. 12086 Princeton University Geological Museum, the right ramus of a lower jaw, unassociated with the horns but from the same collecting locality (Fig. 18). The species is named in honor of my assistant in the field, Mr. A. C. Whitford. Horn bases about one third wider than in *D. borealis,* with the posterior upper corner of the wing-like expansion at the base of the horn

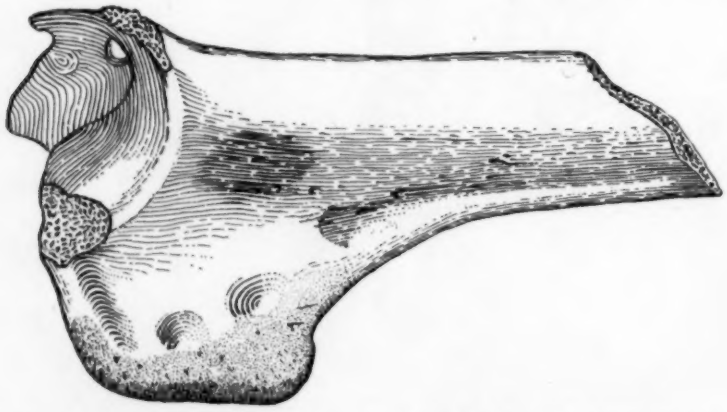

FIG. 17. *Dromomeryx whitfordi,* type specimen, base of left horn, outer side, two thirds natural size. One of an associated pair, No. 12054.

sharply angular instead of a flowing curve as in *D. borealis*. Lower jaw of practically the same size as in that species and dentition not specifically separable therefrom.

The inclusion in the same new species of type material not found associated is most unsafe. In this instance it seems justifiable because the collections made by two parties (American Museum and Princeton) have shown the presence of but one species of *Dromomeryx* in the Snake Creek beds, the so-called *Palæomeryx* of Matthew and Cook being undoubtedly *Dromomeryx* and not separable from the new species here described.

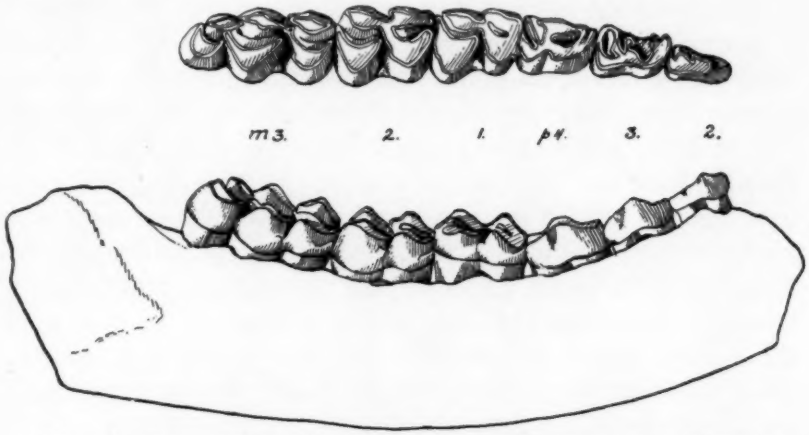

FIG. 18. *Dromomeryx whitfordi*, paratype, right ramus of the lower jaw, side view, and crown view of the teeth, two thirds natural size, No. 12086. The distance from p_2-m_3 is a little greater in the crown view, owing to elimination in the drawing of the fore-shortening due to curvature of dental series.

MEASUREMENTS.

Width of horn-base across middle of wing-like process	73
Anteroposterior diameter of beam three inches above base	30
Transverse diameter of beam three inches above base	25
Legnth, p_2-m_3 measured as chord of arc	109
Length, m_1-m_3	67½
p_2, anteroposterior 12⅛, transverse	6⅔
p_3, anteroposterior 14½, transverse	10
p_4, anteroposterior 15, transverse	10½
m_1, anteroposterior 17, transverse	14
m_2, anteroposterior 19½, transverse	15
m_3, anteroposterior 31, transverse	15
Depth of jaw beneath p_3	31
Depth of jaw beneath m_3	31½

PRINCETON UNIVERSITY, April, 1915.

EXPLORATIONS OVER THE VIBRATING SURFACES OF TELEPHONIC DIAPHRAGMS UNDER SIMPLE IMPRESSED TONES.

By A. E. KENNELLY and H. O. TAYLOR.

(*Read April 22, 1915.*)

The following research was carried on, at the Massachusetts Institute of Technology, under an appropriation from the American Telephone & Telegraph Co. during the year 1914–1915. The experimental work was carried out at Pierce Hall, Harvard University.

The object of the investigation was to explore the amplitude of the small harmonic vibrations of a circular diaphragm of telephonic type, clamped around the edge, and to compare the observed values with those which had been already deduced mathematically. Hitherto, so far as we are aware, the amplitude of vibration of a telephone diaphragm has been determined only at one point on the surface, usually the center,[1] The observations here reported differ from those heretofore obtained, in extending over the entire surface of the diaphragms.

Exploring Apparatus.

The exploring device, or "explorer," devised and constructed for this research, consists of a tiny triangular mirror fastened to a little phosphor-bronze stirrup strip, and having its point applied, by means of torsion in the strip, to the surface of the vibrating diaphragm at the point to be explored. The natural frequency of the mirror being much greater than that impressed on the diaphragm, the mirror is able to follow the vibrations of the latter, without breaking out of contact. The pressure exerted by the mirror on the diaphragm is so small as not materially to affect the diaphragm's vibration. A beam of light, reflected from the mirror on to a translucent scale, was thus set into vibrations synchronous with, and

[1] See Appended Bibliography, Nos. 2, 4, 7, 9 and 10.

proportional to, the vibrations of the diaphragm at the point of contact.

The vibration explorer is shown in side elevation at Fig. 1, in top view at Fig. 2, and in section, through center of the diaphragm, in Fig. 3. A fairly massive rectangular brass frame holds a plate sliding in grooves. The crank at the bottom of Fig. 1 controls this

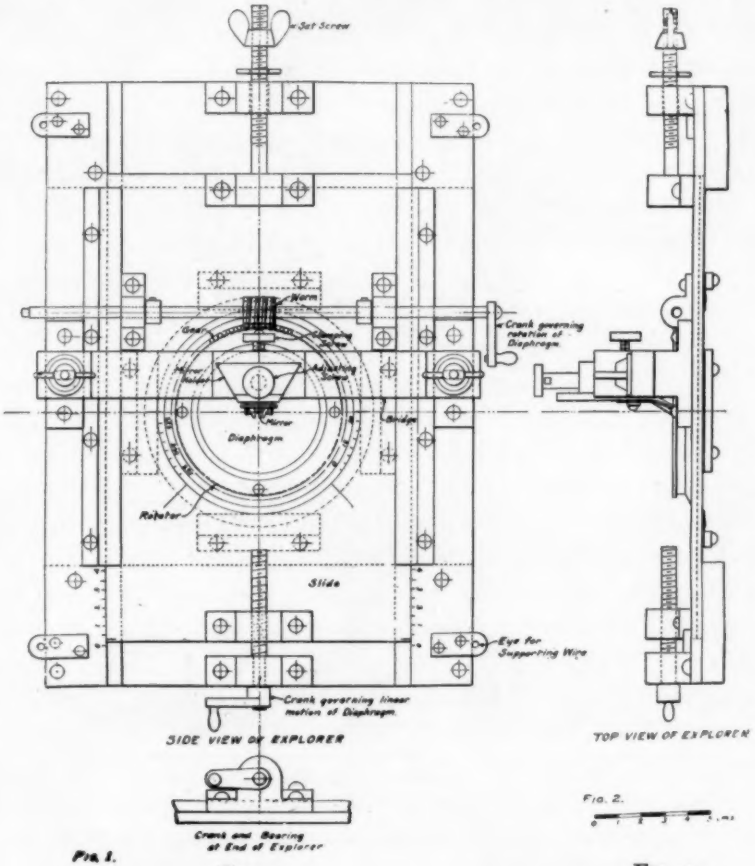

Fig. 1. Fig. 2.

sliding motion, with the aid of the set screw at the other end. At the center of the sliding plate is a circular frame, into which is clamped the diaphragm to be tested. The circular frame can be rotated in its own plane by means of the crank at the right hand of Fig. 1.

A stout brass bridge is fastened to the sides of the rectangular frame. At the center of this bridge is the mirror-holder shown in detail at Fig. 3. The mirror-holder slides in a groove provided in the bridge, and is clamped therein by a clamping screw S. A fine-motion screw M is also provided, for adjusting the position of the mirror. One turn of M advances the mirror 0.8 mm. (1/32 inch). By means of an auxiliary mirror fastened beneath the top of the screw M, the angle through which the screw is advanced may be

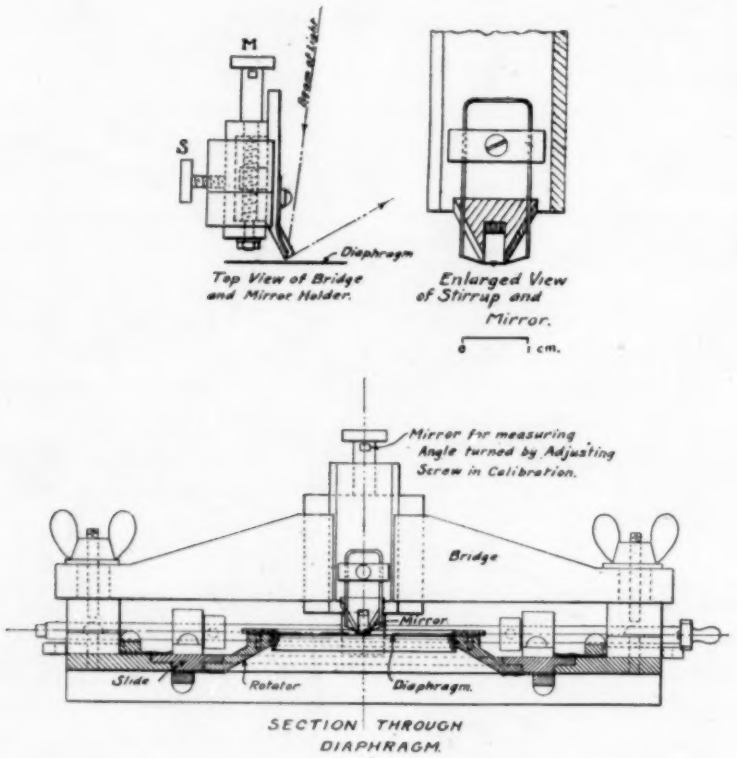

FIG. 3 APPARATUS FOR EXPLORING THE VIBRATION OF DIAPHRAGMS.

measured, for calibrating the indications of the instrument. Adjustment can be made to 1 deg. of rotation, or 2.2 μ; i. e. $\left(\frac{0.8}{360} \text{ mm.}\right)$ assuming that backlash is guarded against.

The construction of the apparatus is such, that the mirror is held at all times at the center of the brass rectangular frame; while by means of the two crank adjustments, the diaphragm to be explored can be moved so as to bring any part of its surface beneath the mirror. With the aid of the scales of distance and angle shown in Fig. 1, the position of the mirror with respect to the diaphragm can be adjusted and read off to polar coördinates (r, θ). The motion in r is controlled by the crank at the bottom, to 0.1 mm.; while the angular motion in θ is controlled by the crank at the side, to 1°, or less if desired. The slide is held in position by flat springs, attached to the rectangular frame, so as to keep the motion of the slide confined to its own plane. A similar construction is used with the circular frame. It is important that the plane of the diaphragm shall not be disturbed when either crank is operated. The weight of the whole explorer is 4.63 kgs. (10.2 lbs).

A magnified view of the mirror, and its stirrup frame, is shown at the top of Fig. 3. The mirror, of silvered glass, about 0.1 mm. thick, is cut in the shape of an equilateral triangle, about 1 mm. in length of side. One vertex of the mirror is applied to the surface of the diaphragm, and the mirror is fastened with sealing wax across a thin phosphor-bronze strip. This strip is approximately 3 mm. long between abutments, 0.02 mm. wide, and 0.013 mm. thick. The weight of the mirror is about 1 milligram, without varnish or sealing wax. Its natural frequency of vibration, as obtained photographically, is about 2,500 $\sim$. These little mirrors are apt to break off the stirrup strip; so that they have to be renewed and recalibrated occasionally. The pressure exerted on the diaphragm by the point of the mirror, as measured by an auxiliary test, is approximately 200 dynes (204 mgm. wt.). A pressure of this order seems to be desirable, so as to obtain a natural frequency of 2,500 $\sim$. If, however, explorations are confined to lower diaphragm frequencies, the natural frequency of the explorer mirror, and its pressure on the diaphragm, may be reduced accordingly.

The diaphragm to be explored is 5.4 cm. in diameter, and is placed in the circular frame. It is clamped tightly into this frame, with the ring clamp shown in Fig. 3, which had a radius of 2.62 cm. when no auxiliary clamping rings were used. The vibration explorer

is then suspended on wires from the ceiling, or other convenient support, in order to suppress building vibrations of high frequency; so as to support the explored diaphragm in a vertical plane. The mirror-holder is then advanced towards the diaphragm, and clamped by screw *S*. The mirror is now carefully brought into contact with the surface of the diaphragm by adjusting screw *M*. A picture of the explorer is presented in Fig. 4. The suspension wires *ww*,

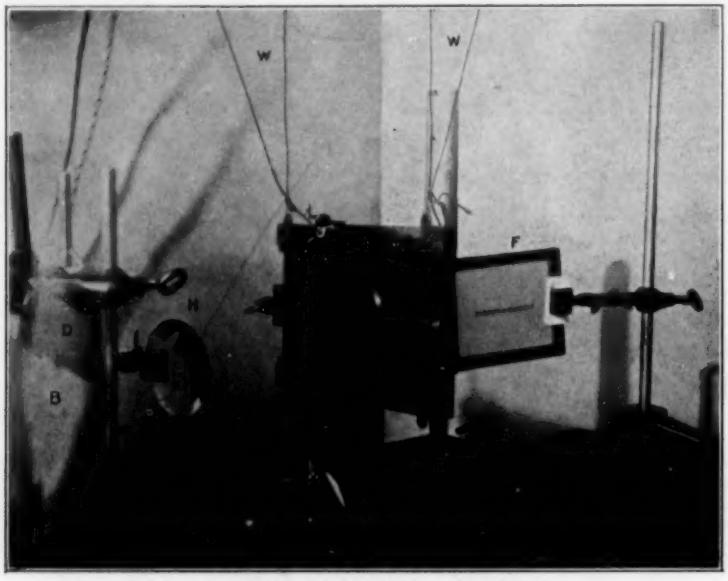

FIG. 4. Vibration Explorer in Booth.

support the instrument. The condensing and focusing lens *H* throws a narrow arc-light beam upon the exploring mirror, which reflects it on to the translucent graduated screen *F*. With the diaphragm at rest, the spot on this screen is a narrow, sharp, vertical, luminous strip. When the diaphragm is set in vibration, the mirror in contact with it vibrates synchronously, and the spot is spread into a luminous band, the limits of which are easily read on the graduated translucent scale. If the motions of diaphragm and mirror are simple harmonic motions, the luminous band shows no discontinuities of intensity. If, however, there is a complex harmonic motion in the diaphragm, the luminous band will show bright and dark

patches, either quiescent, or with beats. By means of the optical magnification of amplitude that can be effected with such an exploring mirror and scale, diaphragm vibrations of amplitude 0.1 μ (*i. e.*, 10^{-5} cm.), or less, can be observed; although the precision of measurement falls off considerably, for a diaphragm amplitude below 0.5 μ (half a micron).

Optical System.

The optical system employed with the vibration explorer is diagrammatically indicated in Fig. 5. The stereopticon arc-lamp *A* throws a powerful condensed beam of light on the pinhole *B*, in a brass vertical screen. A set of small powerful collimating lenses *C*

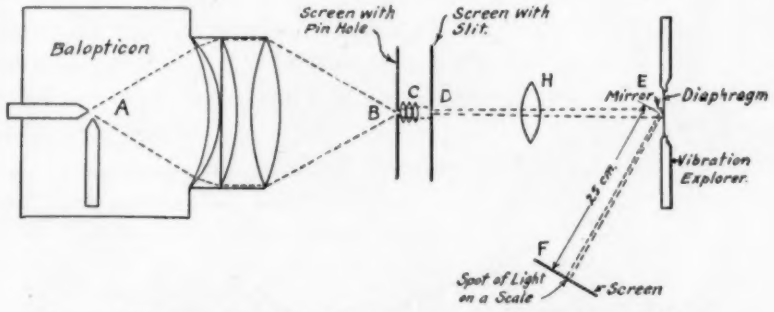

Fig. 5. Diagram of Optical System used with Vibration Explorer.

throws the nearly paralleled beam through the screen and slit *D*, as well as the focussing lens *H*, on the exploring mirror *E*, whence it is reflected to the translucent screen *F*, at a convenient distance, in this case 25 cm. An image of the slit in screen *D* is then sharply focused at *F*. In Fig. 6, it is indicated geometrically that the amplitude c of the diaphragm's displacement is equal to the continued product of the observed amplitude d of the luminous band, the ratio of l (the radius arm of the mirror), to $2L$ the double distance of the mirror from the screen, and the cosine of the angle ϕ between the radius arm of the mirror and the plane of the diaphragm. In order to avoid frequent changes in ϕ, it is desirable to keep constant the zero of the spot at the center of the graduated scale *F*, and with it the contacting angle of the mirror. The numerical

expression $M = 2L/l \cos \phi$ may be called the *magnification-factor* of the explorer. As ordinarily employed, $2L = 50$ cm., $l = 0.05$ cm., $\phi = 45°$ approximately, or $\cos \phi = 0.7$; so that $M = 1{,}400$ approximately, varying in different sets of measurements between

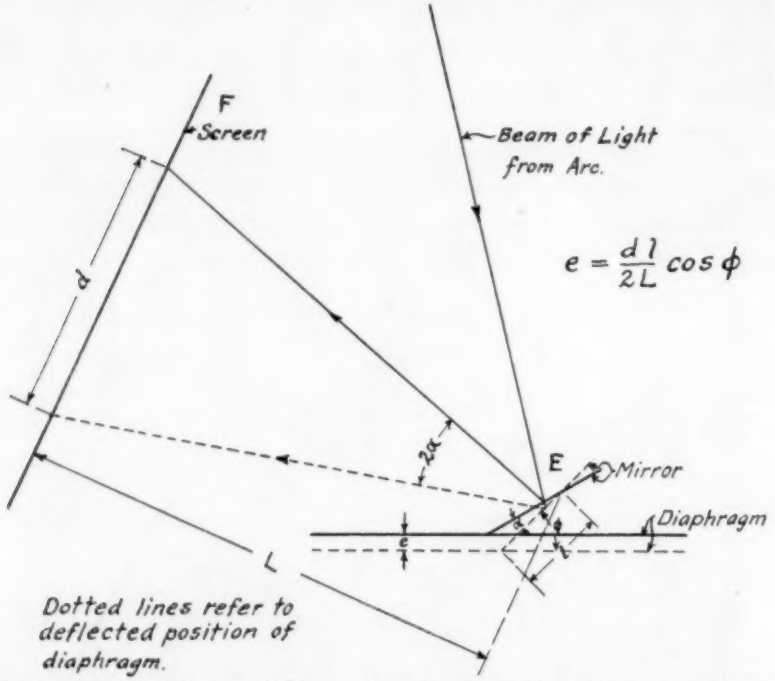

FIG. 6. Diagram Showing Action between Mirror and Diaphragm in Explorer.

800 and 1,500. Had it been necessary, this magnification-factor might have been considerably increased, by increasing the distance L between mirror and scale; although the reduction in luminous-spot intensity, at increasing ranges, prevents the precision of the observations from increasing in the same proportion as the magnification-factor. At $L = 25$ cm., the amplitude of luminous band could be read to 0.1 mm. on the graduated translucent scale F.

SOURCE OF DIAPHRAGM VIBRATIONS.

Two sources of vibrations were used in different series of tests, (1) acoustic, (2) electromagnetic.

(1) The acoustic vibrations were supplied from one of a series of small organ-pipes, giving fairly simple musical tones between C_2 of 128 ~, and C_6 of 2,048 ~. The organ-pipe selected was mounted vertically in a block on the table, at the back of the vibration explorer, and supplied with air at constant pressure (about 18 cm. of water) from a pneumatic tank. The whole apparatus was placed inside a sound-damping wooden-frame booth (274 cm. × 183 cm. × 214 cm. high), lined on the inside with hair-felt, 2.5 cm. thick, surfaced with thin cloth. The observer, after turning on the air to the organ-pipe, observed the amplitude of the luminous band on the translucent screen *F*, Figs. 4 to 6, as the mirror was applied to different successive points on the diaphragm.

(2) The clamping ring of the diaphragm in the explorer was chosen of such dimensions that a standard telephone receiver could be substituted for it. In this case, a steel diaphragm had to be employed. The telephone was then operated by a feeble measured alternating current (2.0 milliamperes) obtained from a Vreeland mercury-arc oscillator having a frequency adjustable, by successive steps, between 430 ~ and 2,500 ~.[2]

Exploration with Diaphragm No. 1.

Diaphragm No. 1 was a telephone-receiver diaphragm of steel, japanned on one side. Its dimensions are given in Table III. The diaphragm was clamped, around the boundary, between opposing circular knife-edges.

TABLE I.

Vibration Amplitudes over Diaphragm No. 1, at Frequency 608 ~, for Nine Different Azimuths θ, and Seven Different Radial Distances r.

Radial Distance, r Cm.	Vibration Amplitude Observed with Explorer (Microns) at Different Azimuths θ.								
	0° μ	40° μ	80° μ	120° μ	160° μ	200° μ	240° μ	280° μ	320° μ
−0.08	13.8	12.1	11.7	14.0	13.4	10.4	10.8	13.3	12.0
+0.31	12.7	10.9	11.3	12.3	12.7	9.7	10.6	12.6	11.6
+0.69	9.7	8.0	8.9	10.4	10.4	8.1	8.8	11.5	9.5
+1.06	6.6	5.9	6.4	6.8	7.0	6.2	6.4	7.1	6.8
+1.44	4.2	3.6	4.2	4.7	4.5	4.1	4.2	4.9	4.3
+1.82	2.5	2.2	2.1	2.5	2.5	2.3	2.4	2.5	2.4
+2.20	0.9	0.8	0.9	0.9	0.9	0.7	0.7	0.9	0.8
+2.54	0	0	0	0	0	0	0	0	0

[2] See Bibliography No. 5.

An organ-pipe of D_4^* (608 ~) was set up with its lip 5 cm. from the back of the diaphragm. An exploration was then made over the surface, at points differing by 40° in azimuth θ, and at successive increases in radius of about 3.3 mm. (7 steps in r, and 9 steps in θ, or 63 observations in all.) The preceding table gives the observed amplitudes of vibration deduced from the scale-deflections, with a magnification factor of $M = 1{,}180$.

It will be seen from the above table, that at any particular radius r, measured from the center of the diaphragm, the amplitudes at varying azimuths θ are substantially equal. The irregularities are small, but nevertheless seem larger than can be accounted for by errors in observations and are, perhaps, due to irregularities in the diaphragm. Fig. 7 shows the contour lines of vibration-amplitude in microns, the maximum amplitude being at or near the center, and amounting to 14 μ. Such vibration amplitudes are larger than were usually obtained, and were specially reinforced in this case, in order to secure large deflections. It will be seen from the contour diagram, that the diaphragm was vibrating with its fundamental or gravest mode of motion; *i. e.*, a motion to-and-fro as a whole, without either nodal diameters or nodal circles. It is known that a circular diaphragm, clamped at the edge, is capable of vibrating in an indefinitely large number of ways, according to the

FIG. 7.

VIBRATION AMPLITUDE
IN MICRONS.
608 ∿
DIAPHRAGM No. I.

FIG. 8.

VIBRATION AMPLITUDE
IN MICRONS.
2100 ∿.
DIAPHRAGM No. I.

number of nodal circles, and also according to the number of nodal diameters present.[3]

A similar exploration was made over the diaphragm, with acoustic excitation from an organ-pipe giving C_6 (2,100 ~). Here the points of observation were in steps of about 3.3 mm. in r, and in steps of 40° in θ, as before, with magnification-factor, $M = 1{,}265$.

TABLE II.

VIBRATION AMPLITUDES OVER DIAPHRAGM No. 1, AT FREQUENCY 2,100 ~, FOR NINE DIFFERENT AZIMUTHS θ, AND SEVEN DIFFERENT RADIAL DISTANCES r, FIVE ONLY GIVING READABLE DEFLECTIONS.

Radial Distance, r cm.	Vibration Amplitude Observed, with Explorer, at Different Azimuths θ.								
	0° μ	40° μ	80° μ	120° μ	160° μ	200° μ	240° μ	280° μ	320° μ
−0.08	0.70	0.95	0.95	0.95	0.87	1.02	0.95	0.87	0.95
+0.31	0.70	0.87	0.87	0.78	0.78	1.02	0.87	0.78	0.87
+0.69	0.62	0.78	0.78	0.62	0.62	0.78	0.62	0.62	0.78
+1.06	0.31	0.39	0.39	0.39	0.39	0.39	0.39	0.39	0.62
+1.44	0.16	0.16	0.16	0.08	0.08	0.08	0.08	0.08	0.23
+1.82	—	—	—	—	—	—	—	—	—
+2.20	—	—	—	—	—	—	—	—	—
+2.54	0	0	0	0	0	0	0	0	0

The vibration contour-lines for this case are given in Fig. 8. Here again it is seen that, setting aside irregularities in the diaphragm, and allowing for errors of observation (which are more noticeable with the small amplitudes of higher pitch), the mode of vibration is essentially fundamental, since there are no perceptible nodal circles or nodal diameters.

Having thus ascertained that both at pitch $D_4^{\sharp}$ (608 ~), and at $\widetilde{C_6}$ (2,048 ~), the first mode of vibration was presented, a series of careful explorations were made at a number of intermediate pitches. These likewise all showed the first or fundamental mode of vibration. See Table II*A*.

Observations were also made, at organ-pipe frequencies down to 128 ~. Explorations would be very difficult to obtain on this diaphragm at such low frequencies, owing to the small vibration amplitudes produced; but the indications were that the fundamental mode of vibration was maintained throughout.

[3] See Appendix 1.

PROC. AMER. PHIL. SOC., LIV, 217, H, PRINTED JULY 6, 1915.

The conclusion, therefore, seems warranted that, for this particular steel telephone diaphragm, acoustically excited to frequencies as high as 2,100 ~, the fundamental mode of vibration is the only one that is maintained. If any higher modes of motion were present, they were too faint to be discerned. This does not mean that higher modes of motion could not be produced by any kind of excitation within the above ranges of frequency. The effects of very powerful vibrations were not investigated.

Since the natural frequency of this diaphragm, with flat clamping, was observed to be $n_0 = 824 \sim$, and since, according to Bessel-Function theory, the natural frequency of the second mode of motion should be $2.09 n_0$, we should naturally expect to find this second mode of motion appearing at and above 1,720 ~. Its non-appearance may have been due to the uniformity of acoustic impressed force over the surface, which would tend to favor the first rather than the second mode of forced vibration.

The vibration-amplitude of the diaphragm was found to vary widely with the pitch of the exciting source. At or near the natural

TABLE II*A*.

SHOWING FUNDAMENTAL MODE OF VIBRATION MAINTAINED FOR A RANGE OF OF FREQUENCIES FROM 400 ~ TO 1,800 ~.

Amplitudes of Vibration in Microns (μ) *along Radius of Diaphragm No. 1, Flat-Clamped.* $n_0 = 704 \sim$.

Radial Distance, r Cm.	Frequency of Vibration.						
	400 ~ μ	500 ~ μ	750 ~ μ	1,000 ~ μ	1,250 ~ μ	1,500 ~ μ	1,800 ~ μ
.04	.8	1.6	7.8	1.3	1.3	.9	.3
.29	.8	1.6	7.7	1.3	1.2	.9	.3
.54	.7	1.5	7.2	1.1	1.1	.8	.3
.79	.6	1.4	6.3	.9	.9	.6	.2
1.04	.5	1.3	5.3	.8	.8	.5	.2
1.29	.4	1.0	3.8	.5	.6	.3	.1
1.55	.2	.7	3.0	.3	.4	.2	+
1.79	.1	.4	1.9	.2	.2	.1	+
2.04	+	.3	1.2	.1	.1	+	−
2.30	−	.1	.8	−	+	−	−
2.65	0	0	0	0	0	0	0

fundamental frequency of the diaphragm, the amplitude of the vibratory response was a maximum. Either above or below this

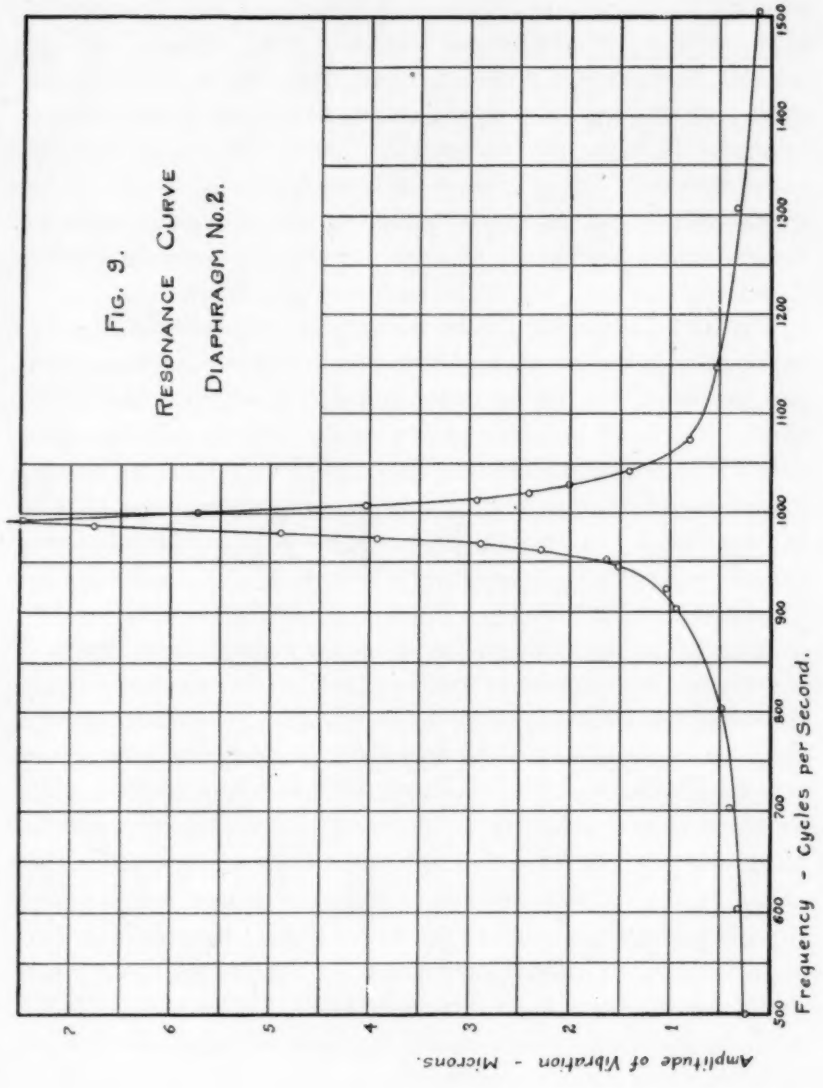
Fig. 9.
Resonance Curve
Diaphragm No. 2.
Amplitude of Vibration - Microns.
Frequency - Cycles per Second.
1
2
3
4
5
6
7
500
600
700
800
900
1000
1100
1200
1300
1400
1500

resonant frequency, the amplitude of vibration, shown by the explorer, fell off very markedly. The curve of relative amplitude at different frequencies is indicated in Fig. 9. It will be seen that when exciting the diaphragm with vibrations remote from the resonant frequency in either direction, the amplitude becomes so small that the degree of precision which may be obtainable near resonance is impossible to secure. The outline theory for this resonance curve, Fig. 9, is given in Appendix II. It is shown that if we multiply the successive ordinates by $\omega = 2\pi n$, the resulting velocity-values correspond to vector chords on a certain velocity circle.

Fig. 1*B* of Appendix I. gives the graph of the explored vibration amplitudes, at successive radial distances from the center of diaphragm No. 1, for the frequency $896 \sim$. It will be seen that the amplitude falls off smoothly from a maximum at or near the center ($r = 0$), to zero at the flat-clamped edge ($r = 2.62$). The application of Rayleigh's theory of free vibration to these curves is given in Appendix I. In general, the agreement between the acoustically forced amplitudes and theoretically computed free amplitudes was satisfactory.

At or near the resonant frequency, or natural frequency of a diaphragm, especially when its damping coefficient is small, so that the resonance is sharp, a small change either in impressed frequency, or in the constants of the diaphragm due to change of temperature, may have an appreciable influence upon the amplitude of vibration. In other words, although the observed amplitudes are relatively large, and the precision of measurement is seemingly high, yet the system is in a virtually unstable condition. Consequently, although there is no reason to suppose that the conditions at resonance differ from those off resonance, nevertheless, when a reliable and reproducible set of observations of amplitude distribution is desired, it is advisable to select a frequency not too close to resonance, or say of about half the resonant amplitude.

Application of Circular Velocity-Diagram Theory to Results of Explorations.

It is shown in the first-approximation theory of Appendix II., that the behavior at the center of a flat-clamped circular diaphragm, subject to constant vibro-motive force of varying frequency, can be completely predicated, if three constants of the diaphragm are known;[4] namely,

(1) the "equivalent mass" m (gm.),

(2) the elastic constant s (dynes per cm. of displacement at center),

(3) the mechanical resistance r (dynes per unit velocity at center).

All these three constants can be obtained, for an acoustically excited diaphragm, with the aid of the vibration explorer.

Determination of m.

In order to determine the equivalent mass of a diaphragm, it is necessary to know the distribution of amplitude over the entire vibrating surface. As is shown in Appendix III., when the distribution of amplitude conforms regularly with the Rayleigh formula, it would appear that the equivalent mass is 0.183 times the mass of the circular vibrating plate. If, however, the distribution of amplitude is irregular, such as may be produced by bipolar electromagnetic excitation of a telephone-receiver diaphragm, the coefficient 0.183 cannot be depended upon, and the proper coefficient must be determined by some process of quadrature, such as Appendix III. describes.

The Elastic Constant s.

The constant s is the inferred elastic resisting force, which, acting perpendicularly upon the diaphragm's equivalent mass (at its center), would produce the same effect upon the vibratory motion as the distributed elastic forces produce upon the diaphragm's distributed mass, in the presence of the particular impressed force distribution. The simplest way to find s is to measure the natural fundamental frequency n_0 of the diaphragm, by exciting it with an

[4] See Bibliography No. 8.

organ-pipe of adjustable pitch, tuned to produce the maximum vibratory amplitude at the center. As shown in Appendix II., the constant s is then the product of the equivalent mass m and the square of the resonant angular velocity ω_0.

A series of statical measurements were made, by applying small tensions f_s, by means of a calibrated spring, to the center of the diaphragm, and observing, with the aid of the explorer, the central displacements w_s, thereby produced. It was found, as might be expected, that the ratio of f_s to w_s was constant, so long as the latter did not exceed 18μ. Moreover, the value of s obtained from f_s/w_s was approximately the same as that obtained from formula (9), App. II. This static method of finding s, however, is inferior to the resonance method, because precise static measurements are difficult to obtain. The application of electro-magnetic excitation to a steel diaphragm also imposes residual stresses, which make the use of the static method unreliable.

The Mechanical Resistance r.

The constant r was measured, with the explorer, by photographing the decay curve of vibration amplitude on a moving photographic film, when the diaphragm was tapped at the center, and allowed to return to the equilibrium position under its own damping forces. It is shown in Appendix II., that the resistance r is twice the natural frequency multiplied by the equivalent mass and the logarithmic decrement. Fig. 10 is a tracing from a photograph of

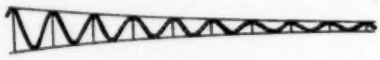

Fig. 10. Tracing from Photograph of Decay Curve. Diaphragm No. 1.

the curve of decay. A small camera, represented in Fig. 11, was set up in front of the explorer, containing a photographic film wrapped around a metal drum. The drum was motor driven at a peripheral speed of approximately 4 meters per second, and the shutter was opened at the time of tapping the diaphragm. The logarithmic decrement of this curve is 0.184, at the frequency of $824\sim$; so that with an equivalent mass m of 1.09 gm. the value of

r becomes 328 dynes per cm. per sec. The precision in measuring r by this method is relatively low, owing to the difficulty in measuring the successive amplitudes with accuracy, on a curve of such small dimensions.

Since, as is shown in Appendix II., a circular diaphragm, in its fundamental mode of motion, ordinarily develops a circular graph of velocity, at varying impressed frequency, with constant vibro-

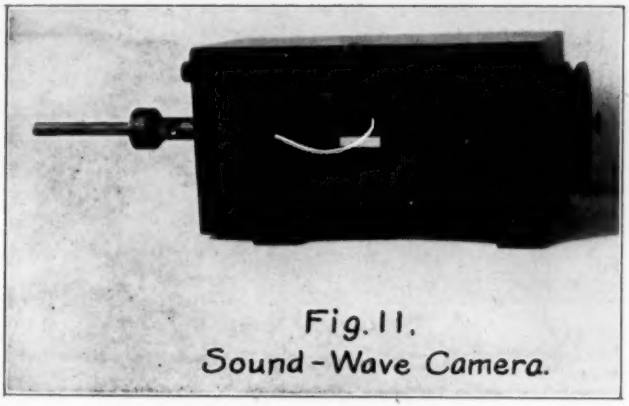

Fig. 11.
Sound-Wave Camera.

motive force, the plan has suggested itself, in the course of this research, to use the circle-velocity diagram of a diaphragm for comparing the vibro-motive forces (vmf.'s) of different organ-pipes. In this connection, the vmf. of a pipe at the exploring diaghragm, may be defined as its harmonically varying pressure $f = Fe^{i\omega t}$ (dynes) produced, at the diaphragm, by the pipe, under the geometrical conditions of the system, including acoustic reflections from walls, or other objects in the room, on both surfaces of the exploring diaphragm. In the simplest, or standard, geometrical condition, the *standard* vmf., which is proportional to the square root of the sound intensity[5] at the diaphragm, would be observed in free space, with the orifice of the pipe facing the diaphragm at a definite distance, and with the diaphragm perpendicular to the line joining them. It is our understanding that there is, as yet, no simple published method of measuring the vmf. of organ pipes, of different

[5] Bibliography 6, Barton, "Text Book of Sound," p. 211, par. 146. Macmillan Co., 1908.

sizes or pitches, at a definite distance from their orifices. If, in a given geometrical environment, pipes of different pitches are set up, in succession, at the same position with respect to the exploring diaphragm, then the observed amplitudes, multiplied by the respective values of ω, should lie on the velocity circle-diagram, if the vmf.'s of the pipes are the same; assuming that the fundamental mode of vibration is produced, that the constants of the diaphragm remain unchanged, and that the overtones of the pipes are negligibly small. The vector departures from the circle diagram would then indicate the inequalities in vmf.'s.

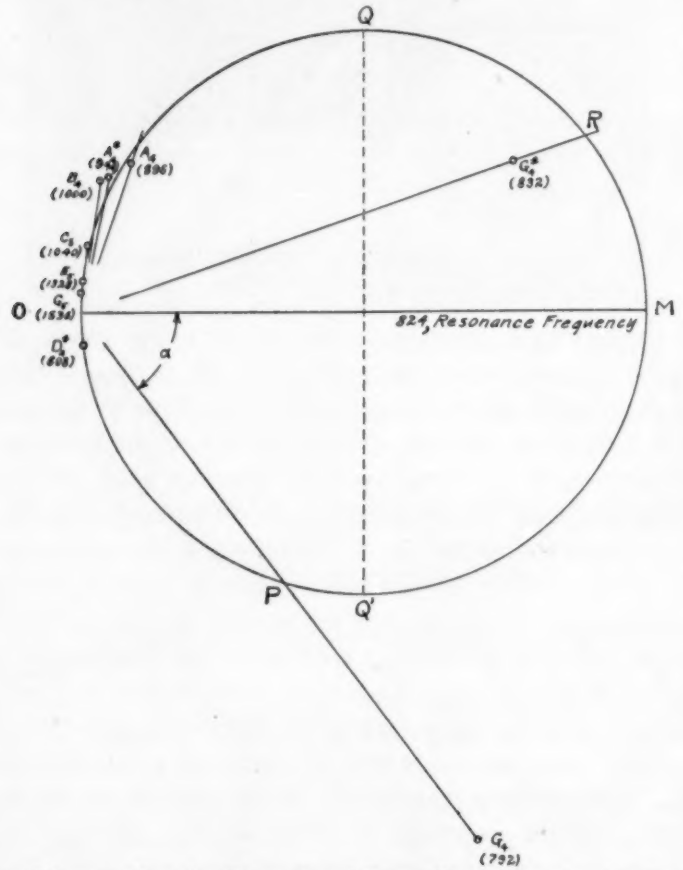

FIG. 12. Diagram Showing Strengths of Organ Pipes Given by the Vibration of a Diaphragm.

Fig. 12 is an inverted velocity-circle diagram for Diaphragm No. 1, based upon its measured values of m, $\mathbf{r}$ and s. If we take the diametral velocity OM as 5 cm. per sec., with $\mathbf{r}=328$ dynes per cm./sec., then the vmf. which, in the particular environment of the experiment, produced this velocity, would be 1,640 dynes, maximum cyclic value. The particular pipe $G_4(792\sim)$, gave an observed amplitude at the diaphragm center, which, multiplied by $\omega=2\pi\times 792$, gives the line OG_4 along the chord OP. The phase-angle α must be obtained by considering the mechanical reactance as in (4), App. II. If the vmf. of this pipe were the same as that which produced OM, this point G_4, would lie on the circle. Consequently, the vmf. of the pipe G_4 is to that of the pipe producing resonance, in the ratio OG_4/OP. Similarly, the vmf. of the pipe $G_4^s(832\sim)$, is less than that producing the resonant velocity, in the ratio OG_4^s/OR. It is evident that the range of any one diaphragm, for the precise comparison of vmf.'s from organ-pipes of different pitch, is somewhat limited. In the case presented, it would not exceed one octave, since the chords far from the resonant diameter become so short. By selecting a diaphragm of relatively large damping constant $\Delta=\mathbf{r}/2m$, this range can be increased. In fact, the range in ω between the quadrantal points QQ' on the velocity circle, is numerically equal to $\mathbf{r}/m$, or twice the damping constant.

A succession of calibrated diaphragms with overlapping ranges might be employed to cover the musical scale. The writers have not attempted to compare organ-pipes for standard vmf. in this manner. The measurements might have to be made out-of-doors. In the sound-absorbing room in which this research was carried on, the effect of sound reflections from walls and other objects prevented any standard comparisons of vmf. from being made.

Explorations with Electromagnetically Excited Diaphragms.

In order to ascertain the effects of exciting a steel diaphragm (No. 2) electromagnetically, a No. 144 Western Electric Bell telephone receiver was screwed into the explorer, behind the diaphragm, so as to obtain the ordinary air-gap between the diaphragm and its two poles. The cap or screw-cover of the ordinary telephone re-

ceiver was here absent. Alternating current of 2 milliamperes (root-mean-square) was supplied from a Vreeland oscillator, giving a close approximation to a pure sine wave, and in connection with a Rayleigh bridge, for the simultaneous measurement of both the resistance and inductance of the telephone receiver, at 32 frequencies varying between 429 and 2,040 ~. Explorations were

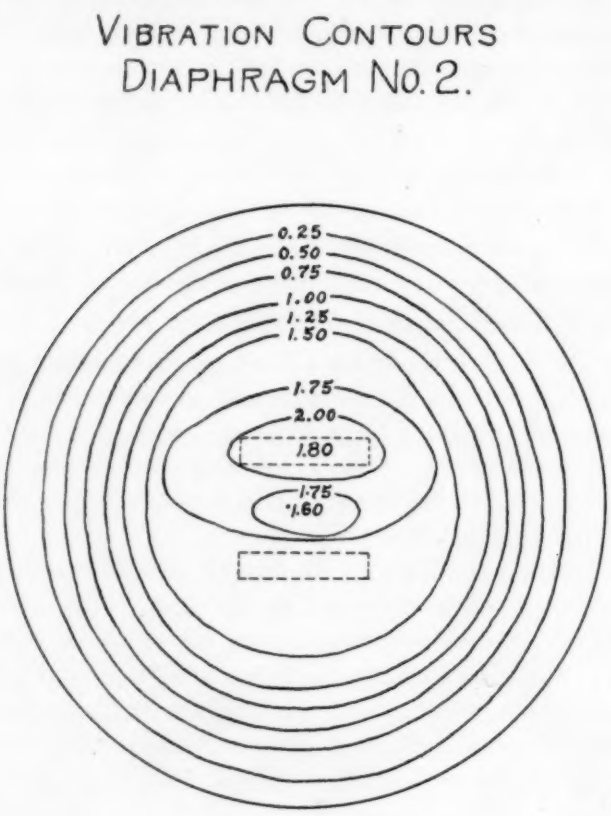

FIG. 13.

made at two frequencies; one, the resonant frequency of 992 ~, and the other slightly below this, or 974 ~. The contour lines for the latter case are presented in Fig. 13, where the outlines of the

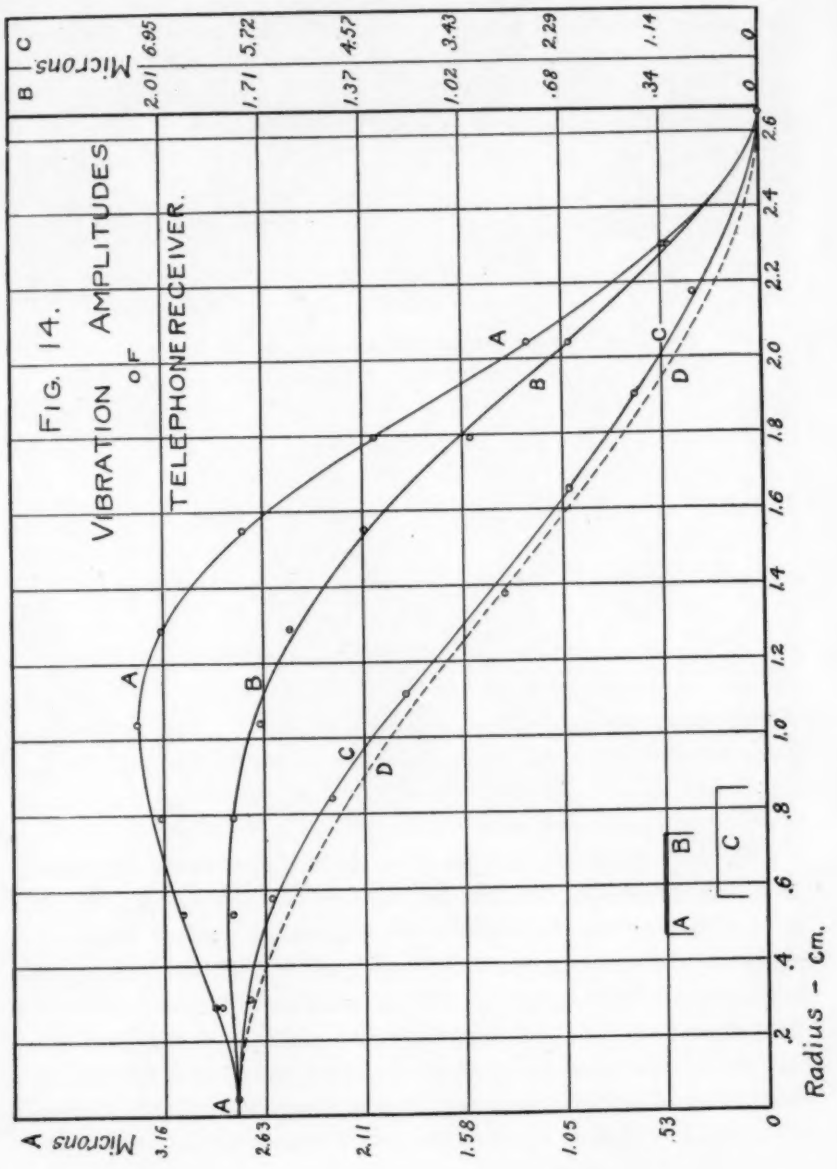
FIG. 14.
VIBRATION AMPLITUDES OF TELEPHONE RECEIVER.
Microns A
Microns B C
Radius - cm.
A
B
C
D

two magnetic poles are indicated in dotted lines. It will be seen that while the mode of motion is essentially fundamental, the amplitude is not a maximum at the center, as in the ordinary acoustic case. The maximum amplitude of 2.0 μ is reached in an elliptical loop embracing the pole at the top. Inside this loop, and immediately over the pole, the amplitude falls off to 1.8 μ. Over the pole underneath, the amplitude is about 1.7 μ, but there appears to be a slight diminution between the poles. If the geometrical and magnetic conditions of the bipolar system were perfectly symmetrical, these dissymmetries would presumably disappear.

The curves of mean amplitude against radial distance are presented in Fig. 14. The curve *AAA* corresponds to that found at resonance, and shows that the amplitude is far from being a maximum at the center of the diaphragm, owing to the attractive forces being established over polar areas on each side of the center. The coefficient of equivalent mass for this curve is over 0.5.

The curve *ABB* gives the corresponding distribution of mean azimuthal amplitude for the frequency of 974 $\sim$. The swelling of the amplitude over the poles is less marked in this case, and does not materially exceed that at the center. The equivalent mass coefficient for this curve is 0.36, or about double that for the Rayleigh-Bessel curve case, which is indicated by *ADD*. The curve *ACC* gives the distribution of mean amplitude in radial distance, for another steel diaphragm (No. 3) in a bipolar telephone receiver, at the resonant frequency of 1,020 $\sim$.

For both steel diaphragms Nos. 2 and 3, a series of central amplitude measurements were made, with the explorer, at constant alternating-current excitation, but adjustably varied frequency. Simultaneous measurements were made by Mr. H. A. Affel, of the resistance and inductance of the telephone-receiver coils, with the diaphragm both free and damped. The explorer measurements in both cases satisfactorily checked the electrically deduced velocity-circle diagrams. It is proposed to report upon the electrical measurements in another paper. Moreover, starting with the amplitudes, measured at the center of the diaphragm, in curves *A* and *C* of Fig. 14, the equivalent masses of the diaphragms, computed from the electrical measurements, agreed, within a few per cent., with those found by integrating curves *A* and *C*.

Temperature Effects.

It was found that changes of temperature in the air surrounding a diaphragm had a marked effect, both upon its resonance frequency, and upon its amplitudes at any frequency. The curves representing w against r, were apt to differ appreciably in outline from day to day. The degree of tightness of clamping also had a marked effect in these measurements. In general, such disturbances due to temperature and clamping, are likely to introduce tensions in the substance of the diaphragm, and to cause some of the characteristics of vibrating membranes to be superposed upon those of a vibrating plate. It is, therefore, desirable that the clamping should be effected tightly, and that the measurements should then be made before the temperature has changed. Strictly speaking, the Rayleigh theory shows that there must be a marked difference in both the resonance frequency and in the distribution of amplitudes, if the diaphragm is clamped between circular knife edges, instead of between circular flat rings at the boundary. The experiments have shown that flat-ring clamping is more likely to give consistent results than knife-edge clamping. These clamping difficulties are accentuated in thin glass diaphragms, for the boundary supporting of which, a special technique had to be developed.

Exploration of Thin Glass Diaphragms.

From a number of thin glass diaphragms, one Diaphragm No. 4, was selected, on account of its uniformity in thickness. See Table III. It was found very difficult to obtain uniform results with this in the explorer, owing to the above mentioned troubles with clamping. Finally, the glass diaphragm was cemented, with water glass, to a boundary ring of glass, and this was lightly supported between the clamping rings of the explorer. The diaphragm was then excited acoustically by organ-pipes. The natural pitch of the diaphragm was found to be 492 $\sim$, in the fundamental mode. On raising the frequency, the mode of motion was found to change suddenly, at 968 $\sim$, to that of a single nodal diameter, the two halves of the diaphragm then vibrating harmonically in opposite phases. This mode of motion continued until the frequency reached 1,696 $\sim$,

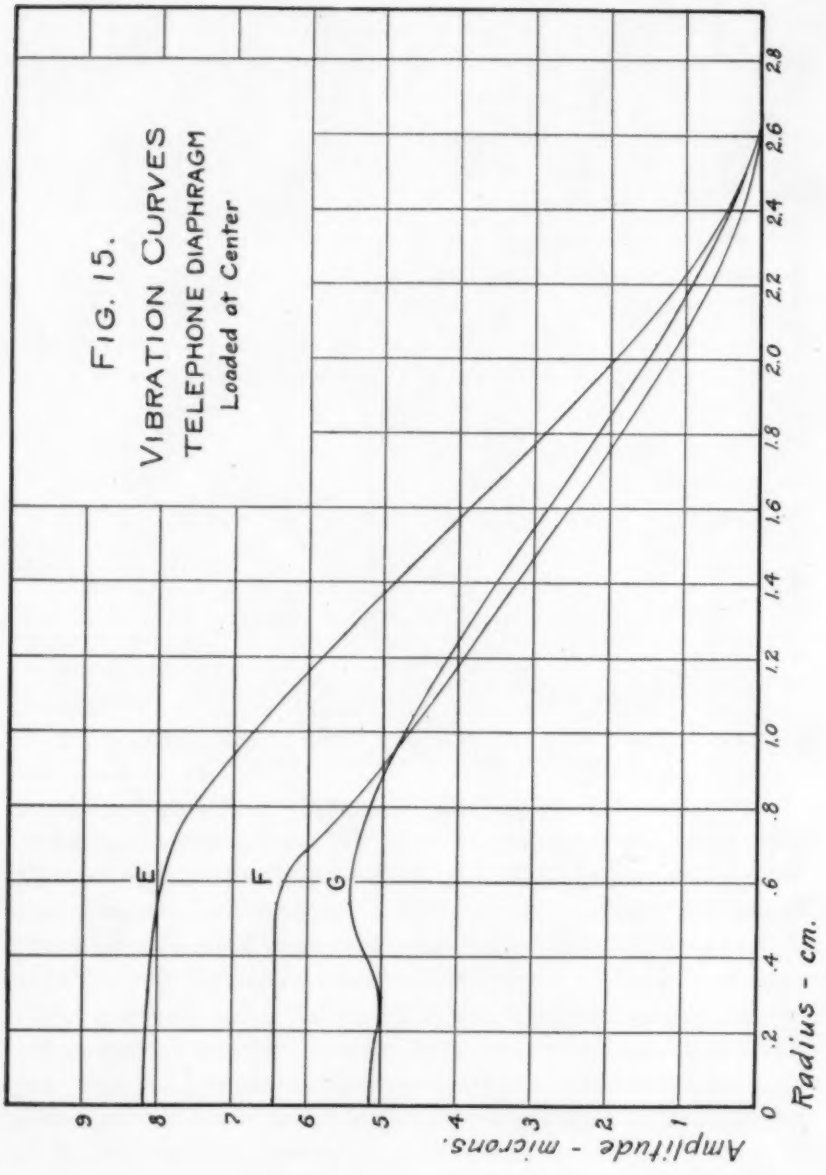
FIG. 15.
VIBRATION CURVES
TELEPHONE DIAPHRAGM
Loaded at Center
E
F
G
Amplitude - microns.
9
8
7
6
5
4
3
2
1
0
.2
.4
.6
.8
1.0
1.2
1.4
1.6
1.8
2.0
2.2
2.4
2.6
2.8
Radius - cm.

when the nodal diameter disappeared and gave place to a single nodal circle. The ratios of the above three frequencies are 1 : 1.97 : 3.44; whereas, according to the Bessel-function theory, they should be 1 : 2.09 : 3.91. The discrepancies may readily be accounted for by imperfections in boundary support, or by temperature effects. Small changes in clamping were found to exercise a marked influence on these ratios.

Loading of Diaphragm.

In the determination of m, r and s, by electrical impedance measurements,[6] only two quantitative relations between these three constants naturally present themselves; whereas, for the evaluation of these three unknowns, three independent quantitative relations must be experimentally obtained. It had been hoped to derive the missing third equation, by applying a small known load-mass at the center of the diaphragm, and by repeating the electrical measurements with this load in place. Electrical experiments showed, however, that while, occasionally, consistent results were obtained in this way, more often the results were discordant. The reason for the discordance has been shown, from explorations of the diaphragm, to be due to a distortion of the amplitude curves; whereby the equivalent mass of the loaded diaphragm is no longer the same as when unloaded.

These conditions are exhibited in the curves of Fig. 15. E shows the w, r curve, for an unloaded telephonic steel diaphragm, excited acoustically at $n = 904 \sim$, its natural frequency being $n_0 = 832 \sim$. The corresponding curve F is for the same diaphragm, after being loaded at the center by a small brass cylinder of 0.536 gm. at $n = 816 \sim$, its new natural frequency being $n_0 = 696 \sim$. After increasing the load to 1.08 gm., the new curve is shown at G ($n = 660 \sim$, $n_0 = 616 \sim$). The shapes of these three curves E, F and G, being so different, it is evident that the equivalent mass of the diaphragm by itself cannot be regarded as constant.

The authors are indebted to Dr. Geo. A. Campbell for a number of valuable suggestions which he made after having read the MSS. of this paper; also to Professor W. C. Sabine for very useful suggestions, during the course of the research.

[6] Bibliography No. 8.

SUMMARY.

1. The distribution of amplitudes over small circular telephonic diaphragms, under simple impressed vibrations, has been measured, it is believed for the first time, by means of a new and specially constructed vibration-explorer.

2. The simple vibrations of the small steel circular diaphragms, used in telephonic receivers, appear to belong to the fundamental mode, within the ordinary telephonic range of intensity and frequency up to 2,000 ~, with the distribution of impressed forces here described.

3. The explorations have confirmed the working theory of the velocity-circle diagram for such vibrations, and have afforded means of determining the three constants m, $\mathbf{r}$ and s, in that theory, for acoustically excited vibrations.

4. In the resonant condition, exploration is somewhat uncertain, owing to slight instability in the vibratory behavior of the diaphragm.

5. The distribution of forced amplitude at varying radial distances, has been found to compare well with the Rayleigh theory of freely vibrating plates, when good flat clamping around the edge can be secured, and with acoustic excitation. The coefficient of equivalent mass appears to be 0.183 for such a case. With electromagnetic excitation, the amplitude distribution may be very different and the coefficient is ordinarily increased.

6. Loading a diaphragm with a small mass at the center, decreases its natural frequency, and tends to reduce the amplitude of vibration at the center, with a relative increase at outlying points; so that the equivalent mass of the diaphragm, considered by itself, is apt to be changed.

7. A means is suggested, based on the velocity-circle diagram, for comparing the acoustic intensities of organ-pipes of different pitches.

8. The distribution of amplitudes over the surface of a steel receiving-telephone diaphragm, with bipolar electromagnetic excitation, was found to be of fundamental mode, but with a tendency to form two maxima, one over each pole.

9. In some small, thin, glass diaphragms, three modes of vibra-

tory motion were observed, in the range of acoustic impressed frequency up to 1,700 ~.

TABLE III.

FLAT CIRCULAR DIAPHRAGMS.

No.	Material.	Diameter, Cm.	Thickness* Over Japan, Cm.	Mass, Gm.	Natural Frequency ~.
1	Steel japanned.....	5.4	0.038	5.615	824
2	Steel japanned.....	5.52	0.0399	5.979	992
3	Steel japanned.....	5.48	0.031	4.181	1020
4	Glass.....	5.4	0.0108	0.6548	492

APPENDIX I.

Application of Bessel-Function Theory to a Diaphragm Vibrating in its Fundamental Mode.

Referring to Lord Rayleigh's "Theory of Sound," Vol. 1, page 352, the formula for the instantaneous amplitude of free vibration in a flat plate is,

$$w_n = P\{J_n(kr) + \lambda J_n(ikr)\}\cos(n\theta + \alpha_n)\cdot\cos(\omega t + c) \quad \text{cm.,} \quad (1)$$

where subscript n = the number of nodal diameters (numeric),

w_n = instantaneous amplitude at a point on the diaphragm whose polar coördinates are r cm., θ radians (cm.)

P = constant of amplitude-magnitude (cm.),

k = a constant of the material defined by:

$k = \sqrt{\omega}/c$ (cm.$^{-1}$),

c = a constant of the material defined by:

$$c = \sqrt[4]{\frac{qb^2}{12\rho(1-\sigma^2)}} \qquad (\text{cm./sec.}^{\frac{1}{2}}),$$

q = Young's modulus for the diaphragm material (dyne/cm.^{2}),

ρ = density of the diaphragm material (gms./cm.^{3}),

σ = Poisson's ratio for the diaphragm material (numeric),

b = thickness of the diaphragm (cm.),

λ = a constant satisfying boundary conditions (numeric),

J_n = a Bessel's Function of the nth order (numeric),

$i = \sqrt{-1}$,

* Thickness of japan 0.0074 cm.

PROC. AMER. PHIL. SOC., LIV. 217 I, PRINTED JULY 6, 1915.

α_n = a phase-angle measured around the diaphragm (radians),
$\omega = 2\pi n$ = angular velocity of vibrating motion (radians/sec.),
n = frequency of diaphragm vibration (cycles/sec.),
t = time elapsed from a given epoch (seconds),
e = a time-phase determined by the epoch (seconds),
a = radius of the diaphragm (cm.).

For the fundamental mode of motion, $n = 0$; or there must be no nodal diameters. Consequently (1) reduces to:

$$w_0 = P\{J_0(kr) + \lambda J_0(ikr)\} \cos(\omega t + e) \qquad \text{cm.} \quad (2)$$

Here the amplitude of vibration at any point w_0, ceases to be a function of θ, and depends only on Bessel functions of r. Since we shall consider only the fundamental mode of vibration in what follows, the subscript will be unnecessary, and we may substitute w for w_0.

Continuing Lord Rayleigh's method of demonstration, if a flat circular diaphragm is clamped at its edge between a pair of flat circular rings, then, referring to (2), we have w vanishing at $r = a$, the clamping radius, and since there is to be no bending or slope of the diaphragm at the clamped boundary, we have also $(dw/dr) = 0$ at $r = a$.

Entering (2) with $w = 0$, we have:

$$\lambda = -\frac{J_0(ka)}{J_0(ika)} \qquad \text{numeric.} \quad (3)$$

Also differentiating (2) with respect to r, for $r = a$, we obtain:

$$\frac{1}{k}\frac{dw}{dr} = J_0'(ka) + i\lambda J_0'(ika) = 0 \qquad \text{numeric,} \quad (4)$$

whence

$$\lambda = -\frac{J_0'(ka)}{iJ_0'(ika)} \qquad \text{numeric.} \quad (5)$$

Combining (3) and (5) we obtain:

$$\frac{J_0(ka)}{J_0(ika)} = \frac{J_0'(ka)}{iJ_0'(ika)} = \frac{J_1(ka)}{iJ_1(ika)} \qquad \text{numeric.} \quad (6)$$

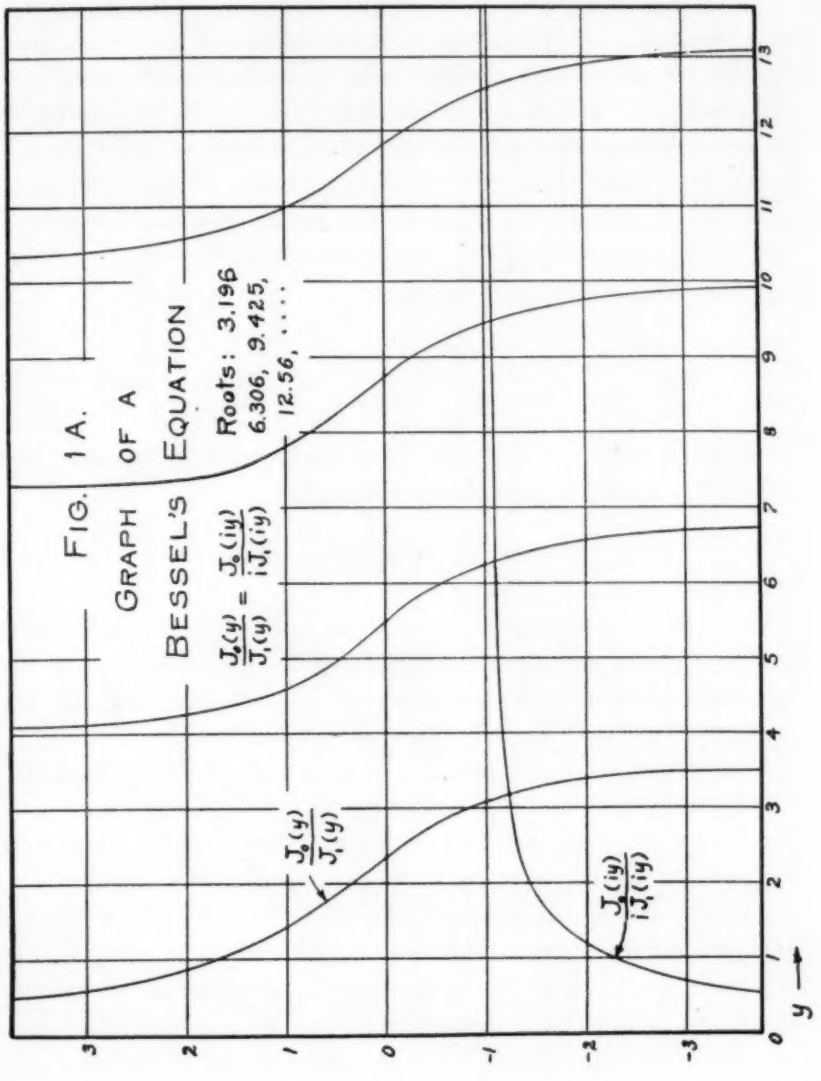
FIG. 1A.
GRAPH OF A BESSEL'S EQUATION
$\frac{J_0(y)}{J_1(y)} = \frac{J_0(iy)}{iJ_1(iy)}$
Roots: 3.196
6.306, 9.425,
12.56, ...
$\frac{J_0(y)}{J_1(y)}$
$\frac{J_0(iy)}{iJ_1(iy)}$
y

This is a transcendental equation involving Bessel's Functions of the zeroth and first orders. It is capable of being satisfied, by trial, with an indefinitely great number of roots, each corresponding to a possible mode of vibration with nodal circles. Fig. 1*A* indicates graphically the method of determining the successive roots of (6). The points of intersection of the lower curve with the successive descending branches, indicate the values of $y = kr$ which satisfy (6). In order to have the fundamental mode of vibration, there must be no nodal circles, which means that the first and lowest root for ka must be taken in (6). This root is at $ka = 3.196$. . . . Placing this value for ka in (3) we have:

$$\lambda = \frac{-J_0(3.196)}{J_0(i3.196)} = -\frac{-0.3197}{5.730} = +0.05571 \quad \text{numeric.} \quad (7)$$

Re-entering (2) with this value of λ, we have for the fundamental mode of vibration of the circular diaphragm:

$$w_{max} = P\{J_0(kr) + 0.05571 J_0(ikr)\} \quad \text{cm.} \quad (8)$$

In Fig. 1*B*, the abscissas correspond both to kr, where $k = 1.21$ cm.$^{-1}$, and to r in cm., the relation being as already pointed out that at the boundary $r = a = 2.62$ cm. and $kr = 3.196$. The ordinates are the numerical values of Bessel's functions as taken from Tables. They also represent vibratory amplitudes of the diaphragm, taking the maximum amplitude at the center ($r = 0$) in microns, corresponding to the heavy curve. The upper faint curve shows the graph of the first Bessel function $J_0(kr)$; while the lower faint curve shows the corresponding graph of λ times the second Bessel function, or $0.05571 J_0(ikr)$. Adding these two graphs, as called for by (2), we obtain the heavy curve, which represents the theoretical amplitude of vibration along any radius of this particular diaphragm, assuming such a scale that 1.056 corresponds to the maximum or central amplitude. The small circles near this curve show the amplitudes observed with the aid of the vibration explorer.

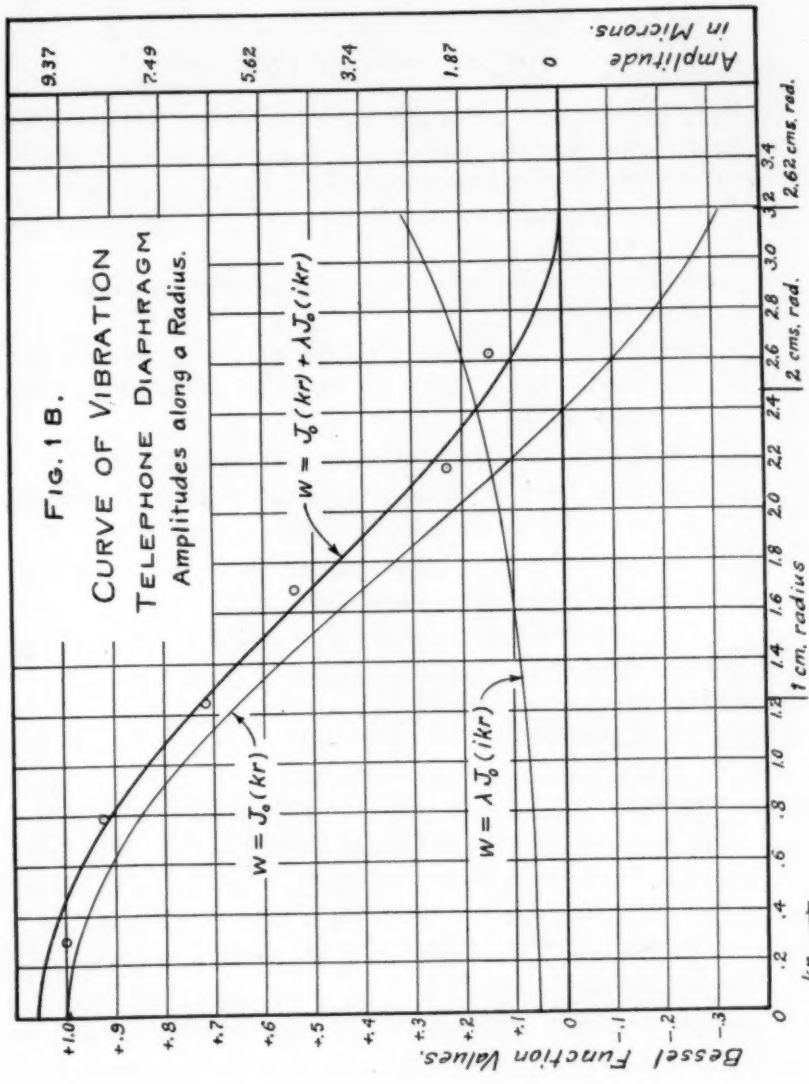
FIG. 1 B.
CURVE OF VIBRATION
TELEPHONE DIAPHRAGM
Amplitudes along a Radius.
$W = J_0(kr)$
$W = J_0(kr) + \lambda J_0(ikr)$
$W = \lambda J_0(ikr)$
Bessel Function Values.
Amplitude in Microns.
9.37
7.49
5.62
3.74
1.87
0
+1.0
+.9
+.8
+.7
+.6
+.5
+.4
+.3
+.2
+.1
0
-.1
-.2
-.3
.2 .4 .6 .8 1.0 1.2 1.4 1.6 1.8 2.0 2.2 2.4 2.6 2.8 3.0 3.2 3.4
1 cm. radius
2 cms. rad.
2.62 cms. rad.
kr

Appendix II.

Elementary Theory of the Steady Vibration Amplitude of a Diaphragm Vibrating in its Fundamental Mode, as a Function of the Impressed Frequency.

Let w = the vibration amplitude at the center of the diaphragm[8] (cm.$\angle$),

w_r = the vibration amplitude at the radius r (cm.$\angle$),

$\dot{w}$ = the vibration velocity at the center of the diaphragm (cm./sec.$\angle$),

$\ddot{w}$ = the vibration acceleration at the center of the diaphragm (cm./sec.$^2\angle$),

$\mathbf{r}$ = frictional resistance to motion of the diaphragm, referred to the equivalent mass, see below (dynes/cm. per sec.$\angle$),

t = elapsed time from a given epoch (seconds),

s = elastic force of the diaphragm per cm. of displacement, referred to the equivalent mass (dynes per cm.$\angle$),

$f = Fe^{i\omega t}$ = impressed simple harmonic moving force on the diaphragm tending to produce displacement w, and measured in the direction of w, referred to the equivalent mass (dynes$\angle$),

$i = \sqrt{-1}$,

$\omega = 2\pi n$ = the angular velocity of a simple harmonic motion of frequency n (radians/sec.),

m = equivalent mass of the diaphragm, defined by the condition that the energy of motion of this mass with the velocity $\dot{w}$ at the center, is equal to the actual energy of the diaphragm with its distributed mass and velocities, according to the equation:

$$\frac{m}{2}(\dot{w})^2 = \frac{2\pi\rho'}{2}\int_0^a r(\dot{w}_r)^2 dr \qquad \text{ergs,} \quad (1)$$

where ρ' = superficial density of the diaphragm (gm./cm.^{2}),

$$m = \frac{2\pi\rho'}{w_{max}^2}\int_0^a (w_r)^2 r dr \qquad \text{gm.,} \quad (2)$$

[8] The sign $\angle$ after a unit indicates a "complex quantity."

since the velocities $\dot{w}$ and $\dot{w}_r$ being assumed simply harmonic, are respectively proportional to their maximum displacements w_{max} and w_r.

Then on the assumptions that the diaphragm vibrates like its equivalent mass collected at the center, with its observed central velocity, with an elastic opposing force sw on this mass, proportional to the displacement, and with a resisting force $r\dot{w}$ on this mass proportional to the velocity, then the equation of motion of the diaphragm in terms of equivalent mass will be[9]

$$sw + \mathbf{r}\dot{w} + m\ddot{w} = f = Fe^{i\omega t} \qquad \text{dynes } \angle. \quad (3)$$

The solution of this equation, in terms of velocity $\dot{w}$, and the steady state, is known to be

$$\dot{w} = \frac{f}{\mathbf{r} + i\left(m\omega - \frac{s}{\omega}\right)} = \frac{f}{\mathbf{r} + ix} = \frac{f}{z} = \frac{F}{z}e^{i\omega t} \qquad \frac{\text{cm.}}{\text{sec.}} \angle, \quad (4)$$

where x is the "mechanical reactance," and z is the complex "mechanical impedance," by analogy to alternating electric current theory. Both x and z have the same dimensions as $\mathbf{r}$.

The mechanical impedance relations are indicated in Fig. II*A* at the left-hand side. OX and OY being rectangular coördinates, the "mechanical resistance" $\mathbf{r}$ in dynes per unit velocity, is measured along OX, and is assumed to remain constant at all frequencies. As the frequency n is increased (and with it the vibratory angular velocity ω) from zero to infinity, the reactance $x = (m\omega - s/\omega)$ varies from $-\infty$ to $+\infty$ along the line yXy'. The mechanical impedance z which is the vector sum of $\mathbf{r}$ and ix, will be represented by a complex quantity, or plane vector Op, the extremity of which remains on the line yXy'. At the particular or resonant value of ω, for which $m\omega - s/\omega = 0$, the reactance vanishes, and the impedance z coincides with the resistance $\mathbf{r}$. As shown in the figure, p lies above OX, corresponding to a value of ω somewhat greater than the critical or resonant value.

[9] See Bibliography No. 8.

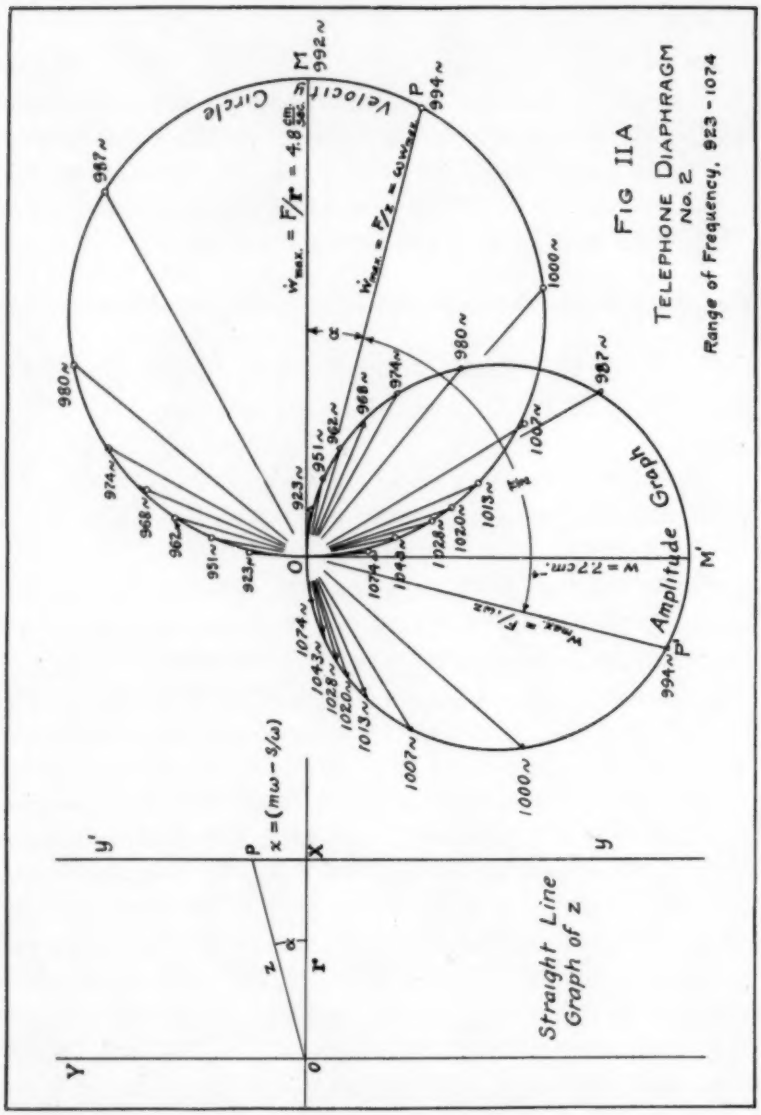
Velocity Circle
Amplitude Graph
Straight Line Graph of z
FIG IIA
TELEPHONE DIAPHRAGM
No. 2
Range of Frequency, 923 - 1074
M
P
O
M'
P'
992~
994~
987~
980~
974~
968~
962~
951~
923~
1000~
1007~
1013~
1020~
1028~
1043~
1074~
Y
y'
y
x = (mω - s/ω)
z
α
r

Equation (4) shows that the displacement velocity $\dot{w}$ is equal to the impressed vibro-motive force f, divided by the impedance z. The locus of this velocity, as ω varies from 0 to ∞ with constant F, becomes a circle OMP, the diameter OM of which is equal to $F/\mathfrak{r}$ cm. per sec., while the angle α of the chord OP, measuring the velocity, is equal and of opposite sign to the angle α of the impedance z. In the case represented by Fig. II*A*, the telephone diaphragm No. 2 was actuated electromagnetically at constant alternating-current strength, under varying frequency. At the frequency $n = 992 \sim$, the vibratory velocity $OM = 4.8$ cm. sec., was a maximum, and was in phase with the impressed vibro-motive force F. At $n = 994 \sim$, the mechanical impedance had increased to op at the angle $\alpha = 14°$, and the vibratory velocity had fallen from OM to OP or from 4.8 to 4.65 cm. per sec. lagging in phase behind the impressed vibro-motive force by 14°. The diagram shows that between the frequencies of 923 and 1,074 $\sim$, the vector displacement velocity $\dot{w}$ had moved over nearly the entire circumference of the velocity circle OMP, and from a phase nearly 90° ahead of the impressed vibro-motive force to nearly 90° behind it.

If we integrate (4) with respect to time, we obtain, for the steady state of motion,

$$w = \int \dot{w} dt = \int \frac{F\epsilon^{i\omega t}}{z} dt = \frac{F\epsilon^{i\omega t}}{i\omega z} = -\frac{iF\epsilon^{i\omega t}}{\omega z}, \quad \text{cm. } \angle. \quad (5)$$

This shows that the instantaneous displacement is ω times less than the corresponding instantaneous velocity, and is 90° behind it in phase. If we consider the maximum displacement, we have

$$w_{\max} = -\frac{iF}{\omega z} \quad \text{cm.} \quad (6)$$

The locus of $w_{\max}$ is therefore a closed curve distorted from a circle by the effect of varying ω in the denominator. Considering it as an approximate circle for this case, the diameter OM' corresponding to $n = 992 \sim$ represents a displacement amplitude of $7.7\,\mu$, lagging approximately 90° behind the maximum velocity OM. At the frequency $994 \sim$, the displacement would be $OP' = 7.48\,\mu$,

lagging 90° behind OP. As the frequency varies between 923 and 1,074 ~, the displacement amplitude almost covers the entire graph of the approximate circle $OM'P'$, commencing at about 1 μ, nearly in phase with the vibro-motive force, and ending at about 1 μ in nearly opposite phase. These amplitudes correspond to the ordinates of the resonance curve in Fig. 9.

It follows from (4) that if the vibro-motive force f is kept constant, and the angular velocity adjusted until the central vibration velocity is a maximum, this will occur when the mechanical reactance is zero, or when

$$m\omega_0 - \frac{s}{\omega_0} = 0 \qquad \frac{\text{dynes}}{\text{cm./sec.}}, \quad (7)$$

that is

$$\omega_0 = \sqrt{\frac{s}{m}} \qquad \frac{\text{radians}}{\text{sec.}}. \quad (8)$$

So that

$$s = m\omega_0^2 \qquad \frac{\text{dynes}}{\text{cm.}}. \quad (9)$$

When the vibro-motive force f is made to vanish in (3) with the diaphragm in motion, the solution of the equation is

$$w = We^{-\frac{rt}{2m}} \sin(\omega t + e) \qquad \text{cm.}, \quad (10)$$

where W is the initial displacement (cm), and e a suitable phase (radians). If we obtain two successive values of w, (w_1 and w_2), corresponding to two successive elongations in the same direction, we have

$$\frac{w_1}{w_2} = \epsilon^{r/2mn} = \epsilon^{\Delta/n} \qquad \text{numeric}, \quad (11)$$

whence

$$r = 2mn \log_\epsilon (w_1/w_2), \qquad \text{dynes/(cm./sec.)}, \quad (12)$$

where Δ is the damping constant (1/sec.).

The quantity $\log_\epsilon (w_1/w_2)$ is well known as the logarithmic decrement of the decay curve.

Appendix III.

Elementary Theory of Equivalent Mass.

In (2) of Appendix II., the expression for equivalent mass m is

$$m = \frac{2\pi\rho'}{w^2_{max}} \int_0^a w_r^2 \cdot r \quad dr \qquad \text{gm.} \quad (1)$$

or m is the mass which, vibrating at the center of the diaphragm with the observed maximum ampltiude w_{max}, would have the same kinetic energy as the total distributed kinetic energy of the diaphragm.

In order, therefore, to determine the equivalent mass of a diaphragm, it is necessary to integrate r times the square of the amplitude over its surface. Assuming that the vibration follows Rayleigh's Bessel-function theory as outlined in Appendix I., it should be sufficient to integrate $w_r^2 \cdot r$ over the surface, mathematically. We are indebted to Dr. Geo. A. Campbell for an indication of the solution of this integral.[10]

In (1)

$$w_{max} = P[J_0(0) + \lambda J_0(i0)] = P(1 + \lambda) \qquad \text{cm.} \quad (2)$$

by reference to (8) Appendix I., putting $r = 0$.

Also

$$w_r = P[J_0(kr) + \lambda J_0(ikr)] \qquad cm. \quad (3)$$

$$\therefore m = \frac{2\pi\rho'}{P^2(1+\lambda)^2} \int_0^a P^2 \{J_0^2(kr) + \lambda^2 J_0^2(ikr) + 2\lambda J_0(kr) J_0(ikr)\} r dr \quad (4)$$

$$= \frac{2\pi\rho'}{(1+\lambda)^2} \left[\int_0^a J_0^2(kr) r \cdot dr + \int_0^a \lambda^2 J_0^2(ikr) r \cdot dr + \int_0^a 2\lambda J_0(kr) J_0(ikr) r \cdot dr \right]$$

$$= \frac{2\pi\rho'}{(1+\lambda)^2} \left[\frac{a^2}{2} \{J_0^2(ka) + J_1^2(ka)\} + \frac{\lambda^2 a^2}{2} \{J_0^2(ika) + J_1^2(ika)\} + \frac{2\lambda a}{k^2 - i^2 k^2} \{k J_0(ika) J_1(ka) - ik J_0(ka) J_1(ika)\} \right], \quad (5)$$

[10] Bibliography (11), (12), (13).

where

$$J_0^2(kr) \text{ stands for } \{J_0(kr)\}^2.$$

But $M = \pi\rho' a^2$ is the total mass of the vibrating diaphragm area.

$$\therefore \frac{m}{M} = \frac{1}{(1+\lambda)^2}\Big[\{J_0^2(ka) + J_1^2(ka)\} + \lambda^2\{J_0^2(ika) + J_1^2(ika)\} + \frac{2\lambda}{ak}\{J_0(ika)J_1(ka) - iJ_0(ka)J_1(ika)\}\Big]. \quad (6)$$

Applying the ratios of (6) Appendix I., this reduces to:

$$\begin{aligned}\frac{m}{M} &= \frac{1}{(1+\lambda)^2} \cdot 2J_0^2(ka) \\ &= \frac{1}{(1.05571)^2} \cdot 2J_0^2(3.196) \\ &= \frac{0.20378}{1.1145} \\ &= 0.18285\end{aligned}$$

or, to three significant digits, 0.183.

The "equivalent mass coefficient," 0.183, for this diaphragm, had also been obtained by quadrature methods applied to the heavy curve in Fig. 1*B*, before the integration was performed as above.

In the case of steel telephone diaphragms excited by bipolar electromagnets, the curves of w_r, r are likely to depart from simple Bessel-function curves, see Fig. 14. In such cases, the coefficient of equivalent mass must be deduced from the exploration curve. In cases examined, this coefficient varied between 0.2 and 0.5.

A quadrature method employed to find the equivalent mass coefficient from curves of any shape is as follows:

Draw the w_r curve as in Fig. 1*B*. Divide the line of abscissas into an integral number n of annular rings of equal area; so that each ring will have a mass of M/n, where M is the total mass of the circular vibrating area of the diaphragm, in grams. We then multiply this annular mass into the square of the observed amplitudes at the middle points of the successive annuli. The sum of these terms will be equal to the product of the equivalent mass m,

TABLE IV.

	kr	w	w (ave.)	w^2 (ave.)
	.0000	1.0557		(1.1145)
1	.4511	1.008	1.032	1.0650
2	.6380	.962	.985	.9702
3	.7814	.918	.940	.8836
4	.9023	.875	.897	.8046
5	1.009	.833	.854	.7293
6	1.105	.792	.812	.6593
7	1.194	.752	.772	.5960
8	1.276	.713	.732	.5358
9	1.353	.677	.695	.4830
10	1.427	.641	.659	.4343
11	1.496	.606	.624	.3894
12	1.563	.572	.589	.3469
13	1.627	.539	.555	.3080
14	1.688	.507	.523	.2735
15	1.747	.477	.492	.2421
16	1.805	.449	.463	.2144
17	1.860	.421	.435	.1892
18	1.914	.394	.408	.1665
19	1.966	.367	.380	.1444
20	2.018	.341	.354	.1253
21	2.067	.318	.330	.1089
22	2.116	.295	.307	.0942
23	2.163	.273	.284	.0807
24	2.210	.251	.262	.0686
25	2.256	.232	.242	.0586
26	2.300	.213	.223	.0497
27	2.344	.195	.204	.0416
28	2.387	.178	.186	.0346
29	2.429	.162	.170	.0289
30	2.471	.146	.154	.0237
31	2.512	.131	.139	.0193
32	2.552	.117	.124	.0154
33	2.592	.104	.110	.0121
34	2.631	.092	.098	.0096
35	2.669	.080	.086	.0074
36	2.707	.070	.075	.0056
37	2.744	.060	.065	.0042
38	2.781	.050	.055	.0030
39	2.817	.041	.045	.0020
40	2.853	.033	.037	.0014
41	2.889	.026	.030	.0009
42	2.924	0.21	.023	.0005
43	2.958	.016	.019	.0004
44	2.992	.012	.014	.0002
45	3.026	.009	.011	.0001
46	3.060	.006	.008	.00006
47	3.093	.004	.005	.00002
48	3.126	.002	.003	.000009
49	3.158	.001	.001	.000001
50	3.196	.000	.000	.000000
				10.2325

$$m = (M/50)\,(10.2325/1.1145) = .183\,M.$$

and the square of the maximum observed amplitude at the center, or

$$m = \frac{M}{n} \frac{\Sigma w_r^2}{w_{\max}^2} \quad \text{gm.} \quad (7)$$

The preceding table sets forth this process for the curve of Fig. 1*B*, drawn theoretically, and checked observationally, with $n = 50$, or the diaphragm divided into 50 annuli of equal mass. The result is that the equivalent mass is 18.3 per cent. of the actual mass of the vibrating area. This result checks that obtained from the mathematical integration of the Bessel curve.

Although 50 annuli of equal area and mass were taken in the case above worked out, so as to attain a fairly high degree of precision in the evaluated equivalent-mass coefficient; yet, for many purposes, a sufficient degree of precision might be attained by taking only 10 such equal annular areas.

BIBLIOGRAPHY.

1. Rayleigh, "Theory of Sound," Vol. 1, p. 352, Macmillan Co., 1894.
2. R. Kempf-Hartmann, Ann. de Physik, 8, pp. 481–538, June, 1902.
3. W. Wien, Ann. de Physik, 18. S, pp. 1049–1053, December, 1905.
4. Henri Abraham, Comptes Rendus, Vol. 144, 1907.
5. Frederick K. Vreeland, Phys. Review, Vol. 27, p. 286, 1908.
6. Barton, "Text-Book of Sound," p. 211, Sec. 146, Macmillan Co., 1908.
7. Chas. F. Meyer and J. B. Whitehead, Trans. A. I. E. E., Vol. 31, II., pp. 1397–1418, 1912.
8. A. E. Kennelly and G. W. Pierce, "The Impedance of Telephone Receivers as Affected by the Motion of Their Diaphragms," Proc. Am. Acad. of Arts and Sci., Vol. 48, No. 6, September, 1912, p. 138; also *Electrical World*, September 14, 1912.
9. L. Bouthillon and L. Drouet, La Révue Electrique, October 16, 1914 (pub. January 15, 1915).
10. Augustin Guyau, "Le Téléphone Instrument de Mésure," Gauthier-Villars, Paris, 1914.
11. E. Jahnke and F. Emde, "Funktionentafeln mit Formeln und Kurven," p. 166 (3) and (4).
12. Paul Schafheitlin, "Die Theorie der Besselschen Funktionen," pp. 68 and 69.
13. W. E. Byerly, "Fourier's Series and Spherical Harmonics," p. 233.

TABLE OF SYMBOLS.

a = Radius of the diaphragm clamping-circle (cm.),
α_n = A phase angle measured around the diaphragm (radians),
b = Thickness of the diaphragm (cm.),
c = A constant of the material of the diaphragm (cm./second $\frac{1}{2}$),
d = Sign of differentiation
Δ = Damping constant $= n \log_\epsilon (w_1/w_2) = \mathbf{r}/2m$ (second^{-1}),
e = Time-phase (radians),
ϵ = Naperian logarithmic base (numeric),
$f = Fe^{i\omega t}$ Impressed simple harmonic moving force on the diaphragm (dynes) $\angle$
f_s = Statical tension (dynes),
F = Maximum value of a vibratory force (dynes),
$i = \sqrt{-1}$ (numeric),
J_n = A Bessel's Function of the nth order (numeric),
J' = The first derivative of J with respect to r (numeric),
k = A constant of the material of the diaphragm, defined by $k = (\sqrt{\omega})/c$ (cm.$^{-1}$),
L = Distance from mirror to scale of explorer (cm.),
l = Radius arm of small mirror in explorer (cm.),
λ = A constant satisfying boundary conditions (numeric),
M = Total mass of diaphragm (in Appendix III) (gm.),
M = Magnification factor of explorer (numeric),
m = Equivalent mass of the diaphragm (gm.),
μ = Micron, 10^{-4} cm. (cm^{-4}),
n = Frequency of diaphragm vibration (cycles/second),
n_0 = Resonant frequency of diaphragm vibration (cycles/sec),
n = Number of annular rings in equivalent mass theory of App. III (numeric),
n (Subscript) = Number of nodal diameters (order of Bessel's Function) (numeric),
P = Constant of amplitude-magnitude (cm.),
π = 3.1416 (numeric),
ϕ = Angle in the explorer between the plane of mirror and plane of diaphragm (deg.),
q = Young's modulus for diaphragm material (dynes/cm.^{2}),
$\mathbf{r}$ = Frictional resistance to motion of diaphragm $\frac{\text{dynes}}{\text{cm./sec.}}$,

r = Distance along a radius (cm.),
ρ = Density of diaphragm material (gm./cm.^{3}),
ρ' = Superficial density of diaphragm (gm./cm.^{2}),
s = Elastic force of diaphragm per centimeter of displacement, referred to equivalent mass (dynes/cm.),
σ = Poisson's ratio for material of diaphragm (numeric),
Σ = Sign of summation,
t = Time elapsed from a given epoch (seconds),
θ = Azimuth angle measured on surface of diaphragm (radians)
vmf. = Vibro-motive force (dynes) $\angle$,
W = Initial displacement in a vibratory motion (cm.),
w and w_0 = Amplitude of a point on surface of diaphragm for fundamental mode of vibration (cm.) $\angle$,
w_r = Amplitude of vibration of a point at radius r from center of diaphragm (cm.) $\angle$,
w_n = Instantaneous amplitude of vibration (cm.),
w_{max} = Maximum cyclic amplitude at center (cm.),
$\dot{w}$ = Vibratory velocity at center of diaphragm (cm./sec.) $\angle$,
$\ddot{w}$ = Vibratory acceleration at center of diaphragm (cm./sec.^{2}) $\angle$,
w_s = Statical displacement of center of diaphragm (cm.),
$ix = i(m\omega - s/\omega)$ "Mechanical reactance" of vibrating diaphragm (by analogy to alternating-current theory) {dynes/(cm./sec.)} $\angle$,
$z = (\mathbf{r} + ix)$ "Mechanical impedance" of vibrating diaphragm (by analogy to alternating-current theory) {dynes/(cm./sec.)} $\angle$,
$\omega = 2\pi n$ = Angular velocity of vibratory motion (radians/sec.),
$\omega_0 = 2\pi n_0$ = Angular velocity at resonance (radians/sec.),
∞ = Infinity,
$\angle$ = This sign after a unit indicates a "complex quantity,"
$\sim$ = Cycles or vibrations per second (cycles/sec.).

THE RULING AND PERFORMANCE OF A TEN INCH DIFFRACTION GRATING.

By A. A. MICHELSON.

(*Read April 22, 1915.*)

The principal element in the efficiency of any spectroscopic appliance is its resolving power—that is, the power to separate spectral lines. The limit of resolution is the ratio of the smallest difference of wave-length just discernible to the mean wave-length of the pair or group. If a prism can just separate or resolve the double yellow line of sodium its limit of resolution will be $\frac{5896-5890}{5893}$ or approximately one one thousandth, and the resolving power is called one thousand.

Until Fraunhofer (1821) showed that light could be analyzed into its constituent colors by diffraction gratings this analysis was effected by prisms the resolving power of which has been gradually increased to about thirty thousand. This limit was equalled if not surpassed by the excellent gratings of Rutherford, of New York, ruled by a diamond point on speculum metal, with something like 20,000 lines, with spacing of 500 to 1,000 lines to the millimeter. These were superseded by the superb gratings of Rowland with something over one hundred thousand lines, and with a resolving power of 150,000.[1]

The theoretical resolving power of a grating is given as was first shown by Lord Rayleigh by the formula $R = mn$, in which n is the total number of lines, and m the order of the spectrum. An equivalent expression is furnished by

$$R = \frac{l}{\lambda}(\sin i + \sin \theta),$$

[1] The 6½ in. gratings now ruled on the Rowland engine have a much higher resolving power—probably 400,000.

where l is the total length of the ruled surface, λ the wave-length of the light, i the angle of incidence and θ the angle of diffraction, and the maximum resolving power which a grating can have is that corresponding to i and θ each equal to 90° which gives $R = 2l/\lambda$; that is twice the number of light waves in the entire length of the ruled surface.

This shows that neither the closeness of the rulings nor the total number determine this theoretical limit, and emphasizes the importance of a large ruled space.

This theoretical limit can be reached, however, only on the condition of an extraordinary degree of accuracy in the spacing of the lines. Several methods for securing this degree of accuracy have been attempted but none has proved as effective as the screw. This must be of uniform pitch throughout and the periodic errors must be extremely small.

For a short screw, for example one sufficient for a grating two inches in length, the problem is not very difficult, but as the length of the screw increases the difficulty increases in much more rapid proportion. It was solved by Rowland in something over two years.

Since this time many problems have arisen which demand a higher resolving power than even these gratings could furnish. Among these is the resolution of doubles and groups of lines whose complexity was unsuspected until revealed by the interferometer and amply verified by subsequent observations by the echelon and other methods.

Others that may be mentioned in this connection are the study of the distribution of intensities within the spectral "lines"; their broadening and displacement with temperature and pressure; the effect of magnetic and electric fields, and the measurement of motions in the line of sight, as revealed by corresponding displacement of the spectral lines in consequence of the Doppler effect.

All of these have been attacked with considerable success by observations with the echelon, the interferometer and the plane-parallel plate. These methods have a very high resolving power, but labor under the serious disadvantage that adjacent succeeding

spectra overlap, making it difficult to interpret the results with certainty.

Some twelve years ago the construction of a ruling engine was undertaken with the hope of ruling gratings of fourteen inches—for which a screw of something over twenty inches is necessary. This screw was cut in a specially corrected lathe so that the original errors were not very large, and these were reduced by long attrition with very fine material until it was judged that the residual errors were sufficiently small to be automatically corrected during the process of ruling.

The principal claim to novelty of treatment of the problem lies in the application of interference method to the measurement and correction of these residual errors.

For this purpose one of the interferometer mirrors is fixed to the grating carriage, while a standard, consisting of two mirrors at a fixed distance apart, is attached to an auxiliary carriage. When the adjustment is correct for the front surface of the standard, interference fringes appear. The grating carriage is now moved through the length of the standard (one tenth of a millimeter if the periodic error is to be investigated; ten or more millimeters if the error of run is to be determined) when the interference fringes appear on the rear surface. This operation is repeated, the difference from exact coincidence of the central (achromatic) fringe with a fiducial mark being measured at each step in tenths of a fringe (twentieths of a light-wave). As a whole fringe corresponds to one hundred thousandth of an inch, the measurement is correct to within a millionth of an inch.

The corresponding correction for periodic errors is transferred to the worm-wheel which turns the screw; and for errors of run to the nut which moves the carriage. In this way the final errors have been almost completely eliminated and the resulting gratings have very nearly realized their theoretical efficiency.

A number of minor points may be mentioned which have contributed to the success of the undertaking.

(*a*) The ways which guide the grating carriage as well as those which control the motion of the ruling diamond must be very

true; and these were straightened by application of an auto-collimating device which made the deviation from a straight line less than a second of arc.

(*b*) The friction of the grating carriage on the ways was diminished to about one tenth of that due to the weight (which may amount to twenty to forty pounds) by floating on mercury.

(*c*) The longitudinal motion of the screw was prevented by allowing its spherically rounded end to rest against an optically plane surface of diamond which could be adjusted normal to the axis of the screw.

(*d*) The screw was turned by a worm wheel (instead of pawl and ratchet) which permits a simple and effective correction of the periodic errors of the screw throughout its whole length.

(*e*) A correcting device which eliminates periodic errors of higher orders.

(*f*) It may be added that the nut which actuates the carriage had bearing surfaces of soft metal (tin) instead of wood, as in preceding machines. It was not found necessary to unclamp the nut in bringing it back to the starting point.

Finally it may be noted that instead of attempting to eliminate the errors of the screw by long continued grinding—which inevitably leads to a rounding of the threads—it has been the main object to make these errors conveniently small; but especially to make them constant—for on this constancy depends the possibility of automatic correction.

The accompanying photograph made with a ten-inch grating, 6th order (actual ruled surface 9.4 inches by 2.8 inches), used in the Littrow form with an excellent 8-inch lens by Brashear, is given in evidence of its performance. The resolving power as shown by the accompanying scale of Angström units is about 450,000. The original negative shows a resolving power of about 600,000. The theoretical value is 660,000.

Doubtless the possibility of ruling a perfect grating by means of the light waves of a homogeneous source has occurred to many—and indeed this was one of the methods first attempted.

It may still prove entirely feasible—and is still held in reserve if

serious difficulty is encountered in an attempt now in progress to produce gratings of twenty inches or more. Such a method may be made partly or perhaps completely automatic, and would be independent of screws or other instrumental appliances.

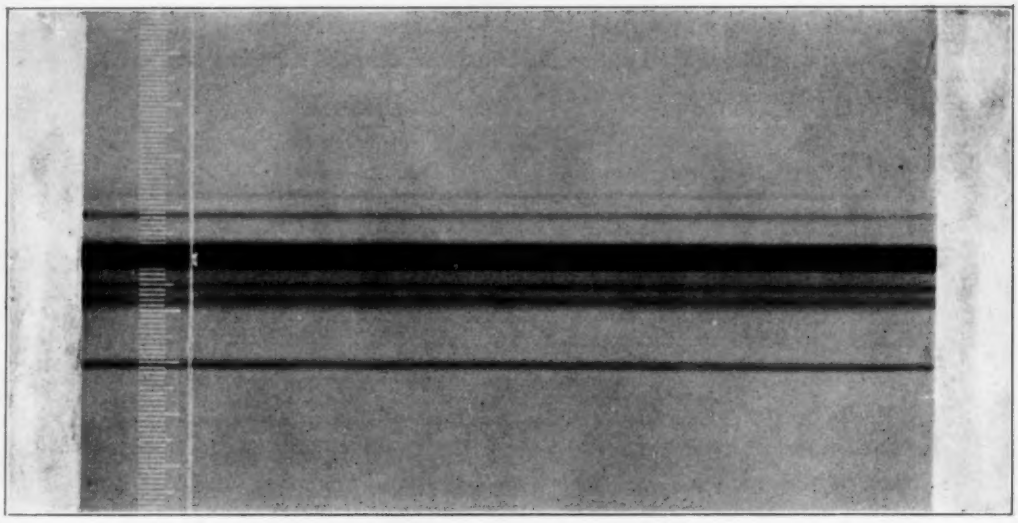

ENLARGEMENT OF PHOTOGRAPH OF THE GREEN MERCURY LINE λ 5461, taken by H. L. Lemon with 10-inch diffraction grating in sixth order. Scale: 1 division = 0.01 A.U.; ruled surface 9⅜ in. × 2⅞ in., 11,700 lines per inch. Mounted in Littrow form with 8-inch lens by Brashear. Focal length 20 feet.

It may be pointed out that an even simpler and more direct application of light-waves from a homogeneous source is theoretically possible and perhaps experimentally realizable.

If a point source of such radiations send its light-waves to a collimating lens and the resulting plane waves are reflected at normal incidence from a plane surface, stationary waves will be set up as in the Lippman plates; these will impress an inclined photographic plate with parallel lines as in the experiment of Wiener; and the only limit to the resolving power of the resulting grating is that which depends on the degree of homogeneity of the light used. As some of the constituents of the radiations of mercury have been shown to be capable of interfering with difference of path of over

a million waves, such as grating would have a resolving power exceeding a million.

This investigation has had assistance from the Bache Fund of the National Academy of Science, from the Carnegie Institution, and from the University of Chicago.

In addition to the grateful acknowledgment to these institutions I would add my high appreciation of the faithful services rendered by Messrs. Julius Pearson and Fred Pearson.

THE CONSTITUTION OF THE HEREDITARY MATERIAL.

By T. H. MORGAN.

(*Read April 23, 1915.*)

There are two ways in which the relation of the egg to the characters of the individual that develops from the egg has been interpreted.

1. The egg has been thought of as a whole and the characters of the individual as the product of its activity as a unit.

2. The egg has been thought of as made up of representative particles of some sort that stand in a definite relation to the parts of the individual that comes from the egg.

Weismann, whose speculations occupied the forefront of interest at the close of the last century, adopted the latter view; namely, that the germ is made up of particles, which he called determiners. For Weismann embryonic development became merely the sorting out of the particles of the germ to their respective parts of the embryo. Each region of the body owed its peculiarities to the particles that came to it by this sorting-out process. In fact, one may go so far, I think, as to say that Weismann borrowed from Roux this particular form of the preformation in order to give a formal explanation of *embryonic differentiation*. But Weismann's theory soon encountered three serious reverses.

In the first place, the study of the minute structure and behavior of the segmenting egg shows no evidence that any such sorting-out process takes place, as Weismann postulated. It has been shown that the chromosomes divide equally at every division, and that every cell of the body contains the entire complex that was present in the fertilized egg-cell itself.

In the second place, it was shown that the sequence of the cleavage planes of the egg could be artificially altered, yet a normal embryo develop.

In the third place, it was shown that in some eggs each of the first two, or first four cells derived from the egg is capable of forming a whole embryo. This result creates a strong presumption against the adequacy of Weismann's interpretation of development.

Meanwhile one of the greatest biological discoveries of the last century—one that had a very direct bearing on the traditional interpretations of predetermination—was forgotten. I refer to Mendel's work. Mendel showed that when two related organisms, differing from each other in a single character, are crossed, and their offspring are again bred together, that in the second generation individuals appear that are like their grandparents. He showed that the numerical proportions, in which they appear, could be explained on the assumption of one factor difference between the original forms. This result might be interpreted to mean either that the two original germ cells, taken as a whole, represent such a factor difference; or it might be interpreted to mean that the original germ cells had one particulate difference. But Mendel went further, and showed that when two related organisms that differ in two, or three, or more different characters are bred to each other, all possible combinations of the original characters appear later. It might seem then that we must abandon the view that each germ cell is to be thought of as a whole, for we see that the parts of each can be separated to become parts of others. In this sense Mendel's results seem to furnish a brilliant confirmation of Weismann's theory, in so far as it relates to preformation in the germ, and in the last edition of his "Vorträge ueber Descendenz Theorie," Weismann put in his claim to this verification.

In fact, Mendel's discovery does furnish a strong argument in favor of that part of Weismann's view that deals with the constitution of the germ-plasm, but it by no means confirms that part of Weismann's theory which postulates that embryonic development is a sorting-out process of representative particles.

Let us turn our attention, then, to Mendel's law and examine in how far it justifies an assumption that there are specific substances in the germ cells.

Mendel's law postulates that the early germ cells (and it may be added all of the body cells too) contain two of each kind of the

hereditary factors,—one derived from each of its parents. Mendel's law postulates further, that, in the ripening of the germ cells, the members of each pair separate (Fig. 1). Each mature germ cell comes to contain but a single element (or factor) of each kind.

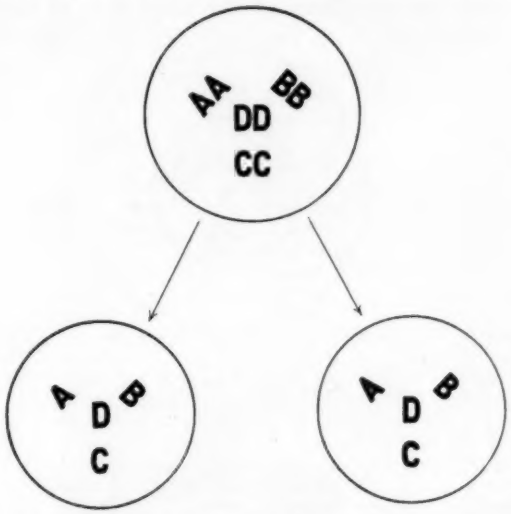

FIG. 1. Diagram to illustrate segregation of factors. The four pairs of factors represented in the upper circle by AA, BB, CC, DD, undergo segregation so that each germ cell comes to contain one member of each pair.

Now students of cytology had quite independently come to this same conclusion in regard to the germ cells. They had found that each cell contains a definite number of chromosomes, and that there are two of each kind of chromosomes in every cell,—one from each parent (Fig. 2, *a*). It had been found that at the ripening of the germ cells the members of each pair of chromosomes conjugate (Fig. 2, *b*), and then separate from each other (Fig. 2, *c*), so that each mature germ cell comes to contain but a single set of chromosomes (Fig. 2, *d*). Furthermore, students of experimental embryology had obtained independent evidence pointing to the chromosomes as the bearers of the hereditary materials.

We find, then, that cytologists had discovered a mechanism in the cell that they had reason to think was the bearer of the hereditary materials, and that the mechanism fulfills the essential

requirements of Mendel's postulates. There were two further steps necessary to bring the two lines of inquiry into complete accord; namely, (1) correspondence between the number of the chromosomes and the groups of inherited characters, and (2) the interchange between the members of the same pair of chromosome.

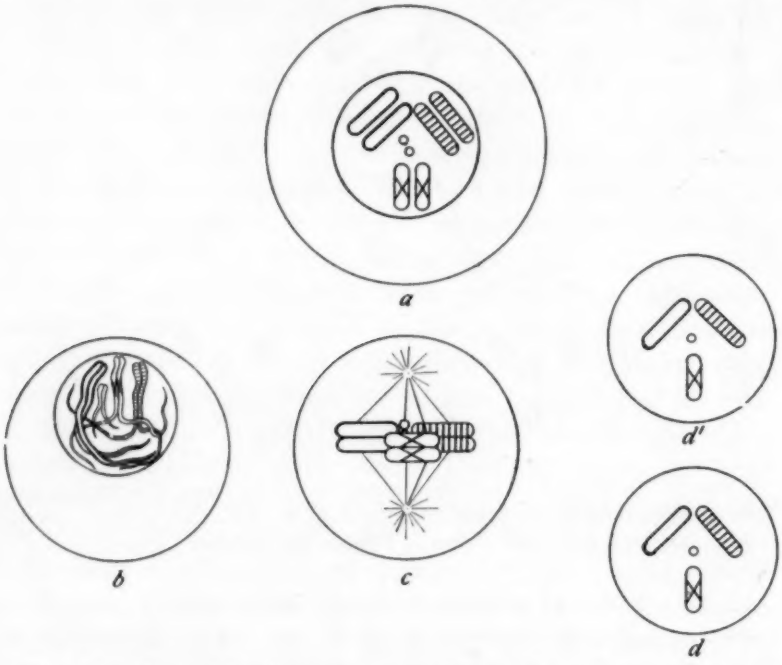

FIG. 2. Diagram to illustrate segregation of chromosomes. The four pairs of chromosomes in the upper circle (*a*), conjugate in (*b*) (synopsis stage), prepare for separation in (*c*) and undergo segregation so that each germ cell (d, d') comes to contain one member of each pair.

The number of chromosomes is small in comparison with the large number of different characters that an animal or a plant possesses. We should expect therefore if in any animal or plant a sufficient number of character-differences were known that the characters would be found to be inherited in groups, and that the number of such groups should be the number of chromosome pairs that such an animal or plant possesses. In very few cases have enough characters been found to make such a comparison of any value.

But in the fruit fly, *Drosophila,* that has been intensively studied for five years, over a hundred new, and inherited characters have appeared. They fall into four great groups. A partial list of the four groups is as follows:

GROUP I.

Name.	Region Affected.
Abnormal	Abdomen
Bar	Eye
Bifid	Venation
Bow	Wing
Cherry	Eye color
Chrome	Body color
Cleft	Venation
Club	Wing
Depressed	Wing
Dotted	Thorax
Eosin	Eye color
Facet	Ommatidia
Forked	Spines
Furrowed	Eye
Fused	Venation
Green	Body color
Jaunty	Wing
Lemon	Body color
Lethals, 13	Die
Miniature	Wing
Notch	Venation
Reduplicated	Eye color
Ruby	Legs
Rudimentary	Wings
Sable	Body color
Shifted	Venation
Short	Wing
Skee	Wing
Spoon	Wing
Spot	Body color
Tan	Antenna
Truncate	Wing
Vermilion	Eye color
White	Eye color
Yellow	Body color

GROUP II.

Name.	Region Affected.
Antlered	Wing
Apterous	Wing
Arc	Wing
Balloon	Venation
Black	Body color
Blistered	Wing
Comma	Thorax mark
Confluent	Venation
Cream II	Eye color
Curved	Wing
Dachs	Legs
Extra vein.	Venation
Fringed	Wing
Jaunty	Wing
Limited	Abdominal band
Little crossover	II chromosome
Morula	Ommatidia
Olive	Body color
Plexus	Venation
Purple	Eye color
Speck	Thorax mark
Strap	Wing
Streak	Pattern
Trefoil	Pattern
Truncate	Wing
Vestigial	Wing

GROUP III.

Name.	Region Affected.
Band	Pattern
Beaded	Wing
Cream III	Eye color
Deformed	Eye
Dwarf	Size of body
Ebony	Body color
Giant	Size of body
Kidney	Eye
Low crossingover	III chromosome
Maroon	Eye color
Peach	Eye color

GROUP IV.

Name.	Region Affected.
Bent	Wing
Eyeless	Eye

GROUP III.—*Continued.*

Name.	Region Affected.
Pink	Eye color
Rough	Eye
Safranin	Eye color
Sepia	Eye color
Sooty	Body color
Spineless	Spines
Spread	Wing
Trident	Pattern
Truncate intensf.	Wing
Whitehead	Pattern
White ocelli	Simple eye

The four pairs of chromosomes of *Drosophila* are shown in the next diagram, Fig. 3.

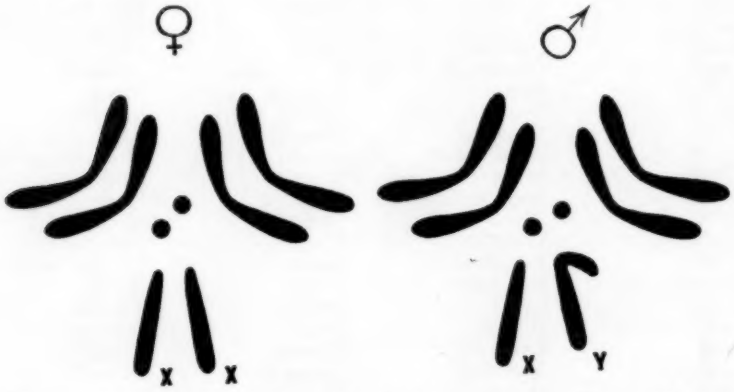

FIG. 3. Diagram of the four pairs of chromosomes of Drosophila ampelophila; to the left the chromosomes of the female; to the right those of the male.

The correspondence between the four character groups and the four pairs of chromosomes is obvious even to the size relations. This relation, or correspondence, does not however tell us anything in respect to the way in which the chromosomes stand for the characters of the group. So far, the result only shows that the characters of a given group are in some way represented in a particular chromosome. Our work has, however, carried us beyond this point. I may illustrate this by an example from the first group, containing sex linked characters. We mean by sex linked characters that they follow the known distribution of the X chromosomes. For in-

stance, the factor that determines the character for white eyes is sex linked, as is also the factor that determines the character for miniature wings. If we cross a female with white eyes and miniature wings to a male with red eyes and long wings, the sons will have white eyes and miniature wings. The explanation of this result is found in the distribution of the chromosomes. The sons get their single X chromosomes from their mother. Hence they show the characters that this chromosome carried in the mother, who had white eyes and miniature wings. The daughters, however, get one of their X chromosomes from their father through his female producing sperm. This chromosome carried a factor for red eyes and another for long wings, which factors dominate those carried by the other X chromosome that the daughters get from their mother, namely, the factors for white eyes and for miniature wings. These relations are shown in Fig. 4.

If these daughters and sons are bred to each other they produce four kinds of individuals, viz., red long, white miniature, red miniature, and white long. These are the four classes that Mendel's law calls for, but they do not occur in the Mendelian proportion (9:3::3:1) when two pairs of factors, as here, are involved. The reason for this is two-fold. In the first place the female alone carries two X chromosomes. The male carries but one. Hence there is an unequal distribution of the X chromosomes in the spermatozoa, for, only half of them can get an X chromosome. These are the female-producing spermatozoa. The result is, as has been shown, that in the first generation the sons inherit their single X chromosome from their mother and none of the dominant characters of the father. Since in this case the sons carry no dominant factor either in their X bearing (female producing), or in their Y bearing (male producing sperm), the second generation here reveals completely the composition of the egg cells that the F_1 female carries.

On Mendel's law of random assortment of two pairs of factors we should expect the four classes that here appear in the second generation to be equal in number. On the contrary we find that two of them are twice as numerous as the other two. On inspection we see that the two larger classes are white miniature and red

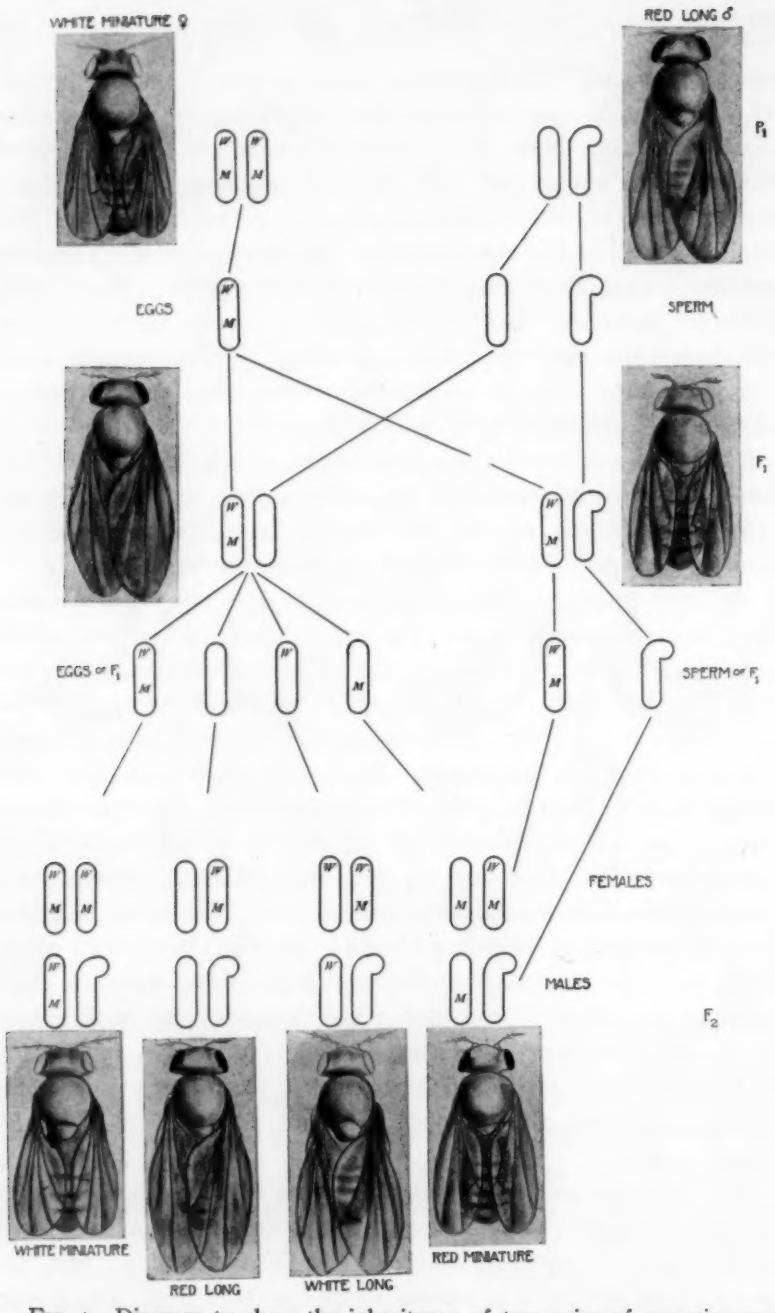

FIG. 4. Diagram to show the inheritance of two pairs of recessive sex linked characters, viz. white eyes (W) and miniature wings (M). The normal, dominant allelomorphs of these factors are omitted.

long. These correspond to the two grandparents. The two smaller classes are white long and red miniature.

We can account for this result if we assume first that the two factors that went in together in the same chromosome tend to hold together. This would account for the two larger classes. Second that the two smaller classes are due to interchanges between the two X chromosomes. Such interchange would here take place only once in three times.

We can test this conclusion by planning the experiment in such a way that white and miniature now go in from opposite sides,—white from one parent, and miniature from the other. When we do this we find that the large classes in the second (back cross) generation will be red miniature and white long and that the small classes will now be red long and white miniature. The ratio of the large to the small classes will be exactly the same as in the first case. In other words the interchange between the X chromosomes is the same regardless of what factors each contains.

If one admits that the chromosomes are the bearers of the hereditary factors he is forced to admit that experiments like these prove that somehow interchange of factors in homologous chromosomes must occur.

If one thinks of the factors as lying in a linear series in the chromosome (and there is certain evidence that I can not consider here that makes this view imperative) then the chance of a crossing over taking place somewhere in the region between two pairs of factors would be greater the farther apart the factors lie. The percentage of times that crossing over takes place becomes then a measure of the distance apart of the factors in question. If we make this assumption we find that we can give a consistent explanation of everything that we have found in the inheritance of linked factors in *Drosophila*. Not only this, but a far more important fact comes to light. If we determine, on the aforesaid basis, the relation to each other of all the known factors in each of the four groups, then, when a new factor appears, we need only determine its group and its relation to two factors in that group. With this information we can predict its relation to all other members of that group. In other words we can predict what the numerical relation

will be in the second generation. There is no other way as yet discovered by means of which this relation can be predicted.

If we compare our conception of the structure of the germ plasm with that of Weismann we find in all of his writings except the last one, that he supposed the chromosomes to be alike and that each consisted of a series of ids that contained the totality of the determiners that influence development.

It is true that in his last writing he partially abandons his earlier idea of *whole ids* for a conception nearer to ours of *partial ids*,—at least for some of the determiners. In this respect his view more nearly approaches the one here maintained. But even then his view not being based on numerical data would leave us entirely helpless in explaining the phenomena of inheritance in any particular case. Without wishing in the least to detract from the value of Weismann's brilliant speculation, nevertheless the difference in the way in which the conclusions were reached in the two cases is one of fundamental significance in all scientific work. Our view is based on accurate numerical data that enables us to predict what any given result in this field will be. It is this power to predict that gives significance to a scientific theory. In this regard we believe that our interpretation is a long step in advance of the purely imaginative conception of the germ plasm that Weismann advanced.

If now we bring our conception of the germ plasm to bear on the problem of development we have a very different view point of that process from the one Weismann pictured.

We think of every cell in the body containing one set of chromosomes received from the mother plus one set from the father. The materials carried by these chromosomes influence development in their entirety. Although we are able to localize certain materials in the chromosomes that when present cause the eyes to be white, and others that cause the eyes to be red, we do not mean that these materials in the chromosomes go directly only to the parts that show their influence more markedly. We mean that given one kind of material and the rest of the cell there is elaborated a white eye; given a different material in the same locus it produces, in conjunction with the rest of the cell, a red eye.

To say that the germinal material that makes a white eye is different from the germinal material that makes a red eye is a platitude. But to be able to locate a particular material in the one case *in relation to other materials* is a very different matter, because by means of this information we are able to explain the results on a mechanistic basis, and are able to predict the results of untried combinations. Without this information the prediction would be impossible.

We are led then to a third conception of predetermination. It is this! That while the hereditary material is made up of different discrete and separable particles (chemical substances) that have a definite position in the chromosomes, the effects of each of these particles must be supposed to be produced in combination with many, or even with all other parts of the cells in which they are contained.

COLUMBIA UNIVERSITY,
NEW YORK.

PROC. AMER. PHIL. SOC., LIV. 217 K, PRINTED JULY 7, 1915.

SPONTANEOUS GENERATION OF HEAT IN RECENTLY HARDENED STEEL.

By CHARLES F. BRUSH.

(*Read April 22, 1915.*)

Two or three years ago, when studying the behavior, under certain conditions, of several specimens of hardened tool steel, I observed that they all spontaneously generated a small quantity of heat, the amount of which diminished from day to day, but which was observable for several weeks. In each case the steel had been hardened only a few days prior to its use. It seemed highly probable that the generation of heat was associated with some sort of "seasoning" or incipient annealing process, perhaps accompanied by slight change of volume, and that it would be most rapid immediately after hardening. I resolved to investigate this curious phenomenon more fully, but failed to spare the time until a few months ago. This investigation forms the subject of the present paper.

Fig. 1 is a diagram of the apparatus employed. *A, B* represent two large silvered Dewar vacuum jars selected to have very nearly equal thermal insulating efficiency. They are supported in a wooden rack inside a thick copper cylinder *C* packed in granulated cork in a wooden box *E*. *D* is a paper extension of *C*, packed with layers of felt by removal of which and the loose copper cover of *C* easy access is had to the Dewar jars. The copper cylinder weighs 52 pounds and its functions are, by reason of its large thermal capacity and high conductivity, to protect the Dewar jars from any rapid change of temperature, and from temperature stratification.

The box *E* is surrounded by a much larger wooden box *F* lagged with a half-inch layer of felt. A long resistance wire is strung back and forth in the air space between the boxes at the bottom and four sides of *E*. Electric current controlled by a thermostat warms the wire, whereby the temperature of the air space may be maintained very nearly constant as many days or weeks as desired. A

thermometer T, easily read to hundredths of a degree, indicates the temperature of the air space.

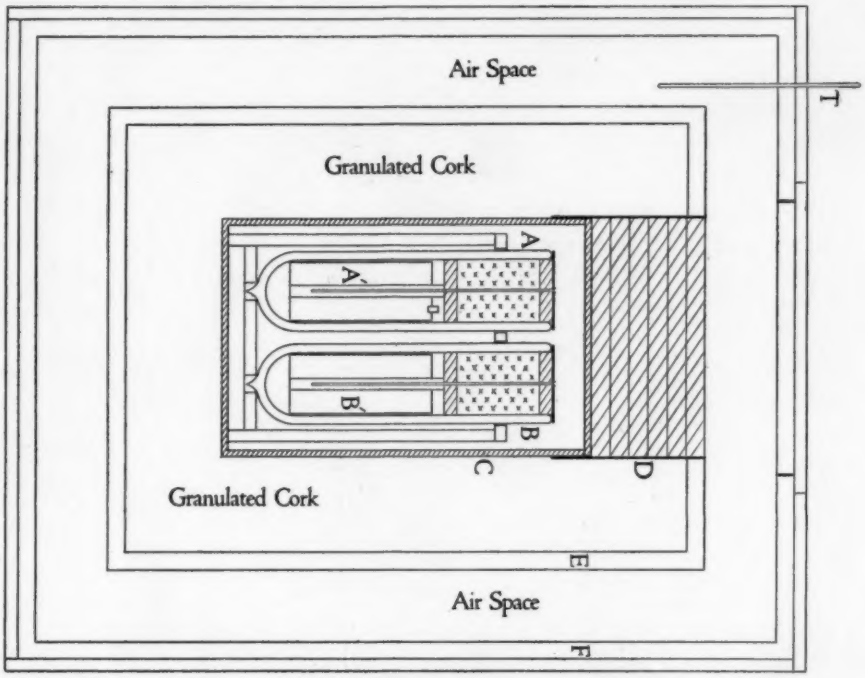

FIG. 1.

Returning now the core of the apparatus: A' is an air-tight cylinder of thin copper, six inches high and two and a half inches in diameter, provided with an open half-inch axial tube also of copper. A small round opening at the top of A' permits the introduction of a weighed quantity of water, after which the opening is tightly corked to prevent any change of temperature by evaporation of the water. B' is another copper cylinder just like A' except that it has a removable top to permit the introduction of the substance whose thermal behavior is to be investigated. The high thermal conductivity of these copper cylinders prevents temperature stratification within them. The Dewar jars are filled above the copper cylinders with layers of felt, and granulated cork, and covered with waxed cardboard carefully sealed on to prevent temperature dif-

ference inside the jars which would follow unequal loss or gain of moisture by the felt and granulated cork. A small thin glass tube, flanged at top and closed at bottom, is located in the axis of each Dewar jar and extends from the waxed cover nearly to the bottom of the inclosed copper cylinder. The glass tubes contain the ends of thermo-electric couples of fine constantan, copper and iron wires, one iron-constantan and one copper-constantan junction at the bottom of each tube. The leading-out wires are copper, and connect the thermo-couples with a reflecting galvanometer having the customary reading telescope and scale. Careful callibration has shown that 55 scale divisions of the galvanometer indicate one degree C. temperature-difference between A' and B', and that temperature-difference and galvanometer deflection are very closely proportional throughout the range used.

In the following experiment A' and B' were removed from the Dewar jars and allowed to attain equal room temperature. Twelve half-inch round bars of tool steel, five inches long and with machined surfaces, were hardened by heating to high "cherry-red" in a reducing atmosphere of a gas furnace and quenching in *cold* water. The bars then had a thin and strongly adhering coating of black oxide. They were next stirred in a large quantity of water at room temperature, to acquire that temperature, wiped dry, and oiled with heavy, neutral mineral oil to prevent generation of heat by further surface oxidation, wiped free of excess of oil and placed in the copper cylinder B'. A weighed quantity of water, also at room temperature, just sufficient to equal the steel bars in thermal capacity had already been placed in A'. The whole apparatus was then assembled as quickly as possible, and galvanometer readings commenced within forty-five minutes of the time of hardening the steel.

The upper curve in Fig. 2 shows the progress of heat generation in the steel bars during the first 150 hours after hardening. A very slow generation of heat was still easily observable at the end of a month.

It is seen that the temperature of the steel bars was rising rapidly when the galvanometer readings commenced, and reached a point (nearly 3° C. at the summit of the curve) where gain and loss of heat balanced each other in about 8 hours.

The "Normal Cooling" curve was obtained five or six weeks after the other, and when the generation of heat had very nearly

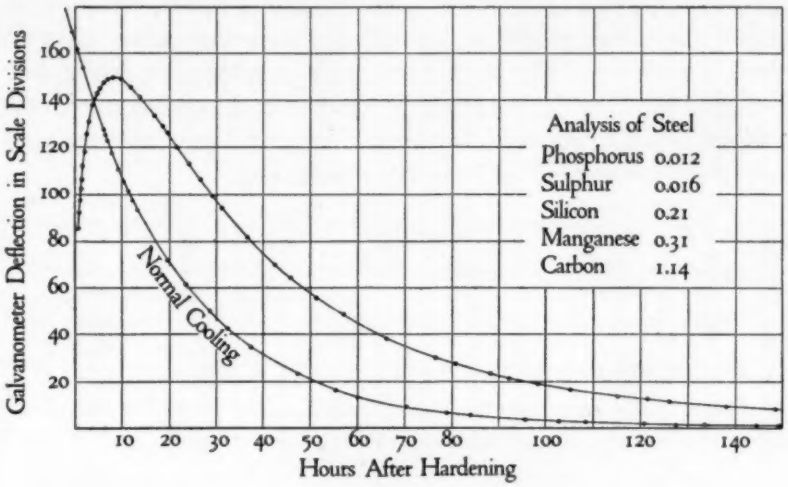

FIG. 2.

ceased. For this purpose the steel bars were removed, warmed a few degrees, and replaced; then galvanometer readings were made from time to time as before. This curve is plotted in a location convenient for visual comparison with the heating curve, but otherwise might just as well be plotted further to the right.

From the two observed curves I have computed a third curve (not shown) which represents the progressive rise in temperature which would have occurred if the thermal insulation of the steel had been perfect, so as to prevent any loss of heat. The curve is strikingly similar in character to the shrinkage curve shown in Fig. 5, and indicates a close association of heat generation and shrinking, to which I shall refer again. The total rise in temperature indicated (about five degrees C.) is of little quantitative importance because it is highly probable that it would have been different if the steel had been hardened at a different temperature, or more uniformly hardened throughout each bar, or had a different carbon content. Yet it is interesting to note that the observed quantity of heat spontaneously generated in the steel, measured by its rise in temperature multiplied by its thermal capacity, indicates internal

work of some sort sufficient to lift the steel bodily about 800 feet high against the force of gravity.

I next prepared a batch of "high-speed" tungsten steel consisting of the same number of bars of the same dimensions as in the first experiment. The bars were water-hardened at white heat, not far below the fusing point, brought to room temperature, oiled and introduced just as in the former case, and galvanometer readings were commenced an hour after hardening.

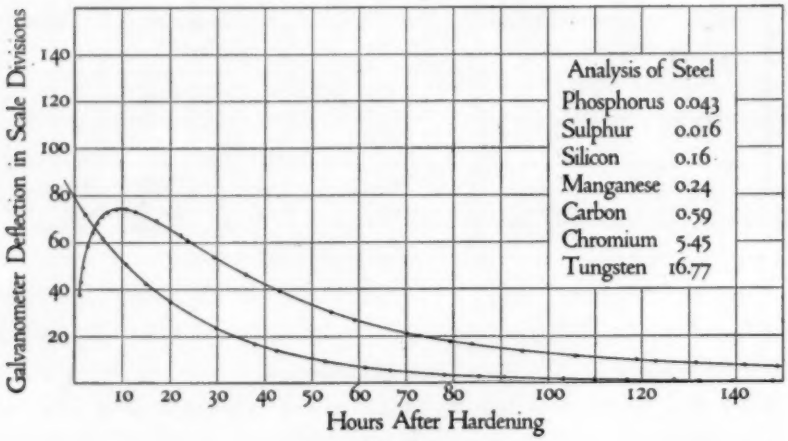

FIG. 3.

Fig. 3 shows the curve of heat generation in the "high-speed" steel, and the curve of normal cooling located with respect thereto as in Fig. 2. The cooling curve here shown is the lower part of that used in Fig. 2. It is permissible to use the same cooling curve for both kinds of steel because the thermal capacity of the two lots was very nearly the same.

It is seen that heat generation in the tungsten steel was the same in character as in the carbon steel of Fig. 2, though much less in amount and somewhat more persistent.

Many workers in steel are aware that the metal expands a little when hardened, and shrinks when annealed; but I have not met with any quantitative data on the subject. With the hope of throwing some light on the spontaneous generation of heat already described, I investigated this phenomenon of swelling and shrinking as follows:

Having no more of the carbon steel used in the first experiment, I procured another half-inch round bar of the same brand, though slightly different in composition as the analyses show. With a piece of this bar two and a half inches long I made a careful determination of its specific gravity under the conditions, and with the results, shown in the following table.

TABLE I.

Specific Gravity		Analysis of Steel	
Commercial Condition	7.8507	Phosphorus	0.015
After Hardening	7.8127	Sulphur	0.021
After Tempering to Light Blue	7.8350	Silicon	0.16
After Annealing	7.8529	Manganese	0.33
		Carbon	1.07

The difference in density and volume between the hardened and annealed conditions is fully a half per cent., which is much more than I expected to find; and nearly half of the total shrinkage was brought about by the very moderate heating necessary for "tempering to light blue." The annealing was very thorough, and, as the figures show, was more complete than in the annealed "commercial condition."

The shrinkage incident to tempering was large enought to encourage the hope that if any spontaneous shrinking, at room temperature, occurs during the generation of heat which follows hardening, it might be detected and measured. For this purpose the apparatus shown in Fig. 4 was designed and constructed.

In Fig. 4 *G* and *H* are two vertical steel rods three feet long and one millimeter in diameter. They are hung from a common rigid metal support *I*, and at their lower ends carry parallel brass bars *G'*, *H'* which move with perfect freedom, yet in close contact, between guides *K*, *K*. The brass bars are accurately machined, and their front edges are polished. The rod *G*, whose function is purely comparative, is kept under moderate and constant tension by the long spiral spring *L;* while the rod *H* carries a four pound weight *M*. An enlarged sectional diagram at the right shows the method employed in mounting each steel rod. Each end of the rod passes through, and is soldered into, a brass head having a hemi-

spherical end which accurately seats itself in a hollow metal cone. The rods are quickly removable through vertical slots in the cones.

After some preliminary experiments, to get acquainted with the apparatus, a fresh rod *H* was hardened by placing it horizontally in a wooden rack just above a trough of water at room temperature, quickly heating it to bright redness by passing suitable electric

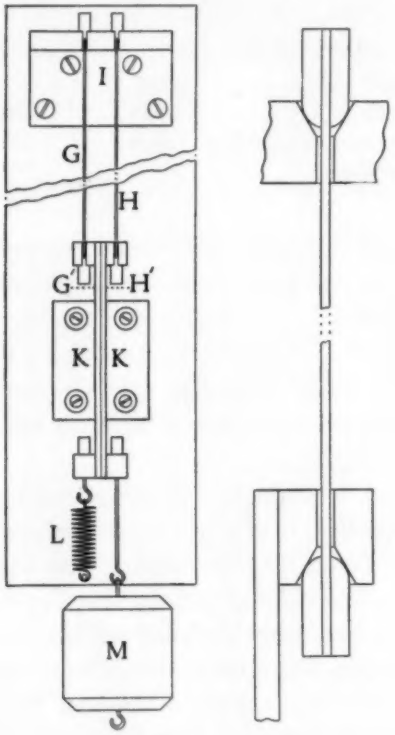

FIG. 4.

current through it and plunging it in the water beneath, the act of lowering the rod serving to break the electric circuit. The rod was kept straight while hot by means of a weak spiral spring which took up the expansion. Preliminary experiments had shown that a rod could be hardened in this way without warping.

The hardened rod, already at room temperature, was quickly wiped dry and put in place beside *G*. Then, without delay, a fine

horizontal scratch was drawn across the polished fronts of the bars G', H' by means of a straight-edge and sharp needle point lightly applied. A microscope, magnifying about 200 diameters and very solidly mounted, was brought into position and focused on the horizontal scratch, which of course consisted of an independent scratch on each bar, the two halves being initially in perfect register. The microscope was provided with a filar micrometer eyepiece carefully calibrated and adapted to measure accurately any departure from register of the two half lines or scratches.

Shrinkage of the hardened rod H was detected within two minutes after scratching the brass bars, and was easily observable at the end of two weeks.

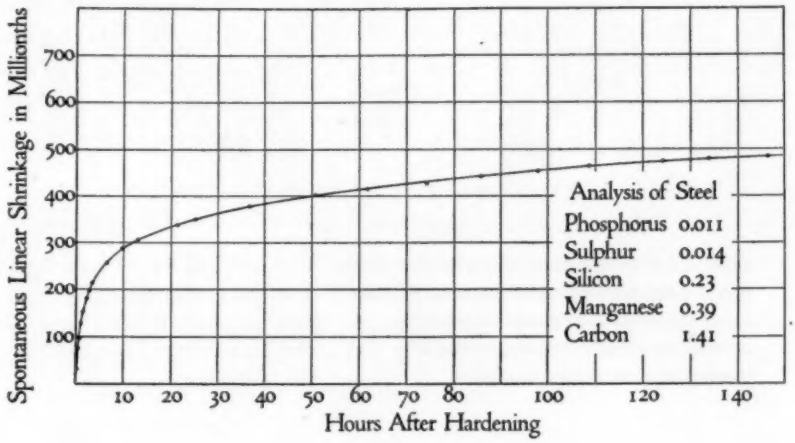

FIG. 5.

Fig. 5 shows the progress of shrinking during the first 150 hours. The curve reached the 500 line a day or two later. The hardened length of the rod was assumed to be 35 inches, so that its actual shrinkage at the 500 line of the curve was 0.0175 inch.

The rod was next scoured clean and tempered to light straw color by electric warming, then to light blue color, and its total shrinkage measured after each operation. Finally, it was thoroughly annealed by bedding in mineral wool, heating to very low redness half an hour, and then gradually reducing the heating current to nothing in the course of two or three hours, after which

the shrinkage was again measured. The rod shrank very considerably in each operation, as indicated quantitatively in Table 2, in which the annealed length is taken as unity or 100 per cent.

TABLE 2.

Length of rod after hardening	100.383
After spontaneous shrinking	100.332
After tempering to light straw	100.182
After tempering to light blue	100.131
After annealing	100.000

Of course the shrinkage in volume must have been very nearly three times the linear shrinkage, or considerably more than one per cent. from the hardened to the annealed condition, which is more than double that observed in the bar steel used in the first experiment. Doubtless this was due to the higher carbon content of the small rod, and more uniform hardening owing to its small size. It is highly probable also that more heat was generated per unit of mass.

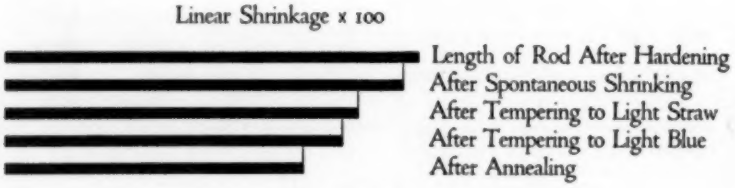
Linear Shrinkage x 100
Length of Rod After Hardening
After Spontaneous Shrinking
After Tempering to Light Straw
After Tempering to Light Blue
After Annealing

FIG. 6.

In Fig. 6 I have visualized the stages of shrinking of the small rod by magnifying a hundred-fold the observed quantities in Table 2.

I have already pointed out the close similarity in character of the spontaneous-shrinkage curve (Fig. 5) and the computed curve of total heat generation; and there seems little room for doubt that the two phenomena are quantitatively related. But it is equally clear that spontaneous shrinking is only incident to, and is not the prime cause of the generation of heat, because the internal work represented by the heat generated is hundreds of times more than necessary to bring about the accompanying change in volume. This

is found as follows: The small steel rod spontaneously shrank 0.0175 inch. To spring it back to its original length required a weight of 15 pounds hung below *M*, Fig. 4 (= 12.400 pounds strain per square inch of cross-section). Hence, in longitudinally shrinking 0.0175 inch, the rod had done work equal to lifting 15 pounds half this distance or 0.00875 inch. The rod weighed about 1230 times less than the weight, so that the work done was sufficient to lift the rod itself $1230 \times .00875 = 10.76$ inches. But this represents one-dimensional shrinking only, and we must take three times this amount of lift, or, say 2⅔ feet, to represent the work done in the three-dimensional shrinking which certainly occurred. We have already seen that the internal work spontaneously done in the steel bars of the first experiment, in generating the observed amount of heat, was sufficient to lift the bars about 800 feet, which is 300 times greater than the work done in spontaneously shrinking the small rod. If spontaneous shrinkage was less in the large bars than in the small rod, which is highly probable, then this ratio was accordingly greater than three hundred to one. The disparity in weight between the twelve large bars and the one small rod does not count, because the work done in each case is computed for the weight of steel which did it.

It has been suggested that loss of the generated heat may perhaps be regarded as a cooling process without change of temperature (which implies reduction in specific heat), and that this may be sufficient to account for the spontaneous shrinkage. But this hypothesis accounts for only a modest fraction of the shrinkage; while the implied change in specific heat is much too large to be admissible.

An attempt was made to measure Young's modulus of elasticity in the small rod both in the hardened condition (after spontaneous shrinking) and after annealing, by hanging various weights below *M*, Fig. 4, and measuring with the microscope the distortions produced,—always far within the elastic limit. But I was unable to obtain reliable results because of an interesting fact which was brought to light, as follows: In the annealed condition the steel exhibited a small amount of viscosity or internal friction which somewhat delayed full distortion and subsequent restitution; but in the

hardened condition the viscosity was *many times greater*. This is a further illustration of the instability of the hardened steel.

In conclusion, I am led to regard the hardened steel as being in a condition of very great molecular strain somewhat unstable, especially at first. Spontaneous relief of a small portion of the strain causes generation of heat until stability at room temperature is reached. Any considerable rise of temperature, as in tempering, permits further spontaneous relief of strain, or molecular rearrangement, doubtless accompanied by more generation of heat, and so on until annealing temperature is reached. It is obvious that the process of tempering or annealing steel is an exothermic one, and conversely that hardening is an endothermic process.

CLEVELAND,
April, 1915.

RELATIONSHIPS OF THE WHITE OAKS OF EASTERN NORTH AMERICA,

WITH AN INTRODUCTORY SKETCH OF THEIR PHYLOGENETIC HISTORY.[1]

BY MARGARET V. COBB.

(PLATES IV–VI.)

(*Read April 23, 1915.*)

I. HISTORY OF THE FAGACEÆ: A RECONSTRUCTION.

Prantl's Classification of the Fagaceæ.

Castaneæ	Quercus.
	Pasania.
	Castanea.
Fageæ	Fagus.
	Nothofagus.

The five or six genera of the family Fagaceæ to which the oaks belong were well differentiated at least as far back as the Cretaceous age. The beeches are sharply separated from the remainder of the family (the pasanias, chestnuts and oaks), and are undoubtedly the more primitive of the two groups. *Nothofagus,* the genus of primitive beeches, is a characteristically sub-Antarctic genus, still surviving in Tasmania, New Zealand, and the southern part of South America (a South Pacific distribution). *Fagus* itself, once more widely spread, is now found only in Japan, North America and Europe.

The pasanias, chestnuts and oaks are at present in possession of the temperate and tropical regions of Asia, North America, Europe and Mediterranean Africa. Species are most numerous in southeast Asia and in Mexico (regions separated by the Pacific). *Pasania* is limited to southeast Asia, except for one species in California

[1] This paper owes a great deal to the extensive knowledge and the never-failing interest and aid of Dr. William Trelease, under whom the work was done at the University of Illinois in the year 1913–14.

and one in New Zealand (ranges separated by the Pacific). *Castanopsis* (the less specialized chestnuts) is limited to southeast Asia, except for two Californian species (ranges separated by the Pacific). *Castanea* is present in southeast Asia, North America and Europe. *Quercus* has most numerous species in southeast Asia and (especially) Mexico and Central America (regions separated, again, by the Pacific), while the subgenus *Cyclobalanopsis* is limited to southeast Asia (monsoon province). In consideration of the facts that the most primitive genus still lingers on the two sides of the southern Pacific, and that so many other groups are found only in regions bordering on the northern Pacific, it is more than plausible that the family Fagaceæ originated in the Antarctic-Pacific region, and moved northward towards its present northern-hemisphere distribution in the region of the Pacific Ocean. This of course involves the hypothesis of an ancient Cretaceous or pre-Cretaceous Pacific continent—for which there is much other distributional evidence and which Scharff,[2] among others, holds to be highly probable. The broad similarity of the ranges of *Pasania, Castanopsis* and *Cyclobalanopsis* was undoubtedly determined at this early time. The problem of the extension of certain species of *Fagus* and *Castanea* to Europe seems entirely separate, and probably belongs to a more recent period. *Quercus* is involved with both the older and the more modern distribution; they have been mapped out here for convenient reference in the coming discussion of *Quercus.*

II. History of Quercus, Hypothetically Reconstructed.

Oaks, living or fossil, have been reported from every continent. Living species, however, are unknown in the southern hemisphere, except that they are found south of the equator in the East Indies, and among the mountains of Ecuador (localities separated by the Pacific). Species, as was said, are most numerous in Mexico and Central America and in southeast Asia; the subgroup *Cyclobalanopsis* is limited to southeast Asia. Remembering that *Pasania* and *Castanopsis* are almost limited to the same region, and that the pasania-chestnut-oak group of the Fagaceæ shows here a concentration, and a profusion of species, seen nowhere else in the world,

[2] Scharff, "Distribution and Origin of Life in North America."

it is natural to suppose that this part of Asia (or more probably, to allow for the outlying species in California, and the oaks in Mexico, a region *east* from southeast Asia) has been the center of distribution, and hence the point of origin of the pasania-chestnut-oak group. And *Quercus* itself, with its black oaks limited to America, its *Cyclobalanopsis* limited to southeast Asia, and its numerous white oak species in both places, undoubtedly differentiated from the pasanias (or their ancestors) in one or other of these regions, or more probably between the two. At any rate, the primitive, little-differentiated *Quercus* must have had a distribution that included both regions, as well as the space between them. We are thus brought again to an hypothetical Pacific continent; for since neither black oak nor *Cyclobalanopsis* exists or gives evidence of having existed in western Asia or Europe, any cretaceous or earlier connection of the two regions in that direction is well-nigh inconceivable. (It is unnecessary to suppose that this Pacific land extended much farther north than the equator).

According to our hypothesis, the disappearance of this Pacific land isolated the two extremes of the range of *Quercus*. The genus had already become differentiated; the Asiatic part of the range received the stock of *Cyclobalanopsis* (found nowhere else) as well as the more typical *Quercus* stock. Certain species of *Quercus*, even today, form a part of the oldest Asiatic flora, which holds its own in isolated regions,—in parts of the Himalayas, for instance. Some of these ancient endemic species are the white oaks *Q. lanata, semecarpifolia,* and *dilatata,* of which the last is said by Schottky to stand nearest of all oaks to the *Cyclobalanopsis* group. (American black oaks, however, show certain features in common with *Cyclobalanopsis*—apical ovules, type of style).

The American end of the range received a group of oaks of which (according to evidence from distribution and palaeontology) *Quercus chrysolepis* is probably our nearest representative; these may have been the basis of both the black and the white oaks of America. It is suggestive to find that *Q. semecarpifolia* (representative of the ancient oaks of Asia) bears some resemblance to this early American oak. Some of the European oaks are also of this ancient type; but since one, *Q. Ilex,* occurs in both Asia and Europe,

the inference is that they all reached Europe westward from Asia. Though the older fossil evidences in this continent have all been referred to *Q. chrysolepis* (these date back to the Cretaceous), it seems not improbable that types such as *Q. emoryi* and *Q. hypoleuca* were soon present, and that differentiation early took the lines towards our American *black oaks* and *white oaks*. Since in *Cyclobalanopsis,* and in the pasanias, the abortive ovules are carried upward in growth till in the mature acorn they are typically apical, this may be considered the primitive condition in *Quercus*. *Chrysolepis,* which has them only lateral, is on the way towards having them in the basal, white-oak, position. The black oaks, on the contrary, have preserved the primitive character in this as in other particulars.

(Since the black oaks resemble *Cyclobalanopsis* in some ways, it may be that they differentiated from *Cyclobalanopsis,* in the Pacific region, before reaching America. Or all three may have diverged together from the primitive *Quercus*. Distribution may have been such that *Cyclobalanopsis* went to Asia, *Erythrobalanus* to America, *Lepidobalanus* to both.)

Having thus some conception of a possible Cretaceous history for American oaks, black and white, and of their relationship to the ancient types of Old World oaks, we may now limit ourselves to the white oak group in North America (*Leucobalanus*). For the black oaks, being limited to the western hemisphere and becoming only more sharply differentiated, can give us no further light on white oak relationships. To begin with, we may mark off *Leucobalanus* as follows:

QUERCUS.

Cyclobalanopsis: Abortive ovules apical, styles short, subcapitate, often recurved, cup scales grown into a solid ring, fruit ripening in one year, leaves evergreen, tertiary nerves very fine.

Erythrobalanus: Abortive ovules apical, styles elongated, subcapitate, often recurved, acorn tomentose within, cup scales thin, appressed, fruit ripening in two years, leaves deciduous or evergreen, lobes when present with bristle points.

Styles slender or very short and flattened, not cephalated at apex. *Lepidobalanus.*

Cerris: Abortive ovules basal, styles long, tapering, cup scales often long, bractlike, fruit ripening in two years, leaves more or less dentate.

Leucobalanus: Abortive ovules basal, styles very short, spatulate, acorn not tomentose within, cup scales often thickened at base, fruit ripening in one year, leaves deciduous or evergreen, lobes when present rounded.

The most stable characters in this classification seem to be the position of the abortive ovules, the lining of the acorn shell and the form of the style. Appression of scales, time for ripening fruit, and time of keeping leaves are all more or less variable among the white oaks.

The earliest home of *Leucobalanus* on this continent, using the term to include the white oaks as they separated themselves from the black oaks in America, seems to have been northern Mexico and the southwestern states. The older type (A. below) still predominates in this region, which has probably long been stable, with a climate similar to the present. It is a region which seems to have been for many species a center of distribution to other parts of the continent. Since the Cretaceous, much differentiation has taken place, the main lines of which may be represented by the following division of North American white oaks:

A. Leaves persistent, usually evergreen, entire, sinuate or dentate, or, if deeper lobed, with pungent tips.
  1. Many species, southwestern U. S. and Mexico.
  2. *Virginiana* and varieties—an early offshoot.
B. Leaves deciduous, lobed or divided, or serrate; lobes rounded, obtuse or acute but not pungent.

The evergreen series, represented, say, by *Q. undulata,* is the more direct continuation of the Cretaceous type, the deciduous the more modern form.

It is barely possible that not all of this differentiation took place on this continent. *Leucobalanus* reached Europe at some time; and the possibility that this took place early (by means of Scharff's Mediterranean land bridge), and that the deciduous oaks originated there, rather than on this continent, must be taken into account. Species of this type occur also in Asia, but there seems to be little doubt that they are sharply separated from the ancient Asiatic species like *semecarpifolia,* and reached Asia in the Tertiary from the eastward. The fact that the range of these species, in the Ter-

PROC. AMER. PHIL. SOC., LIV. 217 L, PRINTED JULY 21, 1915.

tiary, was, at the boreal end, continuous from Asia across America to Europe, gives the possibility of the center of distribution being either in Europe or in America. My data on European oaks are insufficient to decide this point; it seems, however, highly probable that the white oaks with thin, deciduous, lobed leaves originated in or near northern Mexico.

The early members of the group *Leucobalanus,* then, marked by entire, evergreen leaves, gave rise, probably in North America, to a form with thin, deciduous, lobed leaves. This type is now dominant over the greater part of the United States, while the older form holds its own in the southwest and in Mexico, where the climate has probably known no great fluctuations since the Cretaceous, and where it still finds suitable dry and arid habitats. This evergreen type occupies the Mexican highlands, Arizona and New Mexico, extending east into Arkansas, and west into California. *Quercus virginiana* seems also to have been a very early offshoot; with its varieties it forms a well-marked coastal group, ranging from North Carolina south along the shores of the Gulf into Mexico (where it stretches inland up the mountain sides), and appearing also on the California coast.

III. Deciduous White Oaks of North America.

The oaks with which we are familiar in this part of the country are of the lobed-leaf type. Geographically, at least, there are three parts to this group,—the eastern, the Rocky Mountain, and the Californian lobed-leaf oaks. It is not clear, however, whether or not these geographical groups can be separated taxonomically. They may be parallel groups, cut off from one another comparatively recently; or, possibly, the Californian group may be more closely related to the deciduous oaks of Europe (type *Q. robur*) than it is to the oaks of the Rocky Mountains and the east. The habit, leaf form and texture, and bud form of the Californian oaks have suggestive resemblances to those of the English oak; and it is perhaps not venturing too much to speculate as to whether these oaks, like certain other forms on our Pacific slope, may not have their closest relatives, not in America at all, but in Europe. There is besides at least one oak in California, *Q. sadleriana,* which appears to find its

nearest relatives in the modern Asiatic oaks, which were mentioned as having probably reached Asia in Tertiary times from the eastward. The *gambelii* group in the Rockies and the Atlantic group are apparently the separated branches of the latest developed white oaks (and the Californian oaks are perhaps a third corresponding group), which before glaciation may have succeeded in covering the greater part of the continent. Glaciation left survivors of this forest, it would seem, in two parts of the land—mountainous regions which projected above the ice—the southern Rockies, and the southern Alleghanies. From the one *Q. gambelii* has spread northward, keeping rather closely to the mountains and differentiating numerous but similar species; while from the other the early species (possibly *lyratiformis* and *minor*) have recovered an enormous stretch of territory, and have produced a correspondingly large number of varied species.

IV. White Oaks of Eastern North America.

The white oaks found east of the Rocky Mountains comprise the following species (see key):

1. *breviloba* *durandii*	2. *lyrata* *bicolor* *macrocarpa*
3. *chapmani* *minor* *margaretta* *alba*	4. *michauxii* *prinus* *muhlenbergii* group.

These species are all of the deciduous, thin-leaved type of *Leucobalanus*, except that *durandii* and *breviloba*, in ranging from Alabama west and south into northern Mexico, show a series of transitions towards the smaller, more entire, evergreen type of leaf. It might be that a careful study of these forms would show them to be transitional in other features also. Their range seems to indicate an ancient center of distribution in the southwest; this again is in sharp contrast to all the other species, which may be referred to a more recent center in the southeast. In short, there seem to be

several reasons for marking off rather sharply *durandii* and *breviloba* from the remainder of the species present in this area, and for suggesting the possibility that they may be a relic from the time of the differentiation of this deciduous section of *Leucobalanus.*

The remainder of the group has a very wide range. It touches the Rockies in Canada, and reaches Texas, Florida, and Maine. Nevertheless, it is almost true to say that every one of the species includes in its range the region of the southern Alleghanies. This region certainly seems to have been a center of distribution after the retreat of the ice fields, for this as well as for certain other groups of plants and animals (*Cambarus,* and the Unionidæ, for instance). The present distribution must have been largely achieved by the Pleistocene, for late Pleistocene fossils indicate a range broadly similar to that of the present.

The species, aside from (1) *durandii* and *breviloba,* fall into three main groups—(2) *macrocarpa* group, (3) *minor* group, (4) *prinus* group. Their relation to one another is not entirely clear. The *macrocarpa* group in some ways holds a central position, which suggests that it may be the oldest. So do the *persistent stipules* of all members of the group; this is without any doubt a primitive character. Its species moreover have the widest range, *macrocarpa* extending in the north to Saskatchewan and Maine, and in a great southward curve with its lowest point well down the Mississippi Valley; south of this it is replaced by *lyrata.* Again, Tertiary leaf-prints which have been referred to deciduous *Quercus* are limited thus far to types resembling *lyrata* and *minor.* (Cockerell's species *lyratiformis* from the Florissant beds is now reported from the John Day Basin, Oregon, where Knowlton also recognizes leaves of the type of *minor.*) There are so many suggestions of this sort that at present we must assume the *macrocarpa* group to be nearest to the ancestral type; and, though the fruit is aberrant, *lyrata* may well stand near the base of the group.

The *minor* group, or at least *minor* itself, has some affinities with *bicolor* and *macrocarpa.* Its wide range and the Tertiary occurrence of this or a similar species show that it has valid claims to antiquity. Whether *alba* belongs in this group is uncertain; it is difficult to see reasons for connecting it closely with any other species. *Mar-*

garetta, regarded by some as a good species, but which has often been regarded as an *alba-minor* hybrid, suggests such a relationship, but this is more or less doubtful.

The clearest and most highly differentiated group is that of the chestnut oaks. It may be connected with the more typical forms through forms such as *bicolor* (shape of leaf) and *lyrata* (bud-scales). That the serrate leaf is secondarily derived, through a lobed form, and not a persistence of the serration found in older portions of the genus is perhaps not proven; the tendency to lobation rather than serration on young shoots, as well as the general relation of the chestnut oaks to the other oaks of this region make it, however, highly probable.

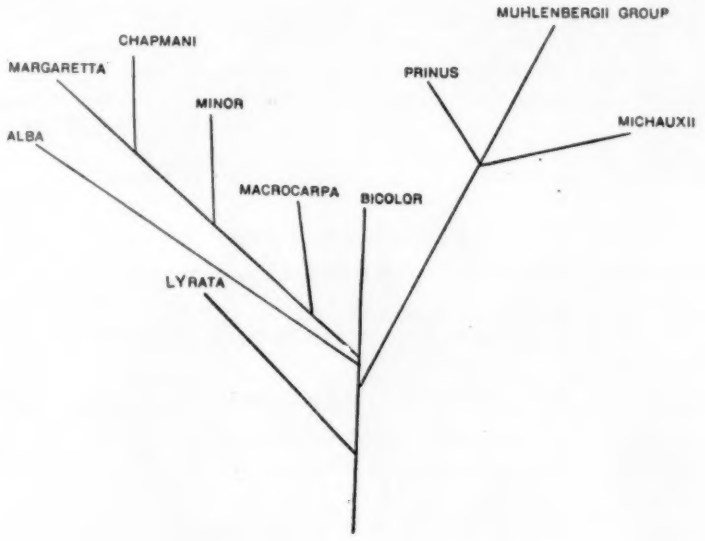

The above diagram may make more concrete these suggestions concerning relationships.

KEY TO DECIDUOUS WHITE OAKS OF EASTERN NORTH AMERICA.

Leaves deciduous, lobed or dentate, not spinulose.

I. Leaves lobed.
  A. Stipules persistent; buds more or less acute.
    1. Twigs slender, smooth. *Lyrata.*
    2. Twigs stout, pubescent.
      a. Fruit sessile, larger; cup usually deeper and fringed. *Macrocarpa.*
      b. Fruit pedunculate, smaller; cup more shallow, seldom fringed. *Bicolor.*
  B. Stipules deciduous; buds rounded.
    1. Twigs smooth. *Alba.*
    2. Twigs pubescent.
      a. Leaves deeply five-lobed, pubescent below. *Minor.*
      b. Leaves undulate, glabrous below *Chapmani.*
II. Leaves dentate.
  A. Buds less elongate, leaves narrower, widest near middle. *Muhlenbergii.*
  B. Buds more elongate, leaves broader, widest above middle.
    1. Cup scales free at tips only; upper scales very small. *Prinus.*
    2. Cup scales free; upper scales often forming a fringe to cup. *Michauxii.*

DESCRIPTION OF PLATES.

PLATE IV. Buds of the rounded type, without stipules. × 3.

FIG. 1. Q. alba (Urbana, Illinois).
FIG. 2. *Q. minor* (collected by H. H. Bartlett, Maryland).

PLATE V. Buds of the more acute type, stipules persistent. × 3.

FIG. 1. *Q. macrocarpa* (Urbana, Illinois).
FIG. 2. *Q. bicolor* (Urbana, Illinois).

PLATE VI. Buds of the elongated, chestnut oak type. × 3.

FIG. 1. *Q. prinus* (collected by H. H. Bartlett, Maryland).

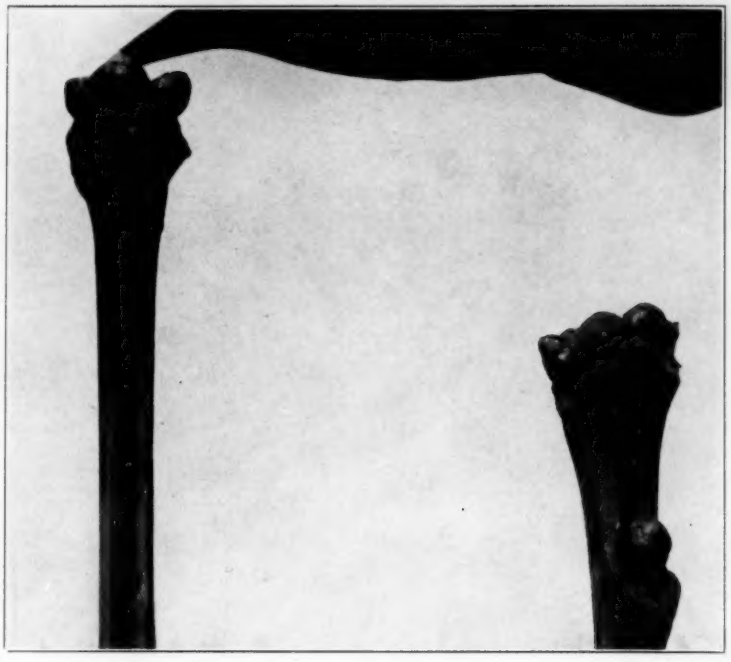

FIG. 1.

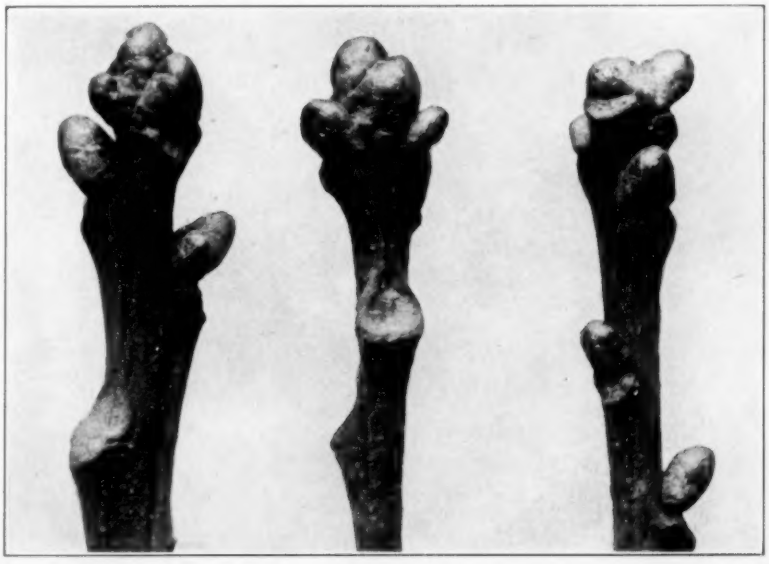

FIG. 2.

FIG. 1.

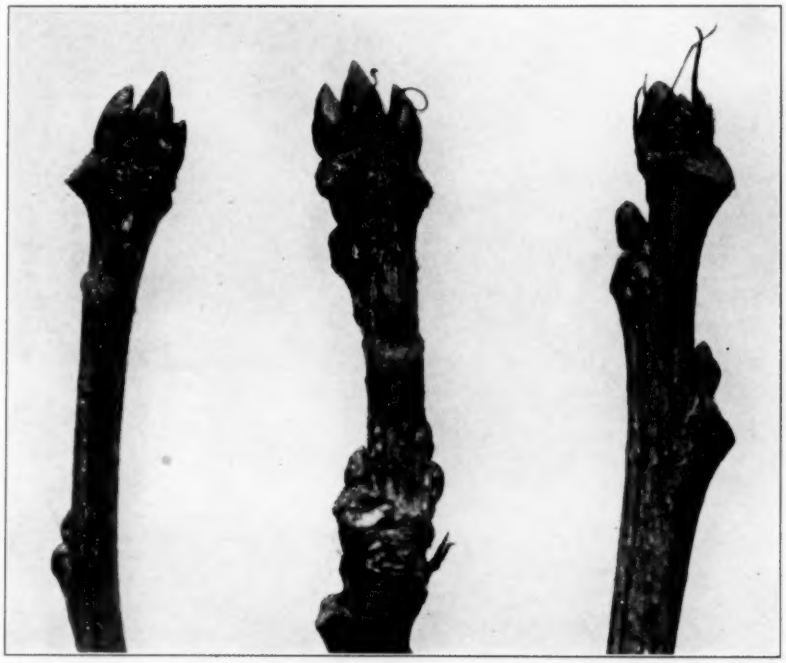

FIG. 2.

FIG. 1.

BIBLIOGRAPHY.

Berry, E. W.

1906. A Note on Midcretaceous Geography. *Science*, N. S., Vol. XXIII., pp. 509–510.

Brenner, Wilhelm.

1902. Klima und Blatt bei der Gattung Quercus. Flora, Bd. 90, p. 114.

1902. Zur Entwicklungsgeschichte der Gattung Quercus. Flora, Bd. 90, p. 446.

Candolle, Alphonse de.

1868. Prodromus Systematis Naturalis Regni Vegetabilis, Vol. XVI, pp. 1–109. Paris, Victoris Masson et Filii.

Engler, A., und Prantl, K.

1894. Die Natürlichen Pflanzenfamilien. III. Teil, 1 Hälfte, p. 47. Leipzig, Engelmann.

Gray, Asa.

1872. Address to the American Association for the Advancement of Science, *Proceedings A. A. A. S.*, Vol 21, p. 1.

Knowlton, Frank Hall.

Fossil Flora of the John Day Basin, Oregon. Bull. U. S. Geol. Survey, No. 204.

Liebmann, F. M., and Oersted, A. S.

1869. Chênes de l'Amérique tropicale. Leipzig, L. Voss.

Saporta, le Marquis G. de.

1888. Origine paléontologique des arbres cultivés ou utilisés par l'homme. Paris.

Sargent, Charles Sprague.

1895. The Silva of North America. Vol. VIII. Cupuliferæ. Boston and New York, Houghton, Mifflin and Company.

Scharff, R. F.

1912. Distribution and Origin of Life in America. New York, Macmillan Company.

Schottky, E.

1911–12. Die Eichen des extratropischen Ostasiens und ihre pflanzengeographische Bedeutung. *Bot. Jahrb. f. Systemik, Pflanzengeschichte, und Pflanzengeographie*, Vol. 47, pp. 617–707.

von Ettingshausen, C., und Krasan, Franz.

1889. Beiträge zur Erforschung der Atavistischen Formen an Lebenden Pflanzen und ihrer Beziehungen zu den Arten ihrer Gattung. Denkschriften der Kaiserlichen Akademie der Wissenschaften (Wien). *Mathematisch-Naturwissenschaftliche Classe*, Bd. 56, p. 47.

A NEW FORM OF NEPHELOMETER.

By J. T. W. MARSHALL and H. W. BANKS, 3d.

(*Read April 23, 1915.*)

The nephelometer (Gr. νεφέλη, a cloud), an instrument for the quantitative determination of small amounts of material in suspension, has attracted considerable attention of late, although the principles involved are by no means new. Since the time of Gay-Lussac attempts have been made to estimate small quantities of material by the turbidity or opalescence of their suspensions. This was generally done by comparing the suspension with a graded series of known suspensions prepared in the same way, and the comparison was made by looking through a column of the liquid and noting the turbidity, or by observing the opalescence, that is, the light reflected from the minute particles when the liquid is illuminated by a powerful beam of light. It is evident that matter in smaller quantities or in a finer state of subdivision may be recognized more easily by the opalescence than by the turbidity of its suspension. That even excessively minute particles possess the ability to diffract light has been shown by the ultramicroscope, while by the Faraday-Tyndall convergent beam of light, the optical in-homogeneity of solutions of crystalloids has been detected.

T. W. Richards in the course of atomic weight determinations in 1894[1] devised a simple instrument to enable the opalescence of very dilute suspensions of silver bromide to be more readily observed, and in a measure, quantitatively determined. Ten years later, Richards and Wells[2] improved the instrument optically and suggested its applicability to suspensions of substances other than the silver halides. Their actual determinations, however, seem to have been arrived at by a process of approximation; that is, the unknown was compared in the instrument to a suspension of known concentration, and from these readings a first approximation of its strength was calculated. A new standard of more nearly the same concentration as the unknown was then prepared

[1] *Proc. Am. Acad.*, XXX., 369, 1894.

[2] Richards and Wells, *Am. Chem. Jour.*, XXXI., 235, 1904.

and comparison again made. This process was repeated until a standard was obtained which when precipitated under the same conditions and compared in the instrument with the unknown gave the same amount of opalescence. The postulate involved, that the same quantities of material precipitated under identical conditions give equal opalescences, is undoubtedly correct, but the method is somewhat tedious in application, although good accuracy was obtained in about three approximations.

Wells in 1906[3] published the results of numerous experiments in which silver chloride was precipitated under different conditions, showing the influence of electrolytes both on the maximum opalescence developed and on the time required for this maximum to be reached. He came to the natural conclusion that the amount of light reflected varies not only with the quantity of material in suspension but also with its state of subdivision. In this investigation he used the Richards instrument of 1904 except that for the usual standard suspension he substituted fixed standards of ground glass as reflecting surfaces.

P. A. Kober[4] in 1913 took up the problem of determining quantitatively by the use of the nephelometric method, proteins and other substances occurring in biochemical investigations for which the ordinary gravimetric methods are either very tedious or inadequate. He used an instrument on the principle of the Richards nephelometer but adapted to the framework and optical parts of the Duboscq colorimeter. In comparing the opalescences of suspensions differing considerably in concentration, he observed that the readings were not quite inversely proportional to the concentration of matter in suspension, and from a large number of experiments with suspensions of different substances he developed an empirical formula expressing the relation between scale readings and concentration. This formula holds very well for ratios up to 1 : 3. He has successfully applied his instrument and method to the determination of a number of organic substances such as casein in milk, uric acid, and other purines. The nephelometer in various modifications has been used by W. R. Bloor to determine the fat

[3] Wells, *Am. Chem. Jour.*, XXXV., 99, 1906.
[4] P. A. Kober, *Jour. Biol. Chem.*, XIII., 485, 1913.

in blood, by McKim Marriot for acetone, and by S. S. Graves in ammonia determinations.

A number of instruments and methods have been devised for determining the amount of substance in suspension by the turbidity of its solution and these find considerable use in industrial chemistry. While the theory underlying this method is undoubtedly simpler than the nephelometric theory, it may easily be seen from the following considerations that the turbidimeter cannot equal the nephelometer in delicacy or sensitivity. Let us suppose that a standard as used in the turbidimeter absorbs about 10 per cent. of the light, then an unknown of twice the concentration will absorb about twice that quantity. However, it is not the amount of light absorbed, but the amount transmitted that is observed in this instrument; consequently the quantities measured would be in the ratio of about 9:8. The reflected lights measured in the nephelometer on the other hand would be nearly in the ratio of 1:2. Clouds which may be measured with considerable accuracy in the nephelometer show very slight absorption when observed by transmitted light in the turbidimeter.

Our reason for devising a new nephelometer may be made more apparent by a brief review of some of the considerations involved in the use of such instruments. The following are the chief factors involved in the amount of light reflected by an opalescent solution. First, the amount of substance in suspension. Second, its physical state, *i. e.*, the number and size of the particles, and their albedo which depends upon their own refractive index and that of the medium in which they are suspended. The amount of light observed is again modified by the fact that the light from any particle is reduced by an amount dependent upon the absorbing power of that part of the liquid above the particle. Thus we receive less light from the bottom layers of the suspension than from those nearer the top. This complex relation between reflection and absorption demands less consideration when the lengths of the illuminated columns are kept equal than when they are varied. As far as we are aware, in the nephelometers hitherto described the light from the two tubes has been equalized by changing the lengths of the illuminated columns of suspension. Although in purely

empirical work the elimination of this factor is not of very great importance, the theoretical consideration of the problem is greatly simplified thereby.

As Wells states, the opalescence of a liquid containing a definite amount of substance in suspension will, owing to the greater total reflecting surface, increase with the continued subdivision of the particles until these reach a limiting size. Rayleigh has pointed out this fact in a mathematical dissertation on the blue color of the sky, stating that as the particles approach the size of a wave length of light their reflecting power decreases. He shows that for very minute particles the amount of light reflected should vary as the sixth power of their radius. The maximum opalescence of the solutions as used in a nephelometer seems, however, to be developed when the particles are much smaller than a wave length of light—in fact of ultramicroscopic size.

The amount of reflected light lost through absorption is also a function of the number and size of the particles.

It is evident that as the refractive index of the medium approaches that of the particles, the amount of light reflected will decrease until, when the two refractive indices become equal, there will be no reflection. This phenomenon may be observed if powdered glass be suspended in a mixture of carbon disulphide and benzol.

With a view to determining some of the underlying laws of opalescent solutions, we undertook to design a nephelometer better adapted both to theoretical and to practical work than those in use at present. By using equal columns of suspension and actually measuring the reflected lights with a suitable photometer, not only is one of the variables eliminated, but also we are enabled to determine the absolute ratio of the lights reflected by various suspensions. The photometric part of the apparatus consists of a wedge of neutral tinted glass by which the light from one of the suspensions may be controlled; and a suitable optical arrangement for observing the two beams of light. A Lummer-Brodhun prism would serve this purpose admirably, but by a simple arrangement of mirrors, a field far more sensitive than that of the Duboscq colorimeter may be obtained.

Briefly the design of the instrument is as follows: The suspensions to be compared are contained in the two cells *A* and *B* shown in the accompanying diagram (Figs. 1 and 2). These consist of cylindrical glass tubes about 4 cm. high and 1 cm. in diameter. A glass plate is sealed into one end, while the other end is covered by a circular plate of glass slightly countersunk and held in place by caps of black fiber. These prevent stray light reflected from the edges

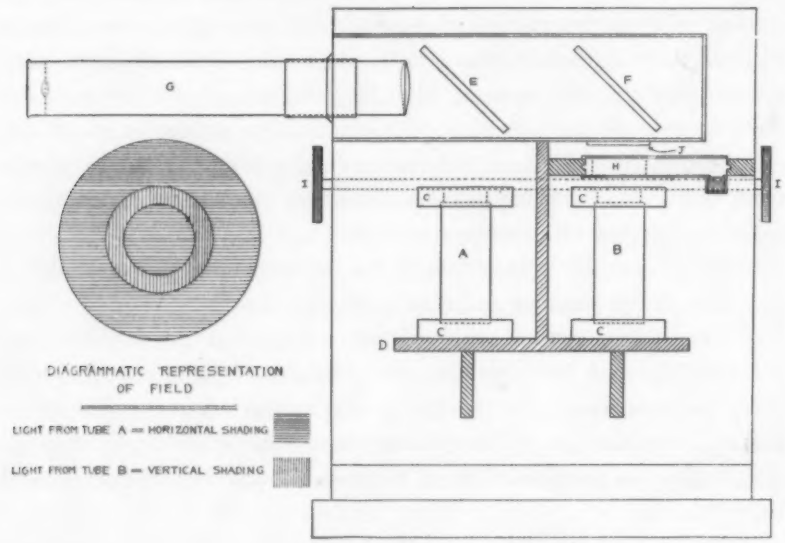

FIG. 1.

of the glass from entering the instrument. Difficulties arising from the agitation of the liquid by plungers are also thus avoided by having the cells completely enclosed. The cells rest on a shelf and are illuminated normal to their axes by a parallel beam of light from a 100 Watt lamp. The rays reflected from the suspended particles pass upward to the two mirrors *E* and *F* whence they are reflected into the magnifying eyepiece *G*. This is focused on mirror *E*. A circle cut through the silvering of mirror *E* permits the juxtaposition of the light from tubes *A* and *B* thus giving the eyepiece a field which is represented diagrammatically in the accompanying illustration. Photometric balance is effected by changing the intensity of the light from tube *B* by means of the sliding wedge of

neutral tinted glass *H*. This adjustment is made by the thumb-screw *I* and the position of the wedge is read on a scale mounted alongside (not shown in the diagram). A compensating wedge wedge may be placed at *J*, but unless the sliding wedge *H* is of fairly steep pitch, this is unnecessary, as the illumination of the field is sufficiently uniform without it. All parts of the instrument from which extraneous light may be reflected are painted a dead black.

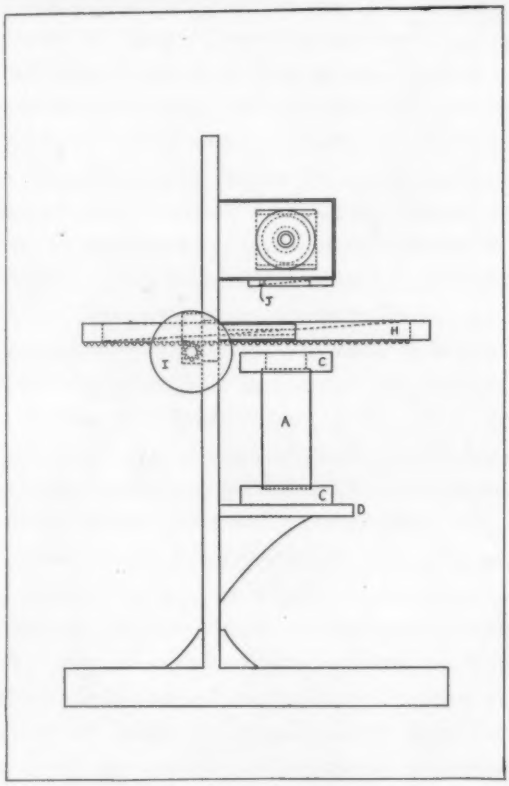

FIG. 2.

The construction of this instrument was delayed owing to difficulties encountered in securing neutral tinted glass. While awaiting its completion we decided to improvise a nephelometer in which several minor changes have been made. Among these may be mentioned the substitution for the glass wedge of a metal plate in which was cut a tapered slot. With this instrument we undertook some

work of rather an empirical nature along biochemical lines. Kober in one of his papers suggested the possibility of a nephelometric determination of albumin in urine, and a turbidimetric method for the same has been developed by Folin and Denis.[5] We therefore decided to apply our instrument to this problem. The standard was prepared from fresh normal human serum as recommended by Folin and Denis, and was standardized by nitrogen determinations and also by gravimetric determination of the heat coagulable proteins.

Difficulty was encountered at the start in comparing in the nephelometer albumin precipitated in the urine with that precipitated in the solution of standardized blood serum, on account of the difference in color due to the urinary pigments. In order to eliminate this interference of color, and also to obtain identical conditions of precipitation for both urine and standard, two equal portions of the urine of from 0.3 c.c. to 10 c.c. depending upon the quantity of albumen present, were taken. To one of these a known amount of standard was added (about 0.5 c.c. of 0.4 per cent. solution of serum protein). Both were then diluted to 75 c.c. with water and finally made up to 100 c.c. by the addition of a 7.5 per cent. solution of sulpho-salicylic acid. This gave a final concentration of 1.87 per cent. sulpho-salicylic acid, while the amount of protein varied from 2 to 5 mg. in 100 c.c. The resulting opalescent solutions were then compared in the nephelometer, the tube containing the urine plus standard being placed under the tapered slot. The light from this tube was then progressively diminished by adjustment of the slotted plate until photometric balance was obtained. From a scale with suitable vernier the position of the plate was read. As the theory has not advanced far enough as yet to permit of a purely formulative interpretation of the readings, the ratio of the concentrations of the two suspensions was determined from a curve. This curve had been obtained by plotting against the concentrations the scale readings obtained when known ratios of serum, made up with albumin free urine and precipitated with sulpho-salicylic acid under identical conditions, were compared. From the ratio R determined by means of the curve, the amount X of albumin originally present in the urine was found by the formula $R = \frac{X}{X+n}$ where n is the amount of

[5] Folin and Denis, *Jour. Biol. Chem.*, XVIII., 273, 1914.

serum albumin added. Quantities of urine and of standard were so taken that *R* would be in the neighborhood of one half. Urines containing large amounts of albumin (1 per cent. or over) were, after suitable dilution, compared directly with standard serum solution. In the case of such urines the high dilution necessary to obtain suitable nephelometric clouds eliminated the differences of color mentioned above. The results were compared with gravimetric determinations made according to Scherer's method. The clear filtrates from the coagulated protein were tested with sulpho-salicylic acid to make sure that none of the protein remained in solution. Duplicate gravimetric determinations gave good agreement. It was immediately evident that the nephelometric determinations were considerably higher than the gravimetric. Moreover, in the case of determinations on daily specimens of urine from one patient, the nephelometric results were consistently about 25 per cent. higher than the gravimetric, while in a similar series from another individual the ratio between nephelometric and gravimetric determinations was very variable, ranging from 1 to about 1.5. This at once suggested that the different proteins of the serum, while closely related chemically and equally precipitable by sulpho-salicylic acid, might give, in the nephelometer, clouds of different intensities. It is a significant fact that in the case of patient *R* where the ratio of nephelometric to gravimetric was variable, half saturation of the urine with ammonium sulphate gave a considerable precipitate of globulin.

In order to determine what differences might exist between the opalescences produced by equal amounts of the various serum proteins on precipitation with sulpho-salicylic acid under identical conditions, albumin, euglobulin, and pseudoglobulin were prepared from horse serum. Solutions of these when compared in the nephelometer gave surprisingly different results. The albumin gave about two and one half times as great an opalesence as the euglobulin and about three times as great as the pseudoglobulin. Compared with casein[6] suspensions, the following ratios, expressing the light reflect-

[6] As standard solutions of casein are easily prepared and also give very satisfactory clouds on precipitation with sulpho-salicylic acid, this substance forms a very convenient standard of reference in nephelometric work with various proteins.

ing power of equal amounts of these proteins, were found: Casein = 0.67 albumin; euglobulin = 0.63 casein; pseudoglobulin = 0.51 casein.

From the results experimentally obtained with various urines and from the differences in the clouds produced by equal amounts of the serum proteins, it may be seen that the nephelometric comparison of urine, in which these proteins may occur in varying amounts, with any definite standard such as serum cannot give a determination of the total protein. We hope by the use of specific precipitants to apply the nephelometric method to the separate determination of albumin and globulin in urine. This may be of value in diagnosis.

As the object of this paper has been to consider mainly the design of the instrument and the reasons for this design, the discussion of its application to the determination of albumin in urine has of necessity been hardly more than a suggestion of the work along that line. The results of the investigation of this particular problem with the experimental details, will be published shortly.

Summary.

1. The previous work in nephelometry has been briefly reviewed and the underlying principles of the nephelometric and turbidometric methods have been compared.

2. A new form of nephelometer has been described in which columns of suspension of equal lengths are used. The lights reflected are equalized and compared by means of a movable wedge of neutral tinted glass. Juxtaposition of the two emergent beams is secured by mirrors.

3. The variations found in preliminary experiments on the nephelometric determination of albumin in urine indicated that equal amounts of the various serum proteins might give different opalescences. Investigation showed that upon precipitation with 1.87 per cent. of sulphosalicylic acid, the same concentrations of serum albumin and serum globulins gave widely different clouds.

Harriman Research Laboratory,
The Roosevelt Hospital,
New York City.